

SOME ASPECTS OF THE SOLUTION CHEMISTRY  
OF TITANIUM (III)

by  
*Frederick*  
John F. Ashton, B. Sc. (Hons.)

Submitted in fulfilment of the requirements

for the

Degree of Master of Science

UNIVERSITY OF TASMANIA

HOBART

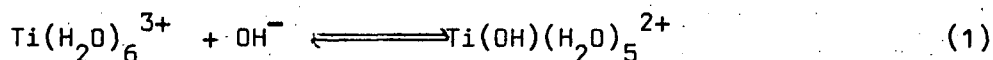
Original manuscript August, 1973

revised October, 1977

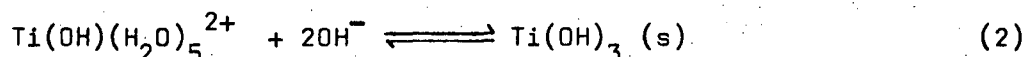
Abstract

In this investigation a combination of physico-chemical techniques namely potentiometric, conductometric and spectrophotometric methods have been used to study several aspects of the chemistry of titanium(III) in aqueous solutions. The results obtained have provided new information about the hydrolysis of the hexaquotitanium(III) ion and complex formation in titanium(III) thiocyanate and sulphate solutions.

It is shown that the hydrolysis of hexaquotitanium(III) ion in chloride solutions takes place in two stages. At low pH values primary hydrolysis occurs as given by the equation



At slightly higher pH values secondary hydrolysis occurs as given by the equation

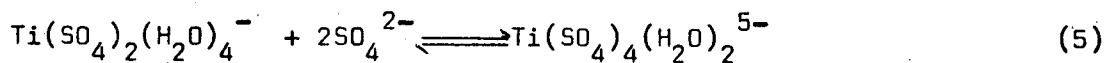
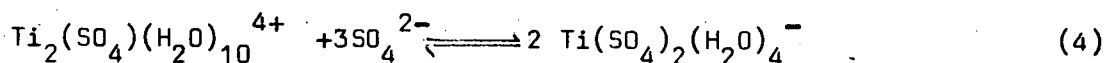
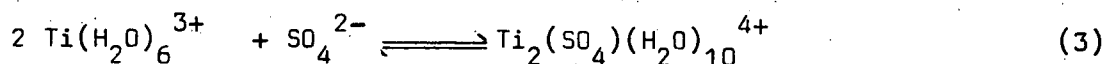


Both the primary and secondary hydrolysis products dimerise on standing forming hydroxy-bridged and oxy-bridged species respectively. Under certain conditions the secondary hydrolysis products oxidise with the evolution of hydrogen to form 1:1 mixed oxidation state species. The rate of evolution of hydrogen is dependent on the hydroxide ion concentration. The pH range over which the respective hydrolysis reactions occur depends on the total chloride ion concentration.

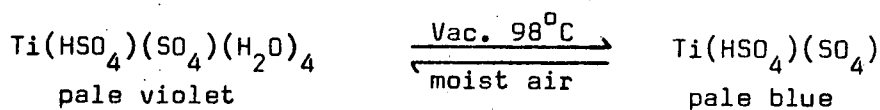
Titanium(III) forms two complexes in aqueous thiocyanate solutions; a 1:1 cationic species  $\text{Ti}(\text{NCS})(\text{H}_2\text{O})_5^{2+}$  and a 1:4 anionic species  $\text{Ti}(\text{NCS})_4(\text{H}_2\text{O})_2^-$ . A 1:1 titanium(III):titanium(IV) mixed oxidation state species is formed during the oxidation of titanium(III) thiocyanate solutions.

In dilute sulphate solutions, titanium(III) forms a series of complexes given by equations (3) - (5)

(iii)



The latter 1:4 complex persists in sulphate solutions up to about 4 molar and at higher concentrations forms polymers. At very high sulphuric acid concentrations i.e. about 15-18 molar, these polymers collapse to form the anhydrous species  $\text{Ti}(\text{HSO}_4)(\text{SO}_4)$ . The relatively stable pale violet 1:2 tetrahydrate can be crystallised from solution and readily converted to the anhydrous form.



Hydroxy sulphate species are formed during the hydrolysis of the above complexes and mixed oxidation state titanium(III) titanium(IV) species are formed when solutions containing the above complexes are allowed to oxidise in air.

Where possible, stability constants are estimated for the complexes formed in each system.

From this new information together with existing data for other systems, trends in the co-ordination behaviour for titanium(III) are discussed.

In each of the systems studied titanium mixed oxidation state species were detected during the oxidation of titanium(III) complexes. Following from this the mixed valence chemistry of titanium has been reviewed and the significance of this type of behaviour in understanding the chemistry of titanium(III) is considered.

To the best of my knowledge, this thesis contains no material which has been accepted for the award of any other degree or diploma in any university and contains no copy or paraphrase of material previously published or written by another person, except where due reference is made in the text.

*John F. Ashton*

John F. Ashton.

to the only God, our Savior through  
Jesus Christ our Lord, be glory, majesty,  
dominion, and authority, before all time  
and now and for ever. Amen.

- Jude 25 (R.S.V.)

ACKNOWLEDGMENTS

Many thanks are extended to Dr. P.W. Smith for his supervision and interest in this work.

The author also wishes to express his appreciation to the following:-

The teaching and technical staff of the Chemistry Department for their help during this work.

Mr. M. Ashton, for assisting with the kinetic runs.

Mrs. J. Roberts, for typing this thesis.

Mrs. H. Hen, for copying the diagrams for this thesis.

The author also acknowledges the award of an Australian Titan Products Research Fellowship.

CONTENTS

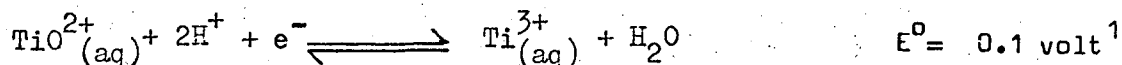
	<u>Page</u>
<u>Chapter 1.</u> Introduction	1
<u>Chapter 2.</u> The hydrolysis of titanium(III) in aqueous chloride media.	3
<u>Chapter 3.</u> Titanium(III) thiocyanate complexes in aqueous media.	42
<u>Chapter 4.</u> Titanium(III) sulphate complexes formed in aqueous solutions.	56
<u>Chapter 5.</u> Some aspects of the solution chemistry of titanium(III).	93
<u>Appendices</u>	99
<u>References</u>	147

## CHAPTER I

### Introduction

In the industrial processing of titanium compounds, titanium is almost always present as titanium(IV). Many processes involve reactions in solution and studies have been made of complexes formed in aqueous titanium(IV) systems. Titanium(IV) can be easily reduced to titanium(III) in aqueous solution. Consequently the use of titanium(III) compounds as alternative intermediates in industrial processes seems feasible. However, by comparison with titanium(IV), much less is known about titanium(III) complexes. For example, it is surprising that only limited studies of the hydrolysis of titanium(III) have been made and the exact nature of titanium(III) hydroxide precipitates has not been investigated in detail. As well, there appears to be very little information available on the nature of the titanium(III) species present in sulphate solutions.

The relatively limited extent of studies of titanium(III) systems may reflect the problems associated with titanium(III) being a reducing agent. Titanium(III) in aqueous solution is a mild reducing agent.



This aerial oxidation of titanium(III) solutions is significantly retarded in strong acid solutions<sup>2-4</sup> and acidic solutions of titanium(III) salts are quite stable in an inert atmosphere e.g., under nitrogen.

In very dilute hydrochloric acid solutions titanium(III) exists as the hexaquo  $[\text{Ti}(\text{H}_2\text{O})_6]^{3+}$  ion<sup>5-7</sup>. When ligands such as  $\text{OH}^{-}$ ,  $\text{F}^{-}$ ,  $\text{Cl}^{-}$ ,  $\text{CN}^{-}$ ,  $\text{NCS}^{-}$ ,  $\text{SO}_4^{2-}$ ,  $\text{C}_2\text{O}_4^{2-}$ ,  $\text{PO}_4^{3-}$  and / <sup>complexing</sup> organic ions are added to solutions containing the hexaquo ion, complexes of the type  $[\text{TiL}_x(\text{H}_2\text{O})_y]^{m+}$  are formed. The chemistry of these complexes was reviewed in 1968 by Clark<sup>8</sup>. Quite a few studies of titanium(III) chloro complexes formed in hydrochloric acid solutions have been made<sup>7, 9-12, 92</sup> and several workers have looked at aqueous titanium(III) fluoride systems<sup>13-19</sup>. However, few other titanium(III) systems have been investigated in detail.



The aim of this present work has been to investigate in more detail the hydrolysis of the hexaquoctitanium(III) ion in chloride solutions and to study the nature of the titanium(III) complexes formed in aqueous thiocyanate and sulphate solutions. The results obtained have enabled complex formation in these systems to be understood. Trends in the co-ordination behaviour of titanium(III) have become more apparent and attention has been drawn to the significance of mixed valence titanium(III) - titanium(IV) species in these systems.

CHAPTER 2The hydrolysis of titanium (III) in aqueous chloride media2.1 Introduction

One detailed study of the hydrolysis of the hexaquotitanium (III) ion in dilute solutions has been reported<sup>20</sup>. However the results presented did not take into account dimerisation reactions which are very common in hydrolytic equilibria. More recent studies in 1968 and 1970 of the hydrolysis reaction<sup>21,22</sup> showed that dimerisation does occur but data are reported only for concentrated halide solutions (ionic strength 3 molar). All the results in the above three studies were based on potentiometric measurements. In additions, the studies were limited in detail to primary hydrolysis behaviour, i.e., the formation of soluble 1:1 Ti (III) : OH<sup>-</sup> species. No detailed studies of secondary hydrolysis behaviour involving the formation of titanium (III) hydroxide precipitates, have been reported.

A preliminary investigation of the system showed that both spectrophotometric and pH measurements were time dependent. In an attempt to understand this behaviour and relate it to the overall hydrolysis picture measurements were made

- (a) as soon as possible after the addition of base and vigorous mixing,
  - (b) after the solutions had equilibrated and measurements were stable
- These are referred to as "initial" and "equilibrated" solutions respectively in this chapter.

It was also noted that hydrogen evolution occurred in the presence of some insoluble species. This behaviour was investigated in a separate kinetic study.

In this chapter, results of a new investigation of both the primary and secondary hydrolysis reactions of the hexaquotitanium (III) ion

are presented. Hydrolysis constants for the primary hydrolysis species in dilute solutions and the solubility product of insoluble titanium(III) hydroxide are reported for the first time. The nature of the insoluble species is discussed and a new explanation for the formation of these different coloured precipitates, is presented with supporting evidence. Also a mixed oxidation state hydrolysis species has been discovered. The results obtained include potentiometric, analytical and spectral data as a function of pH, chloride ion concentration and time, for the hydrolysis system.

## 2.2 Experimental

Rapid potentiometric titrations were used to study the species first formed. Fast stirring was used to ensure rapid mixing of the reactants, total titration time being usually less than 4 minutes. The apparatus for rapid titration measurements is shown in Figure 1. It consisted of a combined pH electrode coupled to a recording pH electrometer, together with a motor driven 20ml piston burette calibrated to 0.01ml. Solutions of titanium(III) in dilute hydrochloric acid (see Appendix 1) were titrated with sodium hydroxide. During the titration the solutions were stirred and nitrogen bubbled through rapidly to prevent aerial oxidation. The total chloride ion concentration was varied by adding  $\text{NH}_4\text{Cl}$ . Ammonium salts have minimal ageing effects on glass electrodes and enable high chloride ion concentrations to be obtained. Consequently solutions high in chloride ion concentration were also titrated with ammonium hydroxide.

Spectroscopic studies were made (see also Appendix 2) to obtain more information about the nature of the hydrolysis species present in solution. The spectra of the initial species present were obtained from solutions where a fixed aliquot of titanium(III) solution was added to prepared solutions containing known amounts of base. These solutions were then transferred after shaking, to glass cells and their absorbance measured immediately. The total time for the operation being about 3 minutes.

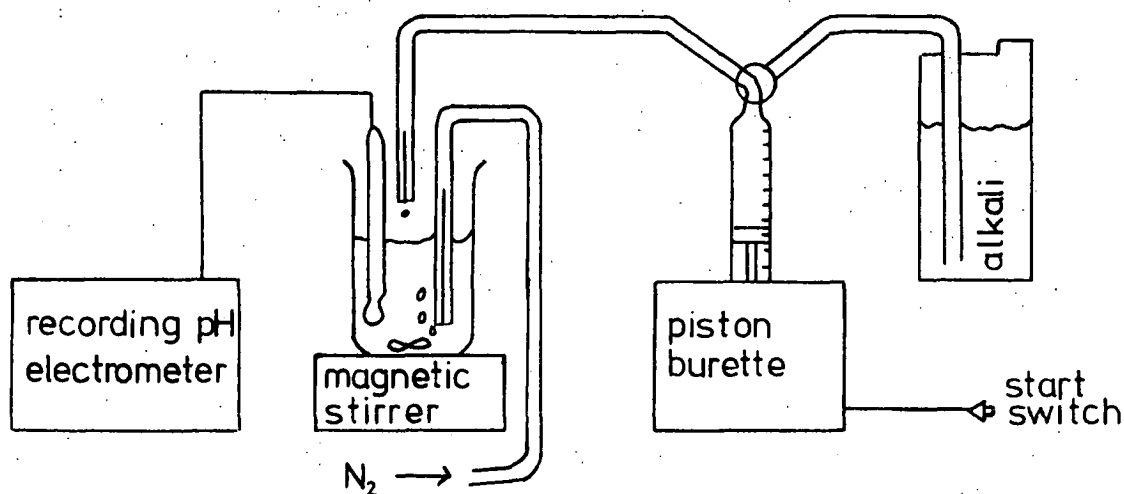
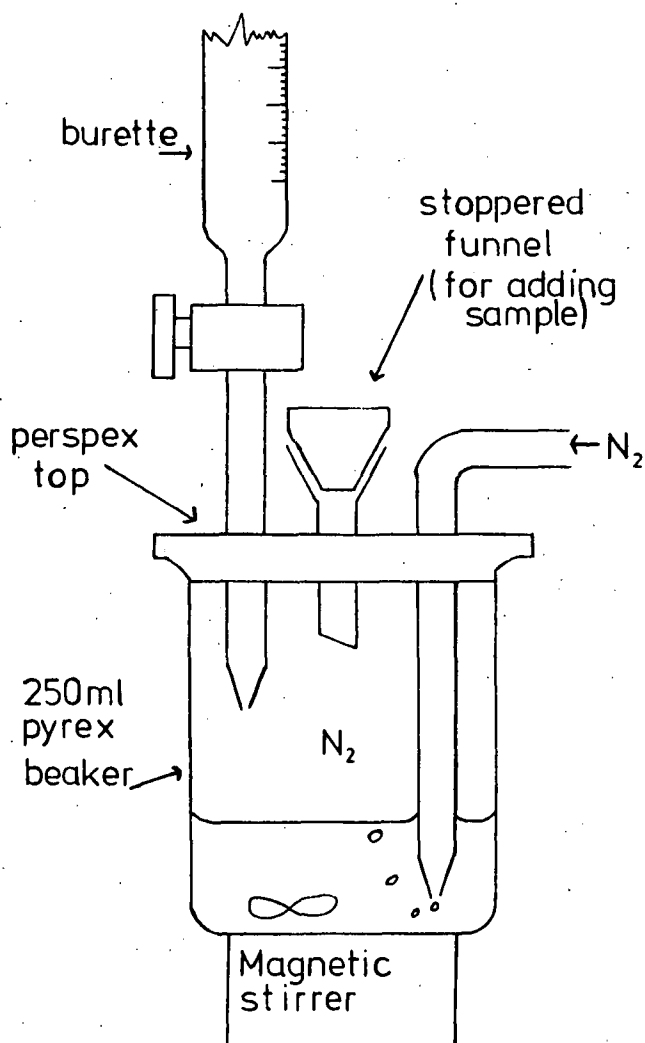


Figure 1. Apparatus for rapid titration measurements.

The final hydrolysis species formed were studied by equilibrium measurements. For all these measurements, series of individual solutions containing fixed titanium(III) and chloride ion concentrations and varying concentrations of base ranging from zero to excess of that required for complete hydrolysis, were prepared and made to constant volume (50mls). The solutions were then allowed to equilibrate by standing in sealed flasks under a nitrogen atmosphere to prevent aerial oxidation. After equilibrating for 20 hours, individual pH, spectral or analytical measurements at room temperature i.e.,  $\sim 21-22^{\circ}\text{C}$ , were recorded.

The latter analytical studies were made to provide additional evidence for the stoichiometry of the hydrolysis reaction. Analysis of the titanium III content of solutions was made using the apparatus shown in Fig 2. 5 ml aliquots of the reaction solution were taken and made to about 20mls with nitrogenated 5M HCl and nitrogen gas was continuously bubbled through the



**Figure 2.** Apparatus for titanium(III) analyses

solution during the titration. A 10%  $NH_4SCN$  solution (5mls) was added as indicator and the solution titrated immediately with nitrogenated 0.020M  $NH_4Fe(SO_4)_2$  solution. Chloride ion determinations were made by Volhard's method, titanium(III) being oxidised to titanium(IV) with nitric acid beforehand, or by estimating the total  $TiCl_3$  and  $HCl$  concentrations by titrating to pH 7.0 with standard sodium hydroxide solution.

Information about the mechanism whereby hydrogen was evolved from certain solutions containing titanium(III) hydroxides was obtained from kinetic studies. The rate of evolution of hydrogen was measured using apparatus consisting of a water manometer (which could be closed off for

high pressures) and a mercury manometer. Both manometers were connected to a glass stoppered conical flask. The apparatus was immersed in a water bath thermostated to  $30.0^{\circ}\text{C}$ , and the solution being studied was stirred magnetically from below. The rate of evolution of hydrogen was followed by measuring the change in pressure (i.e. the change in height of the manometers) with time. The apparatus was initially flushed with nitrogen (by bubbling through the manometers). The volume of the apparatus was determined by water displacement.

### 2.3 Results

Figure 3 shows the typical pH behaviour observed during rapid titrations of titanium(III) in dilute chloride media. In region (a) primary hydrolysis occurs resulting in the formation of a soluble 1:1  $\text{Ti(III):OH}^-$  complex. In region (b) the uptake of another two equivalents of  $\text{OH}^-$  occurs, corresponding to the formation of  $\text{Ti(OH)}_3$  (brown precipitate). Similar titration curves were obtained over the chloride ion concentration range 0.4 to 4.5 M (see also Appendix 3). Equilibrium potentiometric titration data for individual solutions containing varying amounts of base are shown in Figure 4 (see also Appendix 4). A 1:1 complex is still formed in the primary hydrolysis region, although much lower pH values were obtained.

Spectral data for both the initial and final primary hydrolysis species, (at low chloride ion concentrations), for varying concentrations of base are shown in Figures 5 and 6. These studies of the hydrolysis behaviour show that in non-equilibrated solutions where measurements were made immediately after mixing, the intensity of absorption increases with increasing concentration of base and the position of maximum absorption shifts from 495 nm towards 480nm. On standing (to give equilibrated solutions) the intensity of absorption in each solution increases further but there is no change in the position of the peak. From individual absorption measurements at 480nm on a series of solutions (see Appendix 5) and assuming that a stable complex is formed so that  $\bar{n}$  represents the

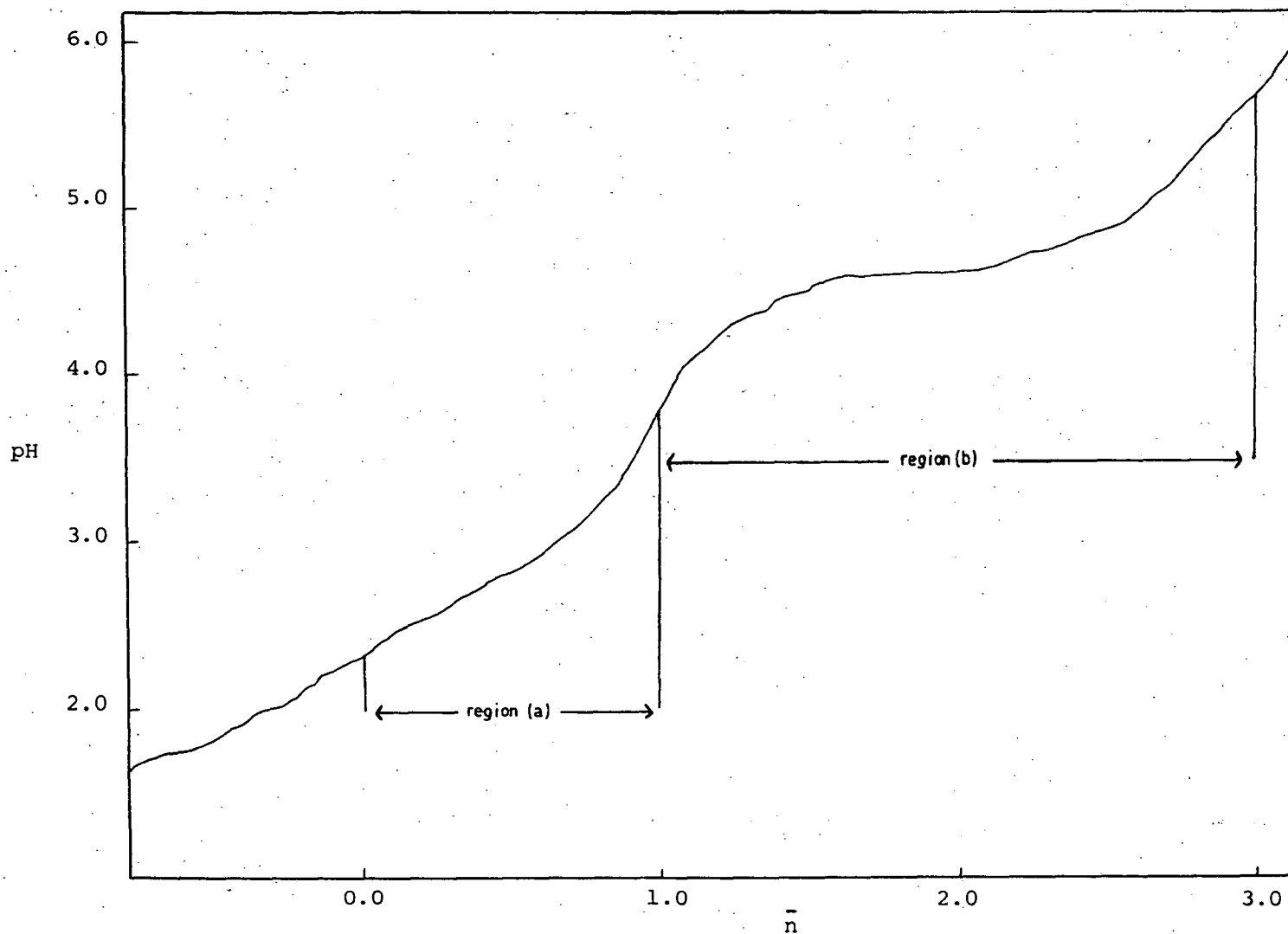


Figure 3. Rapid pH titration curve for 0.113M titanium(III) (80 mls) with 1.97M NaOH.

$[\text{Cl}^-] = 0.45\text{M}$  in the initial solution.  $\bar{n} = \text{ratio}[\text{OH}^-]:[\text{Ti(III)}]$ .

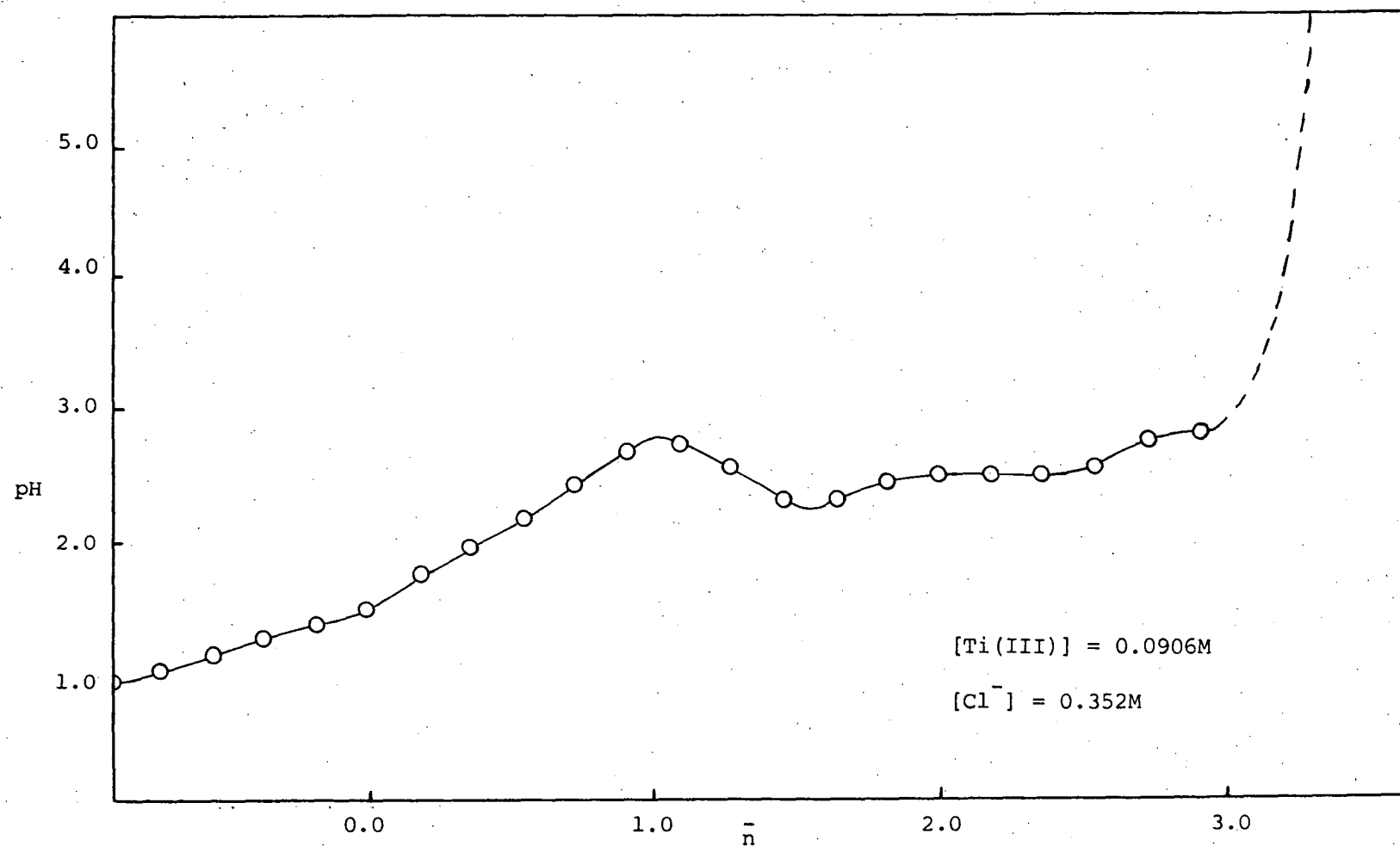


Figure 4. pH of equilibrated titanium(III) solutions.



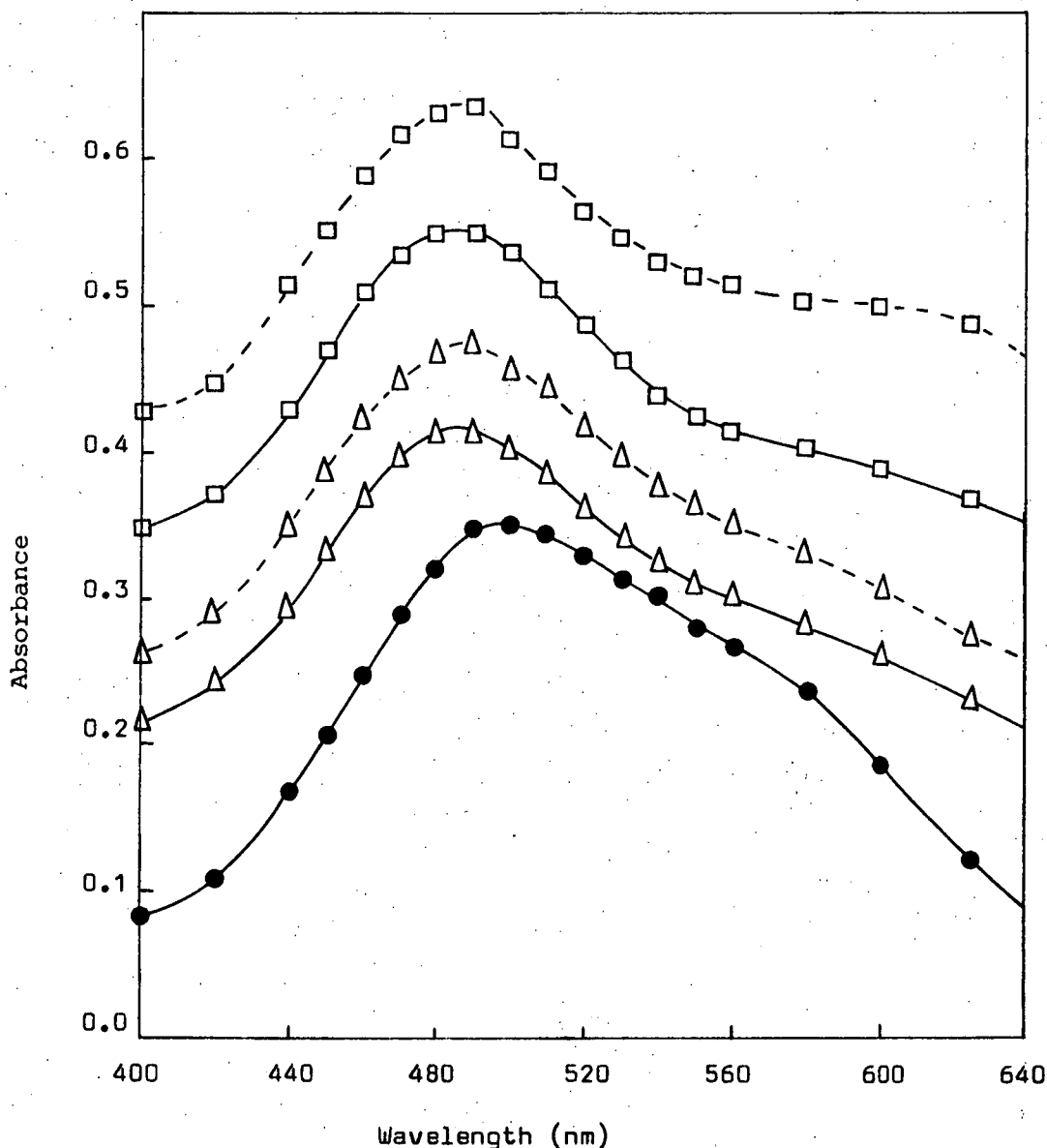


Figure 5. Spectra of initial (—) and equilibrated (---) solutions of titanium(III) where  $\bar{\alpha} = 0.00$  ( $\bullet$ ),  $0.31$  ( $\Delta$ ),  $0.50$  ( $\square$ ), using 1 cm cells.

$$[\text{Ti(III)}] = 0.0892\text{M}. \quad [\text{Cl}^-] = 0.334\text{M}.$$

fraction of titanium(III) which has undergone hydrolysis, the extinction coefficients of the primary hydrolysis species present in the initial and equilibrated solutions were calculated (see Appendix 5) to be  $6.7 \pm 1.0$  and  $10.5 \pm 1.0$  moles<sup>-1</sup> litres cm<sup>-1</sup> respectively. At higher chloride ion concentrations when base is first added to the violet

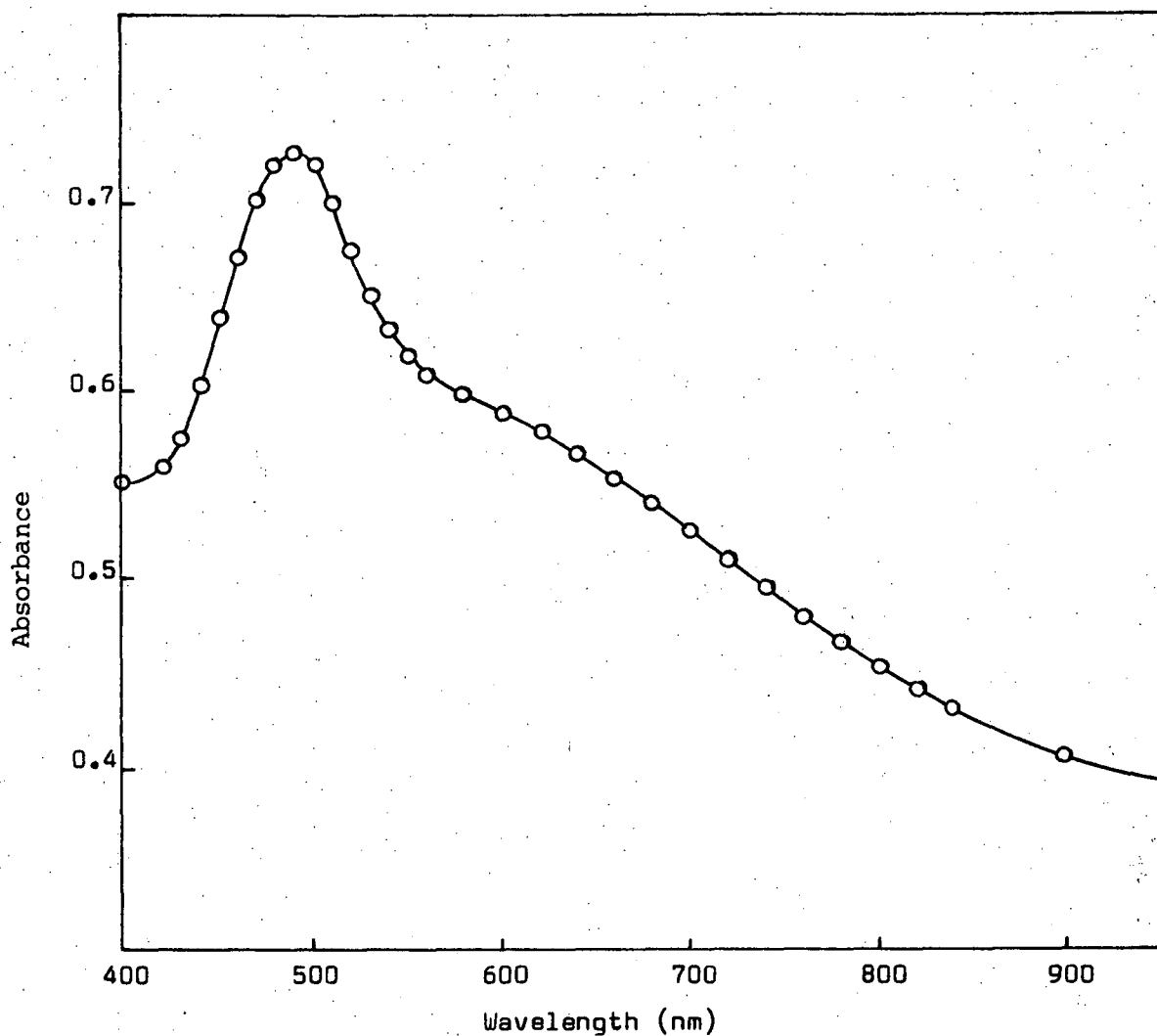
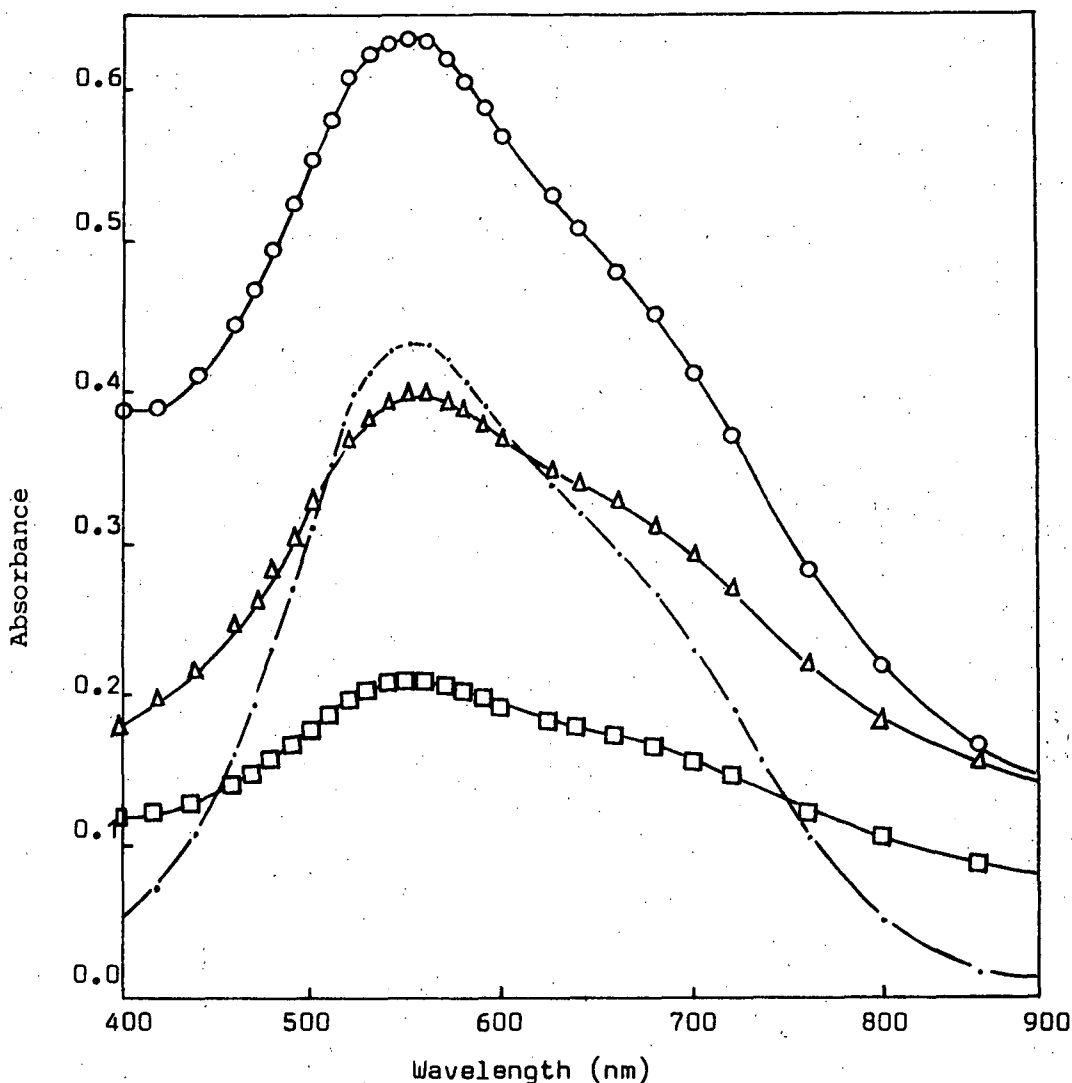


Figure 6. Spectrum of equilibrated titanium(III) solution where  $\bar{n} = 0.64$ , using 1 cm cells.  $[\text{Ti(III)}] = 0.0950\text{M}$ ,  $[\text{Cl}^-] = 0.364\text{M}$ .

solutions the color similarly darkens. However, the solutions then quickly become turbid due to secondary hydrolysis also occurring in this region precluding detailed spectral studies. Generally no solution spectra could be recorded for the secondary hydrolysis region due to the presence of precipitate. However at very high chloride ion concentrations ( $\sim 9$  molar) the precipitate in equilibrated solutions appeared to settle



**Figure 7.** Spectra of equilibrated solutions of titanium(III) where  $\bar{n} = 0.00(\cdot)$ ,  $0.19(o)$ ,  $1.20(\Delta)$ ,  $2.22(\square)$ , using 1 cm cells.  
 $[\text{Ti(III)}] = 0.0880\text{M}$ ,  $[\text{Cl}^-] = 8.80\text{M}$ .

more completely, leaving minimal turbidity in the supernatant solution. Solution spectra for these solutions containing varying amounts of base are shown in Figure 7. No change in the position of maximum absorbance (550 nm) was observed showing that the initial titanium(III) species in solution remains unchanged. i.e. There was no evidence of primary hydrolysis occurring. The variation of the absorbance of individual

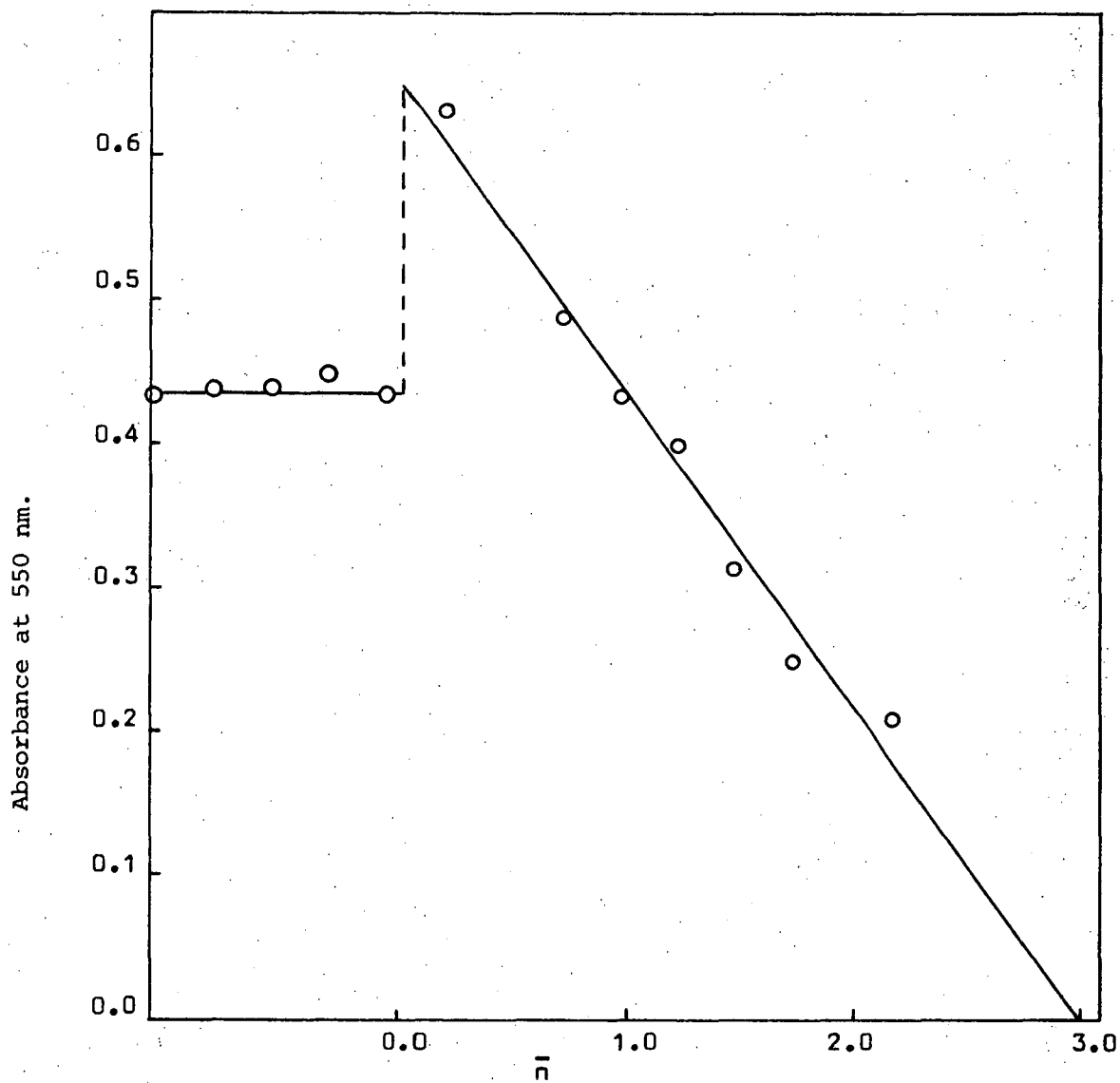


Figure 8. Absorbance (at 550 nm) of equilibrated solutions of titanium(III)

$[\text{Ti(III)}] = 0.0880\text{M}$ ,  $[\text{Cl}^-] = 8.80\text{M}$ . Path length = 1 cm.

solutions at 550 nm, as base is added is shown in Figure 8. No change in absorbance is observed until precipitation occurs. Then the value jumps sharply due to an increase in absorbance caused by scattering of the light by some colloidal particles of the precipitate remaining suspended in the solution. However, overall the absorbance decreased uniformly towards zero as the ratio of hydroxyl ions added tended towards 3. This latter observation being confirmed by the analytical work.

The results of analytical studies of the variation of the titanium(III) content of equilibrated solutions during hydrolysis in dilute chloride media are shown in Figure 9. The titanium(III) content remains constant until precipitation begins at  $\bar{n} = 1.0$ . After this titanium(III) is removed from solution at the rate of 1.00 Ti per 2.00  $\text{OH}^-$  added, by the formation of brown  $\text{Ti}(\text{OH})_3$  precipitate (region (a) in Figure 9) until  $\bar{n} \sim 1.5$ . On standing the brown precipitate initially formed darkens becoming black but no hydrogen evolution is observed in these solutions. In region (b), there appears to be no increase in the amount of black precipitate present. Instead, on standing, hydrogen evolution is observed and a dark blue solution forms. Also the titanium(III) content of the solution decreases at the rate of 1.00 Ti removed per 4.00  $\text{OH}^-$  added, in this region. When an aliquot of the dark blue solution is added to 5.5M HCl solution, a white turbidity forms indicating the presence of titanium(IV). In region (c) the dark blue species coagulates and settles on the bottom, and the rate of removal of titanium is again 1.00 Ti per 2.00  $\text{OH}^-$  added. At high chloride ion concentrations a different analytical curve is obtained. The variation of the titanium(III) content of these equilibrated solutions is shown in Figure 10. A dark blue precipitate settles in the hydrolysed solutions. Hydrogen evolution is also observed. The slope of the curve shows that the titanium(III) is removed uniformly from solution at the rate of 1.00 Ti per 3.00  $\text{OH}^-$  added. This confirms the earlier spectrophotometric result.

The data obtained from the kinetic study of the rate of evolution

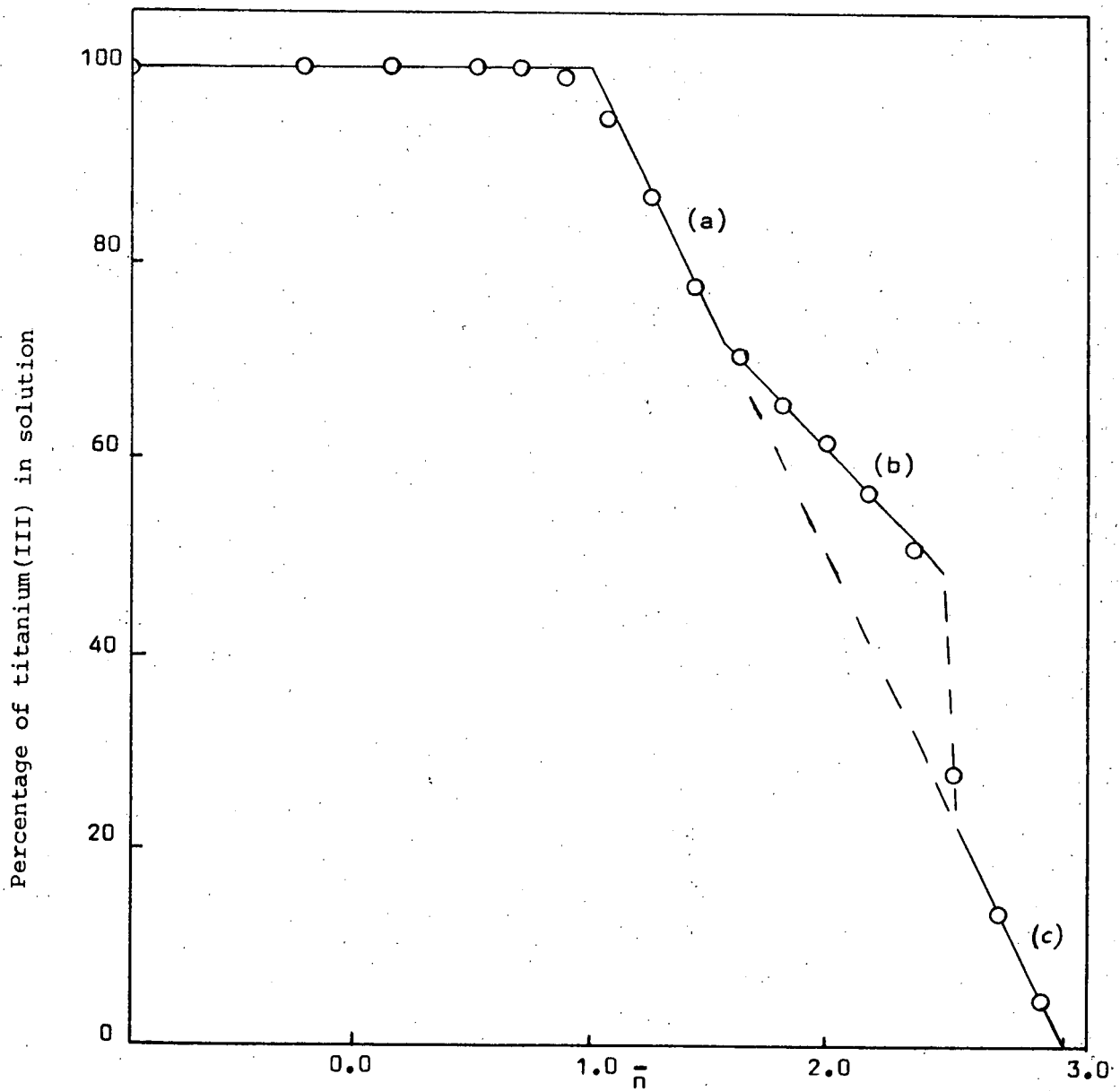


Figure 9. Titanium(III) content of equilibrated solutions during hydrolysis in dilute chloride media.

$$[\text{Ti(III)}] = 0.0906\text{M}, [\text{Cl}^-] = 0.352\text{M}.$$

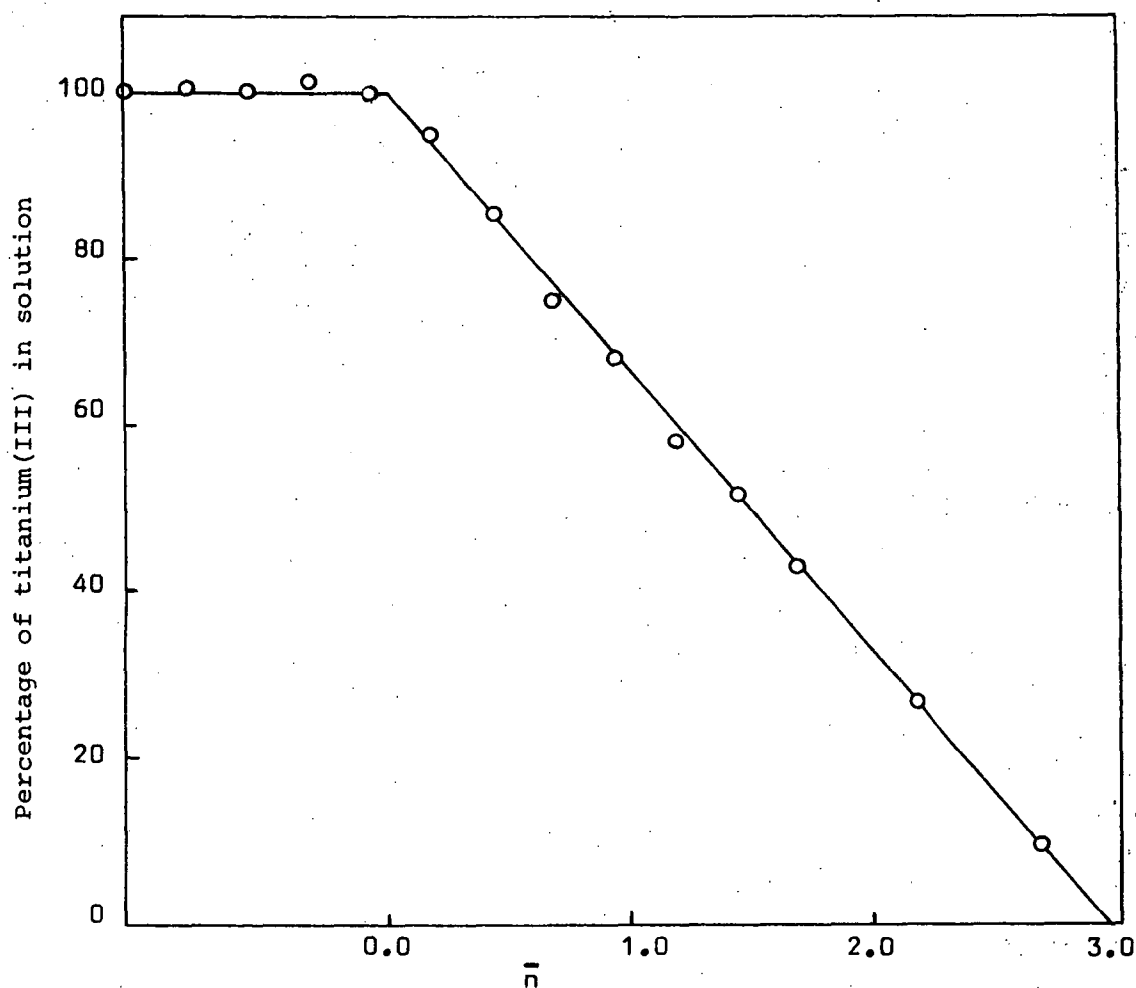


Figure 10. Titanium(III) content of equilibrated solutions during hydrolysis in concentrated chloride media.

$$[\text{Ti(III)}] = 0.0880\text{M}, [\text{Cl}^-] = 8.80\text{M}.$$

of hydrogen are given in Appendix 6. Rate curves show two distinct linear sections in the initial stages. An example is given in Figure 11. The change from one linear section to the other corresponded to the change in color of the precipitate from brown to black. As the reaction proceeded further the rate of evolution of hydrogen decreased gradually to almost zero (see Figure 12) corresponding to the formation of the dark blue species. The "apparent oxidation numbers" in Figure 12 were calculated

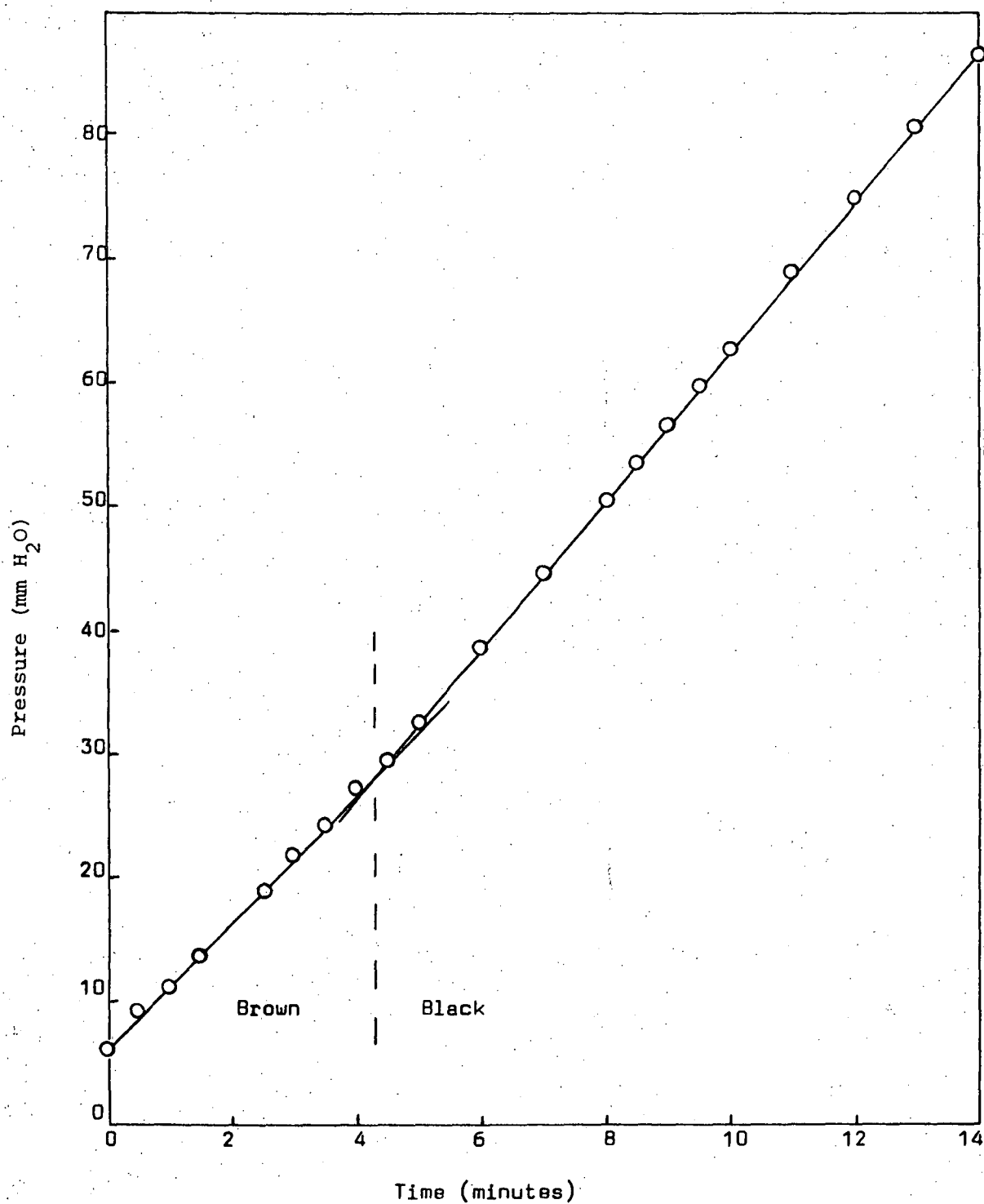


Figure 11. Rate of evolution of hydrogen.

$[\text{Ti(III)}] = 0.184$ ,  $[\text{OH}^-] = 1.680\text{M}$ ,  $[\text{Cl}^-] = 0.668\text{M}$ .



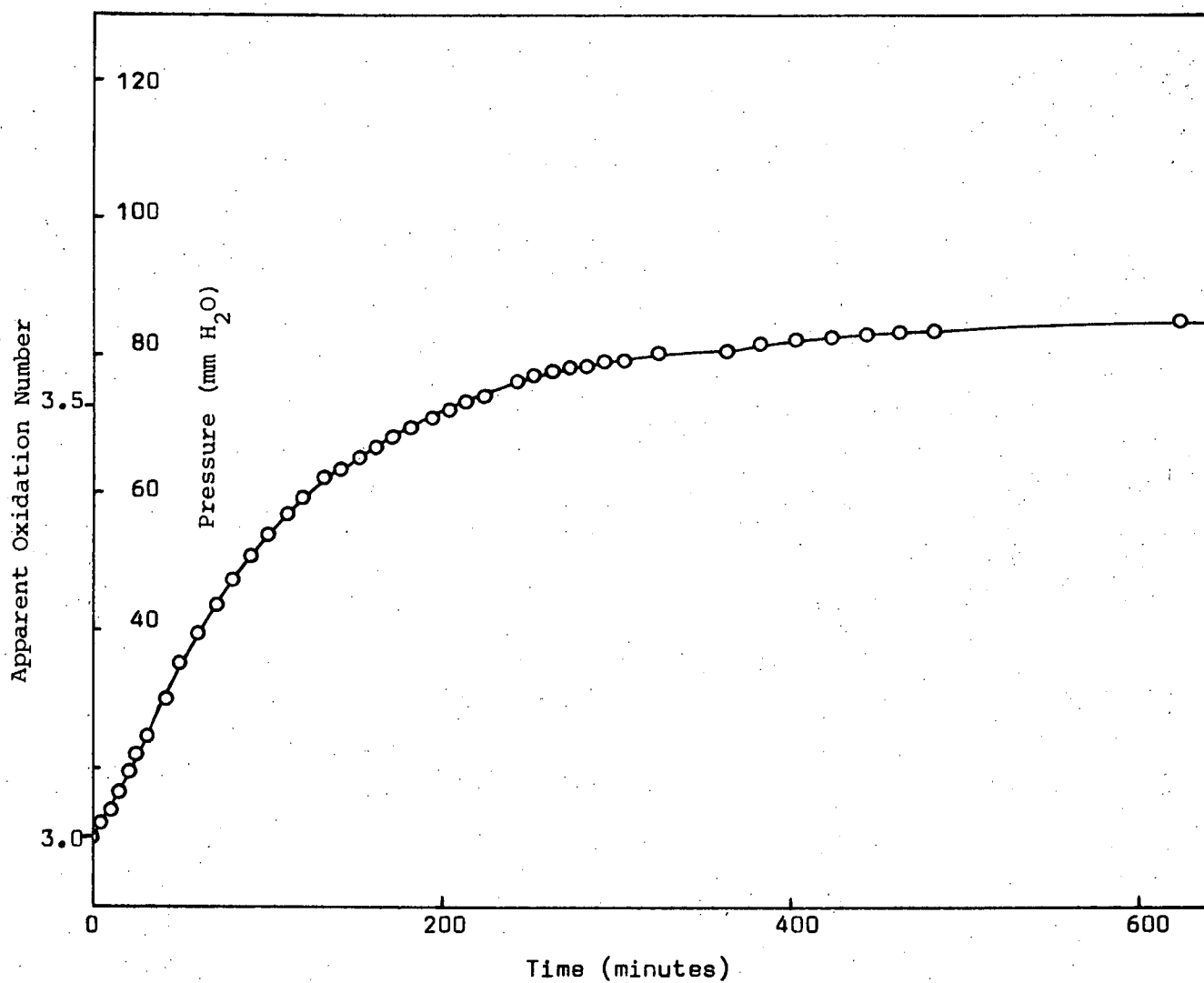


Figure 12. Rate of evolution of hydrogen

$[\text{Ti(III)}] = 0.0391\text{M}$ ,  $[\text{OH}^-] = 0.894\text{M}$ ,  $[\text{Cl}^-] = 0.142\text{M}$ .

from the number of moles of hydrogen evolved, assuming that 0.5 moles of hydrogen are involved for each mole of titanium(IV) produced.

The slopes of the two initial linear sections correspond to the rate of auto-oxidation i.e., hydrogen evolution, for the brown and the black precipitates respectively. Since solid titanium(III) species (precipitates) are involved in the reaction the amount of titanium(III) present should not appreciably effect the rate which is probably 1st order with respect to titanium(III) concentration for both reactions. The effect of base on the rate of hydrogen evolution from solutions initially i.e., in the presence of the brown precipitate, is shown in figure 13. A smooth curve is obtained which when extrapolated to zero rate gives the value 0.20M which corresponds to  $\bar{n} = 1.5$  (see Appendix 7). This is in exact agreement with the earlier observations that no hydrogen evolution is observed up to  $\bar{n} = 1.5$ . After correcting for base concentration at zero rate, a plot of log rate versus log concentration (figure 14) gives a straight line of slope 1.5. Thus initially the rate of hydrogen evolution is given by the equation

$$\frac{d(H_2)}{dt} = k_1 [Ti(III)] [OH]^{3/2} \quad (1)$$

where  $k_1$  is the pseudo 2.5 order rate constant. The effect of base on the rate of the second reaction is shown in figure 15. In this case the rate is proportional to the concentration of base. For this reaction also, extrapolation gave zero rate at 0.20M i.e.,  $\bar{n} = 1.5$ , confirming again that no hydrogen evolution would be observed in solutions where  $\bar{n} < 1.5$ . The rate of hydrogen evolution from solutions in the presence of the black precipitate is given by the equation

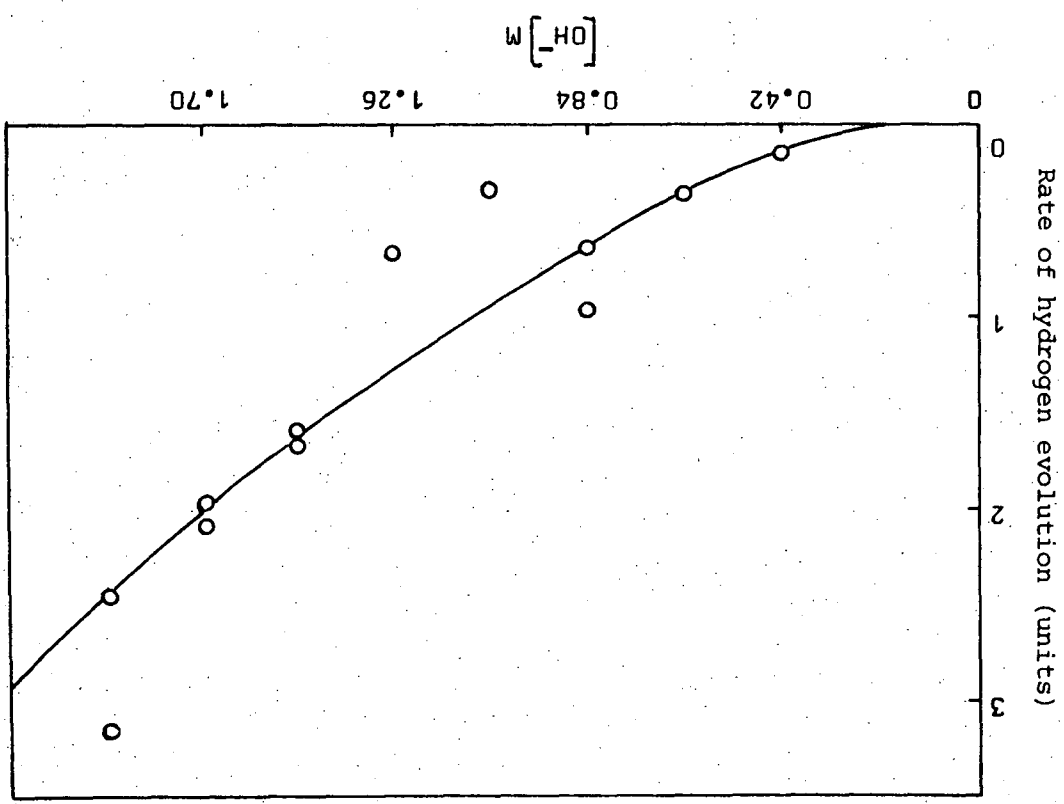
$$\frac{d(H_2)}{dt} = k_2 [Ti(III)] [OH^-]$$

where  $k_2$  is the pseudo 2nd order rate constant. Because the ionic strength was not constant during these measurements no attempt was made to evaluate the pseudo rate constants.

## 2.4 Discussion

The above results have shown that the hydrolysis of titanium(III) takes place in two stages. (i) The formation of soluble titanium hydroxy species when only small amounts of base are added, referred to as primary hydrolysis. (ii) The formation of titanium hydroxide precipitates when further base is added, referred to as secondary hydrolysis. In addition these precipitates, under certain conditions, undergo further auto-oxidation reactions involving the evolution of hydrogen. The hydrolysis of titanium(III) is therefore discussed below in 3 sections: (i) Primary Hydrolysis (ii) Secondary Hydrolysis and (iii) Reactions involving the evolution of hydrogen.

Figure 13. Variation of rate of hydrogen evolution with hydroxide ion concentration for initial reaction.  $[Ti(III)] = 0.0920M$ ,  $[Cl^-] = 0.334M$ .



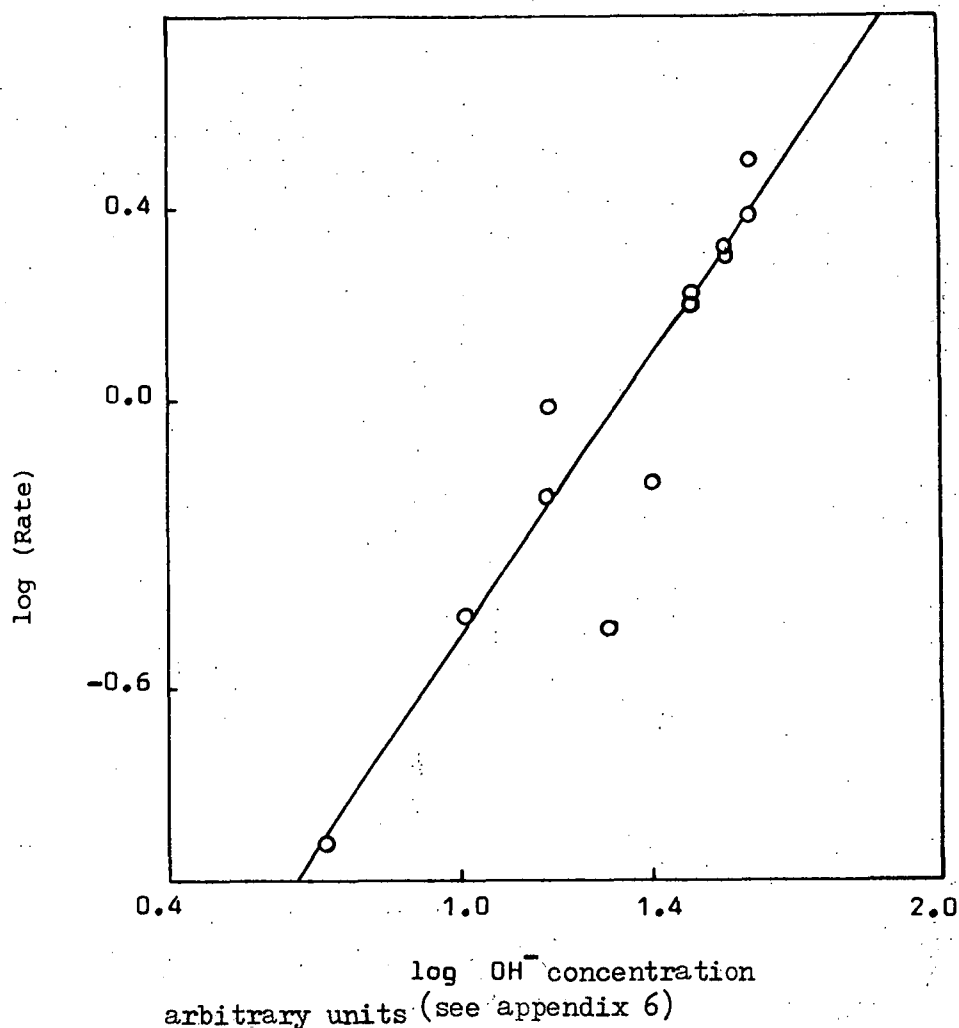


Figure 14.

#### 2.4.1 Primary Hydrolysis

Evidence for the primary hydrolysis reactions has been obtained from pH, spectrophotometric and analytical data.

The pH titration curves Figures (3) and (4) show the formation of a soluble 1:1,  $Ti:OH^-$  complex. The lower pH values obtained for equilibrated solutions as compared with those obtained on rapid mixing could be caused by the following phenomena.

- (i) An oxidation type reaction
- (ii) Slow completion of the hydrolysis reaction
- (iii) Some subsequent co-ordination rearrangement or bridging reaction to form a more stable species.

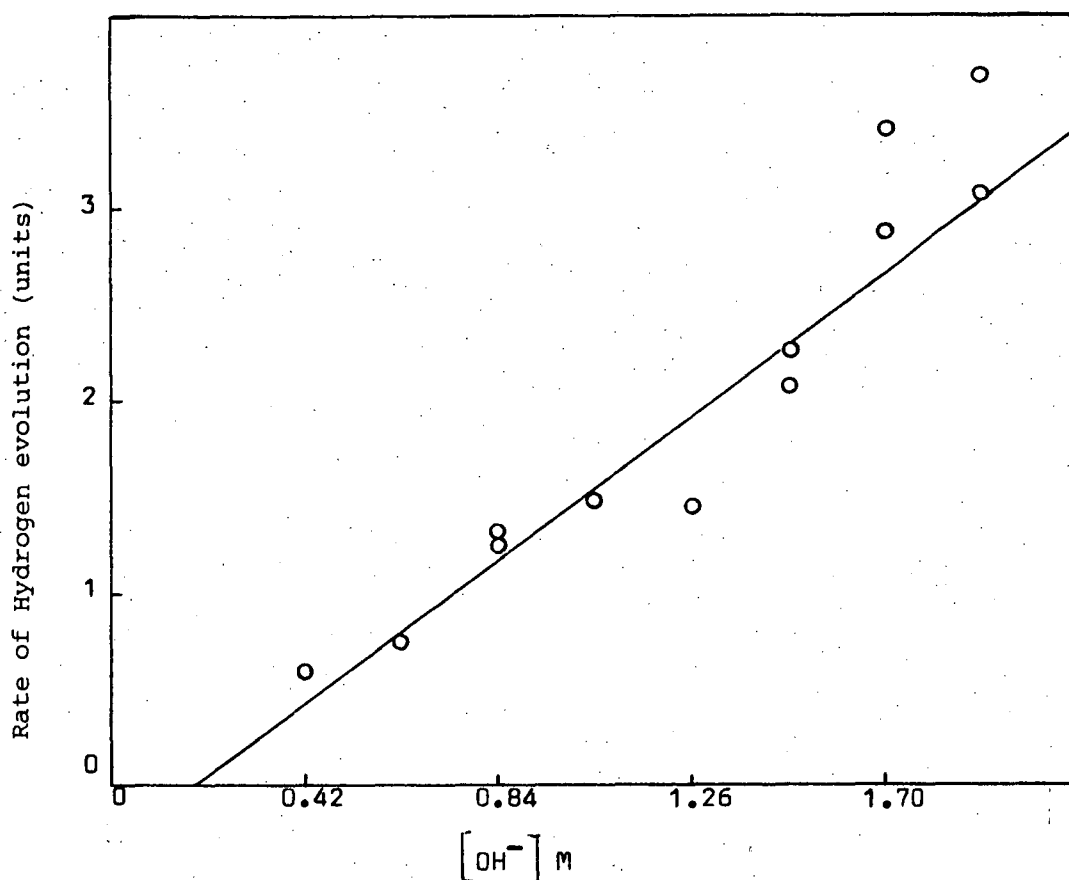


**Figure 15.** Variation of rate of hydrogen evolution with hydroxide ion concentration for second reaction

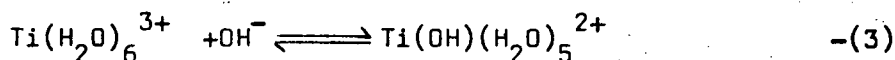
$$[\text{Ti(III)}] = 0.0920\text{M}, [\text{Cl}^-] = 0.334\text{M}.$$

No evidence of oxidation was observed in the primary hydrolysis region. This was confirmed by the analytical data which showed that the titanium(III) content remained unchanged (Figure 9). The possibility of the reaction having not reached completion is also eliminated because the shift in the peak position from 495 nm towards 480 nm (Figure 5) is observed immediately after mixing. The only change in the spectrum on standing is a slight increase in absorbance. This type of behaviour has been observed for other transition metals<sup>23</sup> and it is well known that dimeric species are often formed by the hydrolysis of metal ions<sup>24, 25</sup>.

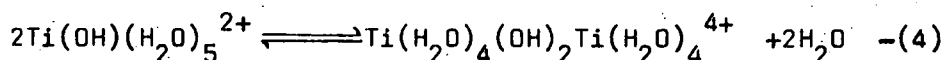
Schaffer and Jorgensen<sup>26</sup>, in their work on binuclear complexes of chromium(III) suggest that the spectra of complexes with central atoms coupled by two hydroxy bridges do not differ greatly from the spectra of mononuclear complexes. The presence of oxygen bridges, however, has been found to influence the spectra quite considerably.

For the titanium(III) solutions, since the dimerisation is accompanied by only a slight increase in band intensity, this suggests the formation of a hydroxy bridged species (i.e.  $\text{Ti}_2(\text{OH})_2(\text{H}_2\text{O})_8^{4+}$ ) rather than an oxy bridged species (i.e.  $\text{Ti}_2\text{O}(\text{H}_2\text{O})_{10}^{4+}$ ).

The potentiometric, spectrophotometric and analytical studies thus suggest that the primary hydrolysis of titanium(III) in dilute chloride solutions involves the formation initially of a monomeric species



followed by dimerisation

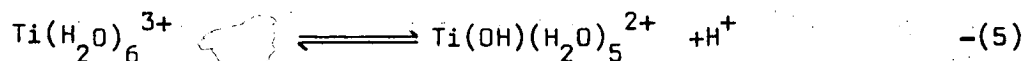


This is in agreement with the conclusions reached by previous workers from limited studies in 3 molar halide solutions<sup>21,22</sup>.

Similar behaviour has been observed in the vanadium(III) system. Pajdowski<sup>23</sup> showed by a spectrophotometric study that the primary hydrolysis involved the formation of both monomeric  $\text{V}(\text{OH})(\text{H}_2\text{O})_5^{2+}$  and dimeric  $\text{V}_2(\text{OH})_2(\text{H}_2\text{O})_8^{4+}$ . The latter species has the higher extinction coefficient. A subsequent magnetic study of the vanadium(III) hydrolysis strongly supported the presence of hydroxy bridges in the dimeric species<sup>27</sup>. Similar behaviour also occurs in the aluminium(III) system as recent <sup>27</sup>Al NMR studies by Akitt et al<sup>28</sup> of the hydrolysis and polymerisation of the  $\text{Al}(\text{H}_2\text{O})_6^{3+}$  cation have shown the positive existence of  $\text{Al}(\text{H}_2\text{O})_6^{3+}$ ,  $\text{Al}(\text{OH})(\text{H}_2\text{O})_5^{2+}$ , and dimeric  $\text{Al}_2(\text{OH})_2(\text{H}_2\text{O})_8^{4+}$ .

The hydrolysis constant  $\beta_1$  for the monomeric species was evaluated using the method outlined below.

For the reaction



$$\beta_1 = \frac{[\text{Ti}(\text{OH})(\text{H}_2\text{O})_5^{2+}][\text{H}^+]}{[\text{Ti}(\text{H}_2\text{O})_6^{3+}]} \quad -(6)$$

If  $\text{Ti}(\text{OH})(\text{H}_2\text{O})_5^{2+}$  is a stable complex, then

$$\beta_1 = \frac{\bar{n}}{(1-\bar{n})} [\text{H}^+] \quad -(7)$$

where  $\bar{n}$  represents the ratio of hydroxyl ion added to titanium(III) ion initially present.

$$\text{i.e.} \quad \log \beta_1 = \log \left( \frac{\bar{n}}{1-\bar{n}} \right) - \text{pH} \quad -(8)$$

Using equation (8) and the potentiometric titration data, the constant for the primary hydrolysis of  $\text{Ti}(\text{H}_2\text{O})_6^{3+}$  was calculated at six equally spaced points in the region  $0 < \bar{n} < 1$  (region (a) in Figure 3) to be  $\log \beta_1 = -2.89 \pm 0.20$  and  $-2.91 \pm 0.20$  on duplicate runs (see Appendix 3). The standard deviation of 0.20 was due to (i) experimental errors associated with very rapid titrations and pH measurements, and (ii) competition from the dimerisation reaction. The ionic strength in region (a) was  $0.41 \pm 0.01\text{M}$ . The effect of the variation of ionic strength on the value of  $\log \beta_1$  is discussed later, but for comparison of hydrolysis data with that for other metals, the ionic strength must be the same. Table 1 compares the present results with those of other metal ions at similar ionic strengths<sup>25</sup>, and shows that titanium(III), vanadium(III) and iron(III) exhibit very similar primary hydrolysis behaviour.

Table 1

Comparison of  $\log \beta_1$  values for the primary hydrolysis in dilute solutions of metals of the first transition series.

Metal	$\log \beta_1$	Ionic Strength	Temperature
Scandium(III)	-4.9	0.1	20
Titanium(III)	-2.9*	0.4	22
Vanadium(III)	-2.9	1.0	20
Chromium(III)	-4.3	0.5	20
Iron(III)	-2.6	0.1	20-22
Cobalt(III)	-1.8	1.0	24

\*This work.

Some workers report stability constants i.e.  $\log K_1$  values, for the hydrolysis species. However this is less practical as it requires knowing accurately the  $pK_w$  value for the solution under the hydrolysis conditions. For the reaction  $\text{Ti}(\text{H}_2\text{O})_6^{3+} + \text{OH}^- \rightleftharpoons \text{Ti}(\text{OH})(\text{H}_2\text{O})_5^{2+}$  -(9)

$$K_1 = \frac{[\text{Ti}(\text{OH})(\text{H}_2\text{O})_5^{2+}]}{[\text{Ti}(\text{H}_2\text{O})_6^{3+}][\text{OH}^-]} \quad -(10)$$

$$\text{and } \log K_1 = pK_w + \log \beta_1 \quad -(11)$$

From published data<sup>29,30</sup>  $pK_w$  was calculated to be 14.38 in 0.41M NaCl at 22°C (see Appendix 8). Thus, from equation (11)  $\log K_1$  equals  $11.48 \pm 0.20$  at 22°C.

The extent of dimerisation can be gauged from the change of pH with time. An example of this is shown in Figure 16. The curve implies that for this solution approximately 25% dimerisation has occurred after 20 minutes. The hydrolysis data reported by Pecsok and Fletcher<sup>20</sup>



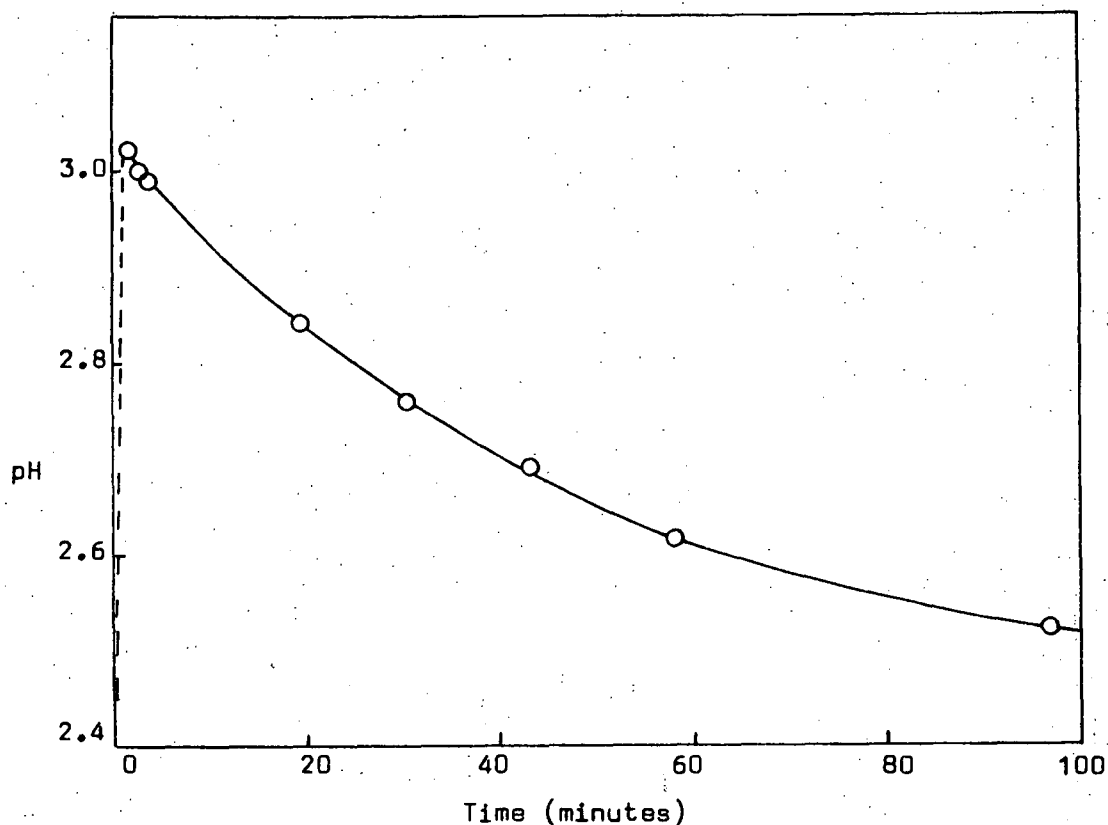


**Figure 16.** Change of pH with time for a solution  $\bar{n} = 0.64$   
 $[Tl(III)] = 0.078M$  ,  $[Cl^-] = 0.4M$ .

were obtained from measurements made over a period of 20-30 minutes.

Obviously significant dimerisation would have occurred during this time.

This would explain the higher  $K_1$  values which they report (e.g.  $\log K_1 = 11.80$  in 0.50 KBr at 25°C).

As the chloride ion concentration was increased up to 5M no significant change in the shape of the rapid titration curve was observed (see Appendix 3). Using the theory outlined by equations (5) to (8),  $\log \beta$  values were calculated (see Appendix 3) at these higher chloride ion concentrations and the results are compared in Figure 17. The hydrolysis

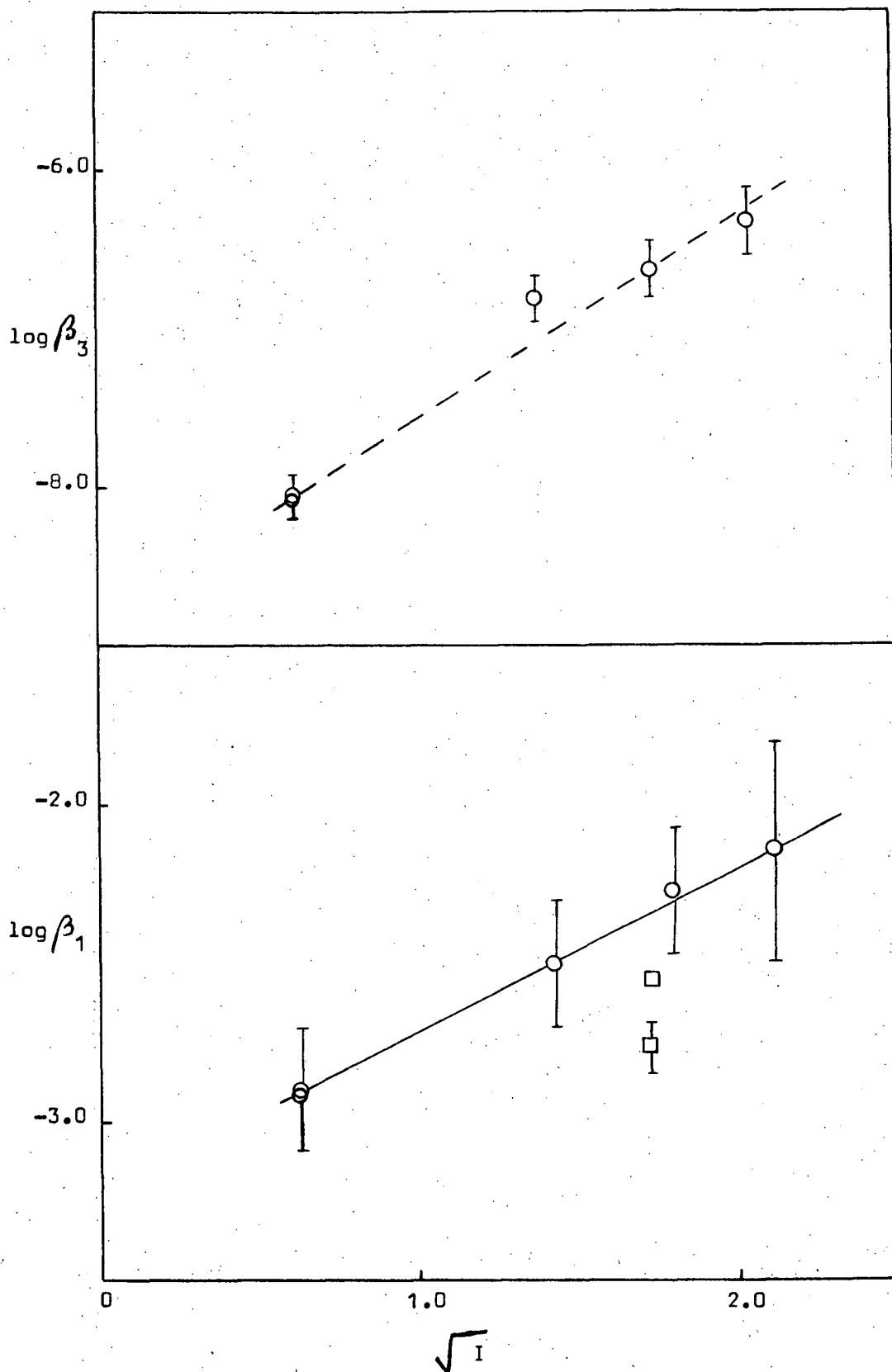


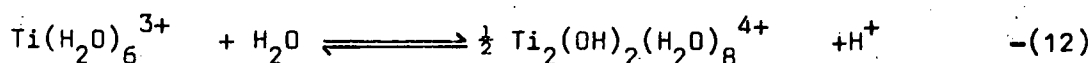
**Figure 17.** Effect of chloride ion concentration on the primary and secondary hydrolysis constants ( $I$  = total chloride ion concentration).

$\square$  = Paris and Gregoire<sup>21</sup> (using bromide ion),  $\Phi$  = Krentzien and Brito<sup>22</sup>,  $\circ$  = this work.

constant values for the monohydroxy species increase with increasing chloride ion concentrations as a result of the increasing ionic strength. Thus the behaviour appears to obey simple Debye-Hückel theory, since under these conditions activity coefficients also increase with increasing ionic strength.

This behaviour also suggests that titanium(III) chloro complexes formed in these solutions have relatively low stability (which is in agreement with reported stability data<sup>7</sup>), as if this were not so, competition from chloride ion to form chloro species would tend to cause a decrease in the stability of the hydroxy species as the chloride ion concentration increased. Other studies of the primary hydrolysis of titanium in 3M KCl<sup>22</sup> and 3M KBr<sup>21</sup> have been reported and these results are also compared in Figure 17.

By using the equilibrium pH data it was also possible to calculate the hydrolysis constant for the dimeric species. For the reaction



$$\beta_{12} = \frac{[\text{Ti}_2(\text{OH})_2(\text{H}_2\text{O})_8^{4+}]^{\frac{1}{2}} [\text{H}^+]}{[\text{Ti}(\text{H}_2\text{O})_6^{3+}] [\text{H}_2\text{O}]} \quad -(13)$$

$$= \frac{\left(\frac{\bar{n}}{2} [\text{Ti(III)}]\right)^{\frac{1}{2}} [\text{H}^+]}{(1-\bar{n}) [\text{Ti(III)}]} \quad \text{for a stable complex} \quad -(14)$$

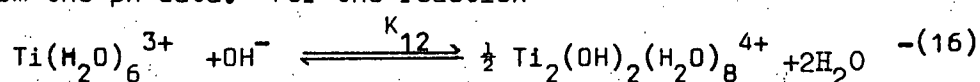
$$\therefore \log \beta_{12} = \frac{1}{2} \log \frac{\bar{n}}{2} - \text{pH} - \log (1-\bar{n}) - \frac{1}{2} \log [\text{Ti(III)}] \quad -(15)$$

Using equation (15) and data as in Figure 4,  $\log \beta_{12}$  values calculated at four points in the region  $0 < \bar{n} < 1$  gave a mean of -1.64 and a standard deviation of 0.04 (ionic strength constant at 0.352M) (see Appendix 4). Other workers report  $\log \beta_{12}$  values at 25°C of -1.65 and  $-1.95 \pm 0.17$  in 3M KBr<sup>21</sup> and 3M KCl<sup>22</sup> respectively.

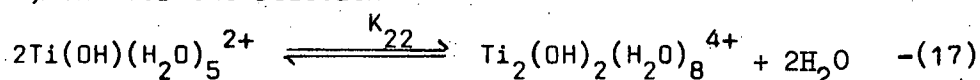
At low chloride ion concentrations e.g. 0.35M, negligible secondary hydrolysis occurs in the primary hydrolysis region i.e.  $\bar{n} < 1$ .

However, as the chloride ion concentration is increased the amount of secondary hydrolysis occurring in the lower pH region also increases until at very high chloride ion concentrations ( $\sim 9$  molar) no primary hydrolysis is observed in the equilibrated solutions. This is discussed in more detail in the next section. For this reason no attempts were made to calculate  $\beta_{12}$  values at higher chloride ion concentrations.

The stability constant  $K_{12}$  for the dimeric species, and the dimerisation constant  $K_{22}$ , at low chloride ion concentrations were calculated from the pH data. For the reaction



$\log K_{12}$  was calculated to be  $12.74 \pm 0.04$  at  $22^\circ\text{C}$  (ionic strength 0.35M) (see Appendix 9) and for the reaction



$\log K_{22}$  was calculated to be  $2.52 \pm 0.24$  (see Appendix 9). The comparative stability of the mononuclear and binuclear primary hydrolysis species for some metals of the first transition series<sup>25</sup> can be gauged from the  $\log K_{22}$  values given in Table 2.

Table 2

Metal	$\log K_{22}$	Ionic Strength	Temperature $^\circ\text{C}$
Scandium(III)	3.9	0.5	25
Titanium(III)	2.5 *	0.4	22
Vanadium(III)	1.8	1.0	20
Chromium(III)	5.3	1.0	25
Iron(III)	2.6	1.0	20

\* This work.

### 2.4.2 Secondary Hydrolysis

From the results section it can be seen that three secondary hydrolysis products are formed, namely brown, black, and blue precipitates. Under certain conditions the brown species changes to black then blue on standing. Thus time is an important variable. As the behaviour is also affected by the chloride ion concentration it too has to be considered. In this section the behaviour at very low chloride ion concentrations is discussed first. Then the effect of increasing the chloride ion concentration up to a very high value (about 9M) is compared.

Information about the brown species was obtained from the rapid titration data. The rapid potentiometric titration curve (Figure 3) shows the uptake of another two equivalents of  $\text{OH}^-$  in the pH range 3.8 to 5.7. It is in this region that a brown precipitate is formed. This corresponds to the reaction

$$2\text{H}^+ + 2\text{OH}^- \rightleftharpoons 2\text{H}_2\text{O}$$

and

$$\text{Ti}(\text{OH})(\text{H}_2\text{O})_5^{2+} \rightleftharpoons \text{Ti}(\text{OH})_3 (\text{s}) + 2\text{H}^+ + 3\text{H}_2\text{O} \quad \text{---(18)}$$

The hydrolysis constant  $\beta_3$  for this reaction was evaluated from the pH data as

$$\beta_3 = \frac{[\text{H}^+]^2}{[\text{Ti}(\text{OH})(\text{H}_2\text{O})_5^{2+}]} \quad \text{---(19)}$$

$$\text{i.e. } \log \beta_3 = -\log [\text{Ti}(\text{OH})(\text{H}_2\text{O})_5^{2+}] - 2\text{pH} \quad \text{---(20)}$$

since  $\text{Ti}(\text{OH})(\text{H}_2\text{O})_5^{2+}$  is a stable complex,

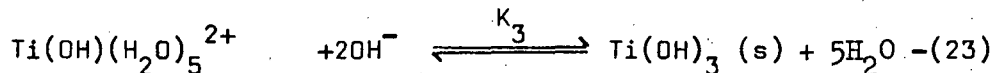
$$[\text{Ti}(\text{OH})(\text{H}_2\text{O})_5^{2+}] = (1-\bar{m}) [\text{Ti(III)}] \quad \text{---(21)}$$

where  $\bar{m}$  is the fraction of titanium(III) precipitated, i.e. the ratio of  $2\text{OH}^-$  added to the titanium(III) ion initially present ( $[\text{Ti(III)}]$ ).

$$\text{i.e. } \log \beta_3 = -\log (1-\bar{m}) [\text{Ti(III)}] - 2\text{pH} \quad \text{---(22)}$$

Using equation (22),  $\log \beta_3$  values calculated at twelve equally spaced points in region (b) gave mean  $\log \beta_3$  values of -8.02 and -8.07 with a standard deviation of 0.08, on duplicate runs (see Appendix 3). The ionic strength in region (b) was  $0.385 \pm 0.012\text{M}$ .

The solubility product value for the brown precipitate was also determined from the pH data. i.e. For the reaction



$\log K_3$  was calculated to be  $20.71 \pm 0.08$ . Thus for the insoluble brown precipitate  $\text{Ti(OH)}_3$   $\log K_{sp} = -32.19 \pm 0.28$  (see Appendix 9).

As no study of the complete hydrolysis of titanium(III) has been reported previously no solubility product data for titanium(III) hydroxide <sup>are</sup> available for comparison. However  $\log K_{sp}$  values for other trivalent transition metal hydroxides<sup>25</sup> are shown in Table 3.

Table 3

Metal	$\log K_{sp}$	Ionic Strength	Temperature
Scandium(III)	-29.7	0	25
Titanium(III)	-32.2*	0.5	22
Vanadium(III)	-34.4	0	25
Chromium(III)	-30.2	0	22
Iron(III)	-38.6	0	25
Cobalt(III)	-40.5	0	25

\* This work.

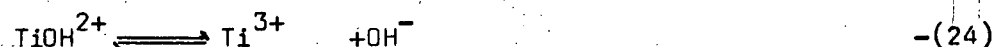
Thus titanium(III) hydroxide has a similar solubility product to other transition metal hydroxides.

$\log \beta_3$  values obtained from titration data for solutions containing higher chloride ion concentrations (see Appendix 3) are compared in Figure 17.

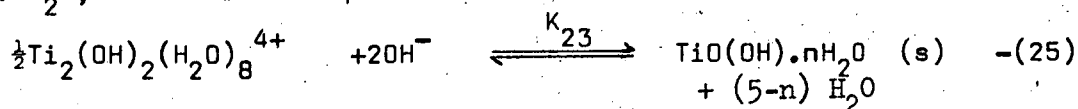
The equilibrium potentiometric titration curve (Figure 4) compared with the rapid titration curve (Figure 3) shows the significant changes in pH which occur on standing. Further information on this unusual hydrolysis behaviour was obtained by analytical studies. The variation of

titanium(III) present in solution after the addition of varying amounts of sodium hydroxide to solutions containing 0.0906M Ti(III) and 0.352M  $\text{Cl}^-$  and allowing them to equilibrate, is shown in Figure 9. The titanium(III) content remains constant until precipitation begins at  $\bar{n} = 1.0$ . After this titanium(III) is removed from solution at the rate of 1.00 Ti per 2.00  $\text{OH}^-$  added, by the formation of brown solid  $\text{Ti}(\text{OH})_3$  (region(a) in Figure 9) until  $\bar{n} \approx 1.5$ .

On standing, the brown precipitate darkens becoming black but no hydrogen evolution is observed, so that it is unlikely that the precipitate contains any titanium in the +4 oxidation state. Instead this darkening is probably associated with the replacement of hydroxide groups by oxide ions. Also in this region after equilibration, the pH values decrease with increasing addition of  $\text{OH}^-$ . If it is argued that in the primary hydrolysis region  $\text{OH}^-$  ions are supplied by the reaction



then in the region  $1.0 < \bar{n} < 1.5$ , as the black insoluble species is formed from the  $\text{TiOH}^{2+}$  ions, it reduces the concentration of this latter ion, consequently reducing the equilibrium concentration of  $\text{OH}^-$  ions and thus the pH. The minimum in the pH curve occurs at  $\bar{n} = 1.5$ , the pH then being 2.30. If as seems likely, the black insoluble compound is the oxy-hydroxy species  $\text{TiO}(\text{OH}) \cdot n\text{H}_2\text{O}$ , then for the equilibrium



$$K_{23} = \frac{1}{[\text{Ti}_2(\text{OH})_2(\text{H}_2\text{O})_8^{4+}]^{\frac{1}{2}} [\text{OH}^-]^2} \quad -(26)$$

$$\therefore \log K_{23} = 2\text{pOH} - \frac{1}{2} \log [\text{Ti}_2(\text{OH})_2(\text{H}_2\text{O})_8^{4+}] \quad -(27)$$

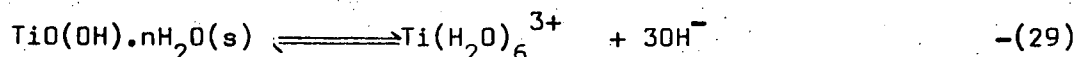
After the addition of 1.5 equivalents of  $\text{OH}^-$ , 0.75 equivalents of  $\text{Ti}_2(\text{OH})_2(\text{H}_2\text{O})_8^{4+}$  remain (0.25 equivalents being precipitated as the hydrated oxide) and

$$[\text{Ti}_2(\text{OH})_2(\text{H}_2\text{O})_8^{4+}] = \frac{0.75}{2} [\text{Ti(III)}] \quad -(28)$$

giving from equation(27), ( $pK_w = 14.38$ ),  $\log K_{23} = 24.89$  (see also Appendix 4).

Since this value was calculated at the minimum in the pH curve, the actual value is  $\log K_{23} \gg 24.89$ .

Therefore, for the equilibrium

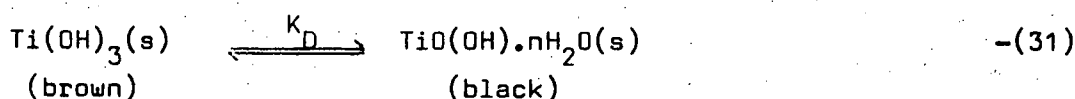


from equations (26) and (16)

$$\log K_{sp} = -\log K_{23} - \log K_{12} \quad -(30)$$

$$\text{i.e. } \log K_{sp} \gg -37.63$$

Also, for the equilibrium



$$\log K_D = \log K_{sp_{\text{brown}}} - \log K_{sp_{\text{black}}} \quad -(32)$$

$$\text{i.e. } \log K_D \gg 5.44$$

The black precipitate was very readily oxidised and extreme care was necessary to eliminate contamination from oxygen. The stability of this precipitate was also very sensitive to chloride ion concentration and as a result it was only present in equilibrated solutions when minimum chloride ion concentrations were used. Otherwise oxidation to the dark blue soluble species discussed below tended to occur.

In region(b) (of Figure 9) the precipitate which forms initially is brown, but this turns black within a few minutes. However, on standing hydrogen is evolved and the additional precipitate which would normally be expected, appears to redissolve to give a dark blue solution. This reaction is completed in about 20 hours. (Note: the amount of precipitate formed in part(a) (see Figure 9) does not appear to increase during the further reaction in region(b).) Because a soluble species is formed, the loss of titanium(III) in this region must be due to oxidation to titanium(IV). The ratio of titanium(IV) formed to  $[\text{OH}^-]$  is 0.5045:2.0000. As the overall change in stoichiometry corresponds to  $\text{Ti(OH)}^{2+} \longrightarrow \text{Ti(OH)}_3$ , this suggests that one



in every two titanium ions which react with hydroxide ions is also oxidised to the +4 oxidation state. That is, the dark blue species contains Ti(III) and Ti(IV) in the ratio 1:1. When aliquots of the dark blue solution are added to 5M HCl solution, a white turbidity forms, confirming the presence of Ti(IV).

The dark blue species is quite stable in solution and no further hydrogen evolution is observed on standing. Absorbance data at 740 nm from a series of solutions gave an extinction coefficient in the order of 500 moles<sup>-1</sup> litres cm<sup>-1</sup> (see Appendix 10) so that the complex probably corresponds to the polynuclear species observed by Pecsok and Fletcher<sup>20</sup>. An example of the solution spectrum is shown in Figure 18. The high extinction coefficient of this complex would seem to be indicative of a mixed oxidation state complex.

In region(c) (of Figure 9) the dark blue species had coagulated and settled as a colloidal gel like precipitate. The rate of removal of titanium(III) confirmed that the stoichiometry outlined by equation(23) was still being obeyed. This salting out effect is typical of the behaviour of the colloidal precipitates often formed by hydrated metal oxide or hydroxide species.

No mixed oxidation state titanium hydrolysis product appears to have been positively identified prior to this work although, Hartmann and Schlafer<sup>5</sup> in 1951 speculated that the dark blue precipitate formed by the addition of base to titanium(III) solutions might be a mixed oxidation state compound.

Investigation of the nature of the brown and black titanium(III) hydroxide precipitates is very difficult because of their extreme sensitivity to aerial oxidation and auto-oxidation, and their colloidal properties. In the similar iron(III) system, which does not have the same oxidation problems, despite innumerable studies of precipitation in hydrolysed iron(III) solutions very little is known about the relationship between hydrolysis products in solution and the mechanism by which a solid phase is produced<sup>31</sup>. However it seems likely that the formation of a solid phase initially involves elimination of co-ordinated water from the iron atoms together with further

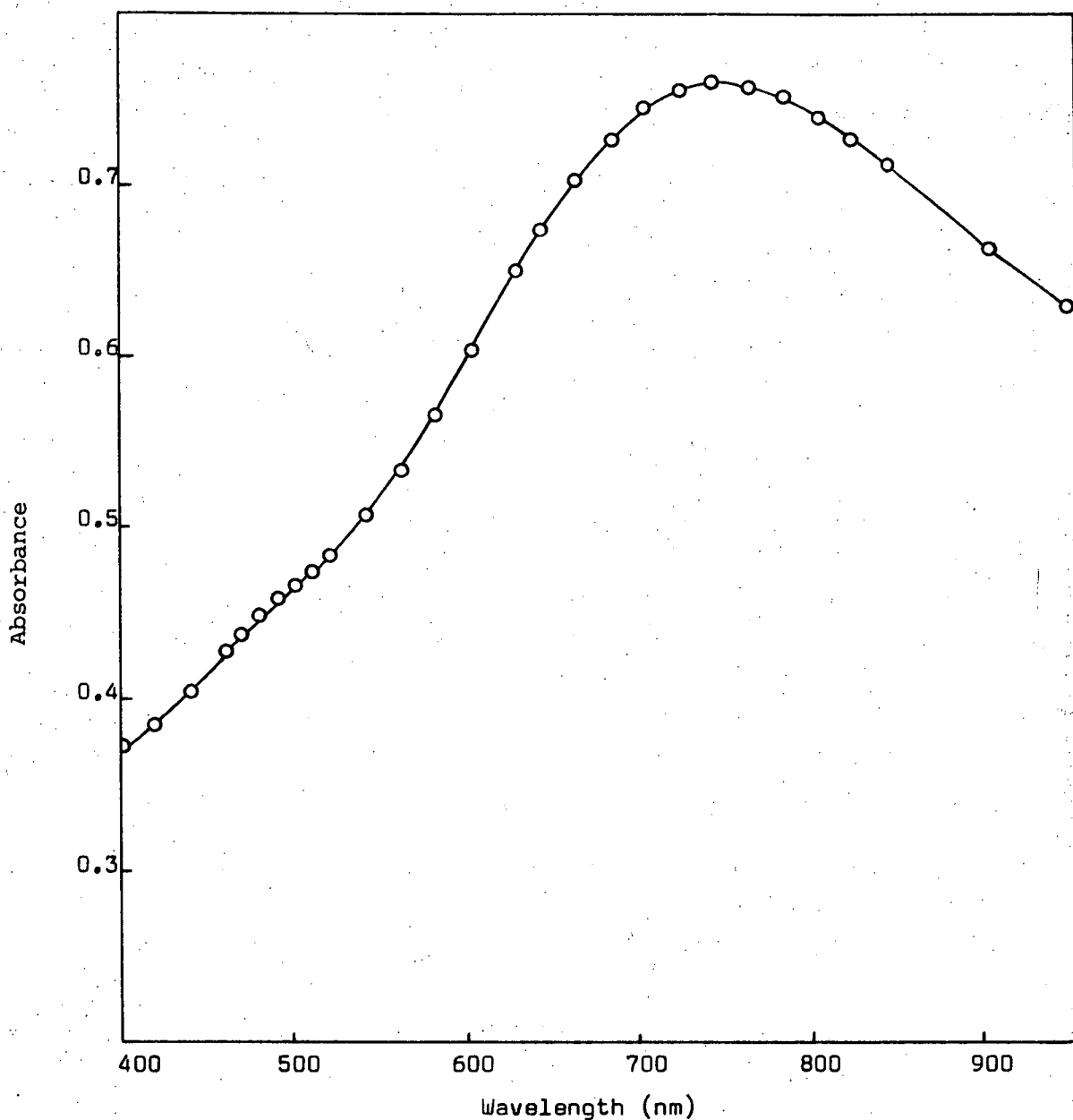


**Figure 18.** Spectrum of the dark blue 1:1 mixed oxidation state species in equilibrium with  $\text{Ti}_2(\text{OH})_2(\text{H}_2\text{O})_8^{4+}$ , using 0.1 cm cells. Fraction of titanium estimated present as dark blue species is 0.16. Total titanium concentration in solution is 0.0950M, and chloride ion 0.364M. The absorbance due to  $\text{Ti}_2(\text{OH})_2(\text{H}_2\text{O})_8^{4+}$  at 740 nm is estimated to be 0.065.

oxolation reactions. Atkinson et al<sup>32</sup> proposed that the hydrolysis proceeds by progressive elimination of  $H^+$  from  $Fe(H_2O)_6^{3+}$ , followed by formation of polymeric species with oxo and hydroxo linkages. Studies of the ageing behaviour of iron(III) hydrolysis products show that if iron(III) is initially precipitated under rapid conditions i.e. using excess base, as iron(III) hydroxide gel, then the ageing of this precipitate produces, depending on the other ions present, ( $\alpha$ ,  $\beta$ , or  $\gamma$ )  $FeO(OH)^{31,32}$ . Analytical studies of iron(III) hydroxide sols by Spiro et al<sup>33</sup> showed that they contain predominantly hydroxyl bridging. In the gallium(III) system which has also been extensively studied<sup>34</sup>,  $Ga(OH)_3$  is precipitated initially by the action of bases on gallium salts. On standing the precipitate ages forming  $GaO(OH)$ . Similar aluminium hydroxides are also known;  $\alpha$ - $Al(OH)_3$  Bayerite,  $\gamma$ - $Al(OH)_3$  Hydrargillite and  $\chi$ - $AlO(OH)$  Boehmite, and the position of the protons in these compounds has been derived from Proton Magnetic Resonance studies<sup>35</sup>.

The change from brown to black in the titanium(III) hydroxide system is a similar ageing process; and by comparison with the more studied iron(III), gallium(III) and aluminium(III) systems it seems reasonable to propose that the brown precipitate is an hydroxy bridged polymeric species represented by the formula  $Ti(OH)_3 \cdot nH_2O$ , and that the black precipitate is  $TiO(OH) \cdot nH_2O$ .

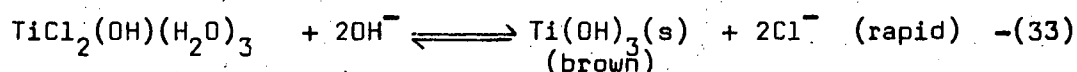
It is known that at very high chloride ion concentrations (greater than about 8 molar) titanium(III) chloro complexes predominate in solution<sup>7,9</sup> and it is interesting to compare the different equilibrium hydrolysis behaviour in these solutions. Using  $LiCl$ , chloride ion concentrations of about 9 molar could be obtained readily, however under these conditions accurate pH measurements could not be made<sup>36-38</sup>. Consequently this section of the work is mainly qualitative and based on spectral and analytical data.

Spectral studies of solutions containing titanium(III), (0.088M) and chloride ion, (8.80M) showed that the observed spectrum ( $\lambda_{max} = 550 \text{ nm}$ , see Figure 7) is very similar to that observed by Schlafer

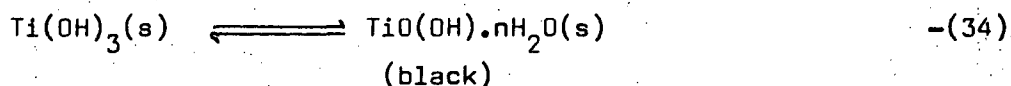
and Fritz<sup>12</sup> for solid trans -  $[\text{TiCl}_2(\text{H}_2\text{O})_4] \text{Cl} \cdot 2\text{H}_2\text{O}$  ( $\lambda_{\text{max}} = 545 \text{ nm}$ ). When base is first added to the violet solutions of  $\text{TiCl}_2(\text{H}_2\text{O})_4^+$  such that  $0 < \bar{n} < 1$ , the color becomes darker. This suggests the formation of the chloro primary hydrolysis species  $\text{TiCl}_2\text{OH}(\text{H}_2\text{O})_3$  which probably dimerises rapidly. The solutions quickly become turbid, precluding spectral studies of the chloro hydrolysis species. When base is first added to the original violet  $\text{TiCl}_2(\text{H}_2\text{O})_4^+$  solutions such that  $1 < \bar{n} < 3$  a brown precipitate is formed which rapidly darkens. In both regions the precipitates are slowly oxidised to a dark blue species, hydrogen being evolved simultaneously. The final result is the formation of a dark blue precipitate in solutions over the range  $0 < \bar{n} < 3$ , with the unhydrolysed  $\text{TiCl}_2(\text{H}_2\text{O})_4^+$  species remaining in solution above the precipitate (see spectra Figure 7). The variation of the absorbance of the solutions at 550 nm, as base is added is shown in Figure 8. No change in absorbance is observed until precipitation occurs. Then the value jumps sharply due to scattering of the light by a small amount of the precipitate remaining suspended in the solution as colloidal particles. However, overall the absorbance decreased uniformly towards zero as the number of hydroxyl ions added tended towards 3. The variation of the titanium(III) content of these equilibrated solutions is shown in Figure 10. The slope of this curve also corresponds to titanium being removed as the dark blue precipitate at the rate of 1.00 Ti(III) per 3.00  $\text{OH}^-$  added and confirmed that complete precipitation of the titanium occurs.

Thus in equilibrated concentrated chloride solutions, secondary hydrolysis probably results from the following reactions

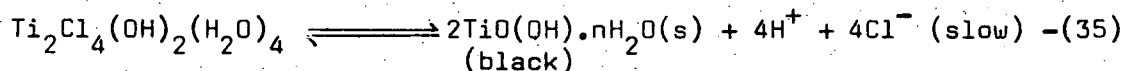
(i) Addition of excess base



and subsequently



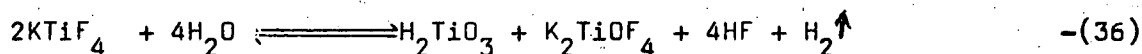
(ii) Slow hydrolysis of a dimeric chloro primary hydrolysis species e.g.



(iii) Auto oxidation of the black precipitate to form the dark blue mixed oxidation state species which settles as a gel like precipitate at these high chloride ion concentrations.

#### 2.4.3 Reactions involving the evolution of hydrogen.

The evolution of a gas from solutions containing titanium(III) hydroxide precipitates is an unusual phenomenon. The gas was observed to cause a lighted match to explode, establishing that it was hydrogen being evolved. Spontaneous hydrogen evolution from a metal hydroxide in solution is relatively rare and only associated with low oxidation states of transition type metals. Titanium(III) hydroxide had been known to undergo this type of behaviour for some time<sup>39</sup> but no detailed study of the reaction appears to have been made previously. Hydrogen evolution also occurs in some titanium(III) - fluoride systems. The very slow evolution of hydrogen from titanium(III) fluoride solutions in hydrofluoric acid has been reported<sup>14</sup> and  $\text{KTiF}_4$  is oxidised by water with the evolution of hydrogen<sup>18</sup> according to the reaction

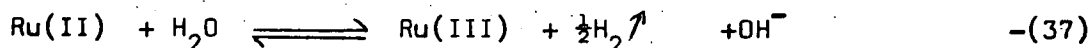


The only other well known case of hydrogen evolution involving a metal in solution in the trivalent state is that of uranium(III). If a red hydrochloric acid solution of uranium(III) chloro complexes is added to aqueous ammonia, a pale orange-red precipitate of  $\text{U}(\text{OH})_3$  is observed which subsequently changes to pale green  $\text{U}(\text{OH})_4$  with the evolution of hydrogen<sup>40-42</sup>.

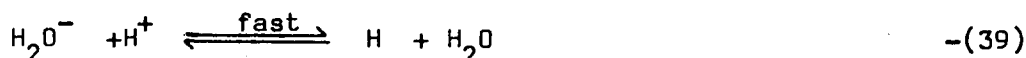
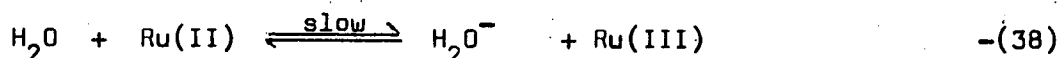
Several metals in the divalent state liberate hydrogen from solution.  $\text{TiCl}_2$  when dissolved in water liberates hydrogen<sup>9</sup> and  $\text{V}(\text{H}_2\text{O})_6^{2+}$  similarly liberates hydrogen but not in acid solution<sup>9,43</sup>. Chromium(II) ions are also unstable in aqueous solution and evolve hydrogen at rates varying with acidity and the anions present<sup>44,45</sup>.

Few studies of the kinetics and mechanisms for these types of hydrogen evolution reactions have been made. The kinetics of the oxidation

of ruthenium(II) in 2.5M KCl (pH 1.5, 30°C) by water has been studied by Rechnitz and Catherino<sup>46</sup>. No pH effect was observed in the pH range 0.5 to 1.5, and the reaction was also independent of chloride ion concentration in the range 1-4 molar. From the evidence it was concluded that water itself acts as the oxidising agent, the overall reaction being

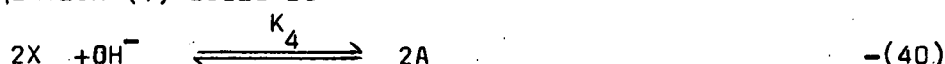


The mechanism proposed was



i.e. a 1st order rate was observed. The ruthenium case is therefore quite different from that for titanium where a strong dependence on  $\text{OH}^-$  concentration was observed.

For the titanium(III) system the dependence of the rate of hydrogen evolution on the hydroxide ion concentration was different for the brown and black hydroxide precipitates. A simple reaction mechanism suggested by equation (1) would be

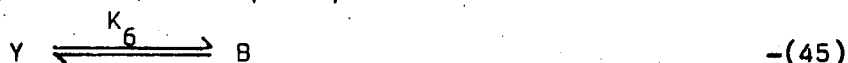


$$\text{thus rate} = k_3 [\text{A}] [\text{OH}^-] \quad -(42)$$

$$[\text{A}] = K_4^{\frac{1}{2}} [\text{OH}^-]^{\frac{1}{2}} [\text{X}] \quad -(43)$$

$$\therefore \frac{d(\text{H}_2)}{dt} = k_3 K_4^{\frac{1}{2}} [\text{X}] [\text{OH}^-]^{\frac{3}{2}} \quad -(44)$$

and from equation (2) for the black precipitate would be



$$\text{thus rate} = k_5 [\text{B}] [\text{OH}^-] \quad -(47)$$

$$[\text{B}] = K_6 [\text{Y}] \quad -(48)$$

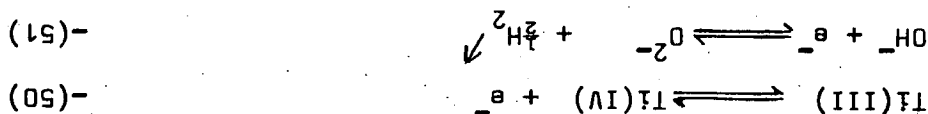
$$\therefore \frac{d(\text{H}_2)}{dt} = k_5 K_6 [\text{Y}] [\text{OH}^-] \quad -(49)$$

with both reaction systems connected by a slow equilibrium of the type

$\text{X} \rightleftharpoons \text{Y}$  where X and Y are the initial titanium(III) species, i.e.

brown  $Ti(OH)_3 \cdot nH_2O$  and black  $Ti(OH)_3 \cdot nH_2O$ , and A and B are intermediate species. However because of the complex solution chemistry involved, the number and nature of intermediate species in the reactions is not known. This would require an extensive kinetic study, which is outside the scope of this work.

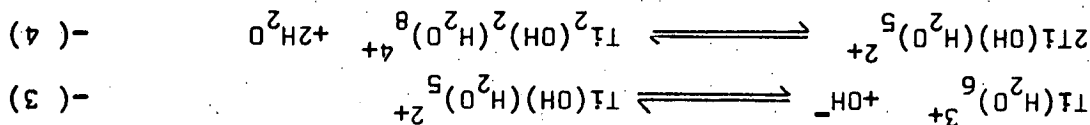
The redox equilibria involved are summarised by the equations



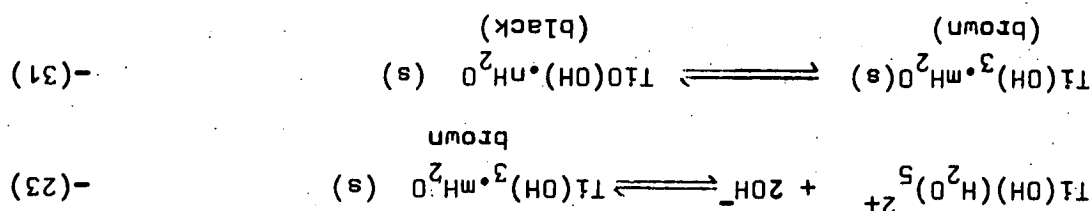
i.e. the evolution of hydrogen results from the reduction of hydroxyl groups. This is the first time that behaviour of this type has been studied.

## 2.5 Conclusion

The investigation carried out in this work has given for the first time an understanding of the complete hydrolysis of the hexaquotitanium(III) ion. It has been shown that the hydrolysis consists of two steps. The formation of a soluble primary hydrolysis species which dimerises on standing



and the formation of an insoluble secondary hydrolysis species, if more base is added, which also subsequently dimerises on standing.



Consequently the nature of the brown and black titanium(III) "hydroxide" precipitates can now be understood for the first time. Evidence has been presented to show that the dark blue "hydroxide" precipitate obtained is a mixed oxidation state species containing equal amounts of titanium(III) and titanium(IV). This latter species is formed at certain hydroxide ion concentrations by the auto oxidation of either the brown or the black precipitates.

At high chloride ion concentrations the formation of titanium(III) chloro-aquo species tends to promote the dimerisation reactions, the auto oxidation reactions and the formation of the secondary hydrolysis species. Thus the effect of chloride ion concentration on the hydrolysis behaviour would seem to support the suggestion of Glebov<sup>47</sup> that the replacement of water molecules by chloride ions in the co-ordination sphere of titanium(III) increases the rate of exchange of the molecules in the hydration shell of the titanium ion.

The studies of the rate of evolution of hydrogen which takes place during the auto-oxidation of the brown and black precipitates, appear to be the first studies of this type carried out for the titanium(III) system and have suggested that the actual species reduced is hydroxide ion. It has also been noted with interest that, if excess base is not present, this oxidation process stops once the composition of the 1:1 titanium(III) titanium(IV) mixed oxidation state species is reached. This emphasises the importance of mixed valence compounds in titanium chemistry.



## CHAPTER 3

### Titanium(III) thiocyanate complexes in aqueous media

#### 3.1 Introduction

Several studies of complex formation between the thiocyanate ion and titanium(III) in aqueous solution have been made<sup>3,40,48-51</sup>. However these have been limited in extent and the reported data appear to contain some inconsistencies. For example, Jorgensen<sup>40</sup> suggests that a 1:3 Ti(III) : NCS<sup>-</sup> species is formed in solution, while from a similar solution Sutton<sup>52</sup> isolated a 1:4 complex. Van der Pfordten<sup>53</sup> reports the preparation of a 1:6 compound but more recent work has been unable to confirm this<sup>52</sup>. Several workers have proposed the formation of a 1:1 complex in solution<sup>3,49-51</sup> but no direct evidence has yet been presented. Consequently the titanium(III) thiocyanate system in aqueous solution is still not clearly understood.

In this chapter, results of a new investigation of complex formation in aqueous solution over the thiocyanate ion concentration range 0-7 molar are presented. These results enable discrepancies in the literature to be explained. Direct evidence confirming the formation of the previously reported 1:1  $\text{Ti}(\text{NCS})(\text{H}_2\text{O})_5^{2+}$  species has been obtained. The existence of a 1:4 complex  $\text{Ti}(\text{NCS})_4(\text{H}_2\text{O})_2^-$  in solution has been demonstrated and its formation constant estimated. No study of the actual bonding between the thiocyanate ligand and titanium(III) has been made in this work. However a comprehensive infra-red study of vanadium(III) thiocyanates by Bohland and Malitzke<sup>54</sup> has established that the thiocyanate is bonded to the vanadium via nitrogen rather than sulphur and it is assumed from this evidence that the anions in the titanium thiocyanate complexes are also N-bonded.

The oxidation of titanium(III) thiocyanate solutions in air has also been studied and evidence is presented for the formation of a new 1:1 Ti(III) : Ti(IV) mixed oxidation state species.

### 3.2 Experimental

The studies involved conductometric and spectral measurements of titanium(III) - thiocyanate solutions.

Conductometric measurements were used to determine the metal: ligand ratios of the complexes formed in solution. A conductance cell of similar design to that used by Jones and Bollinger<sup>55</sup> was constructed of pyrex glass. Platinum disc electrodes 0.80 cm diameter were used, the separation distance being 25.50 cm. This cell gave relatively high resistance values for the solutions (300-600 ohms) which resulted in good sensitivity being obtained for the measurements. The resistance values were obtained using an A.C. conductance bridge described by Leong<sup>56</sup>. By using an A.C. technique, polarisation errors were minimised. The basic circuit was essentially a modified Wheatstone Bridge (see Figure 19). The ratio arms  $R_3$  and  $R_4$  were kept equal at 100.00 ohms each and the measuring arm  $R_2$  was a separate resistance box, capable of having resistance values between 0.02 and 10000 ohms. Resistance changes of 0.1 ohm were detectable. Conductance measurements were made on a series of carefully prepared solutions. Each solution contained a fixed quantity of titanium(III) in dilute hydrochloric acid and varying amounts of ammonium thiocyanate. The solutions were made to constant volume and allowed to equilibrate to constant temperature.

Spectrophotometric measurements of the titanium(III)-thiocyanate solutions were made to obtain information about the nature of the complexes formed in solution and also to provide data for estimating the formation constants of the various species. Series of individual solutions each containing a fixed quantity of titanium(III) with varying amounts of thiocyanate ion were prepared for different ranges of thiocyanate ion concentrations. Absorbance measurements over a range of wavelength values were made on each solution.

It was necessary to take precautions against aerial oxidation of titanium(III) and all solutions were presaturated with nitrogen.

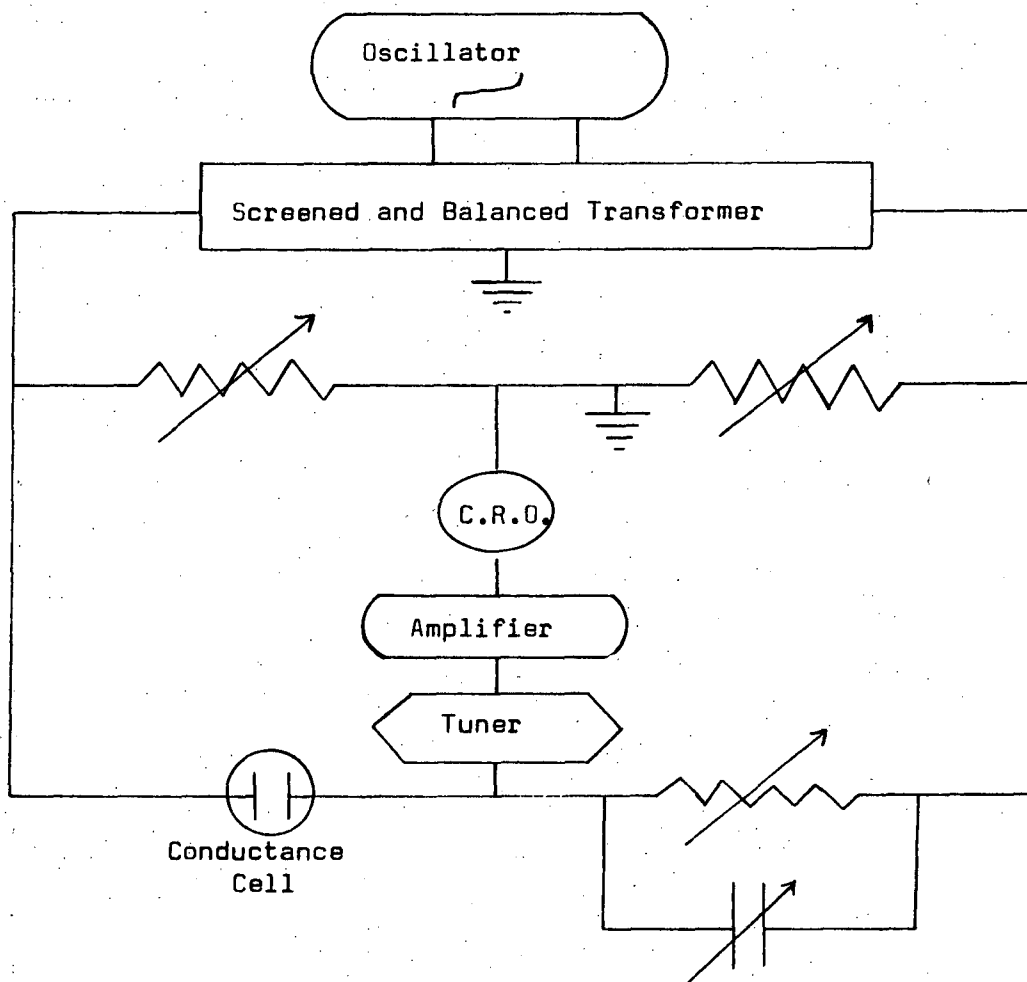


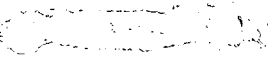
Figure 19. Conductance Bridge circuit.

Spectrophotometric studies were also found to be the most useful for monitoring the oxidation of titanium(III) in thiocyanate solutions. The procedure used involved following the changes in the spectra of solutions with time, during equilibration in air. The titanium(III) content of the solution was determined by direct titration (see Chapter 2.2) immediately following the absorbance measurements.

### 3.3 Results

The change in conductivity as the thiocyanate ion concentration is increased for a series of solutions having constant titanium(III) concentration is shown in Figure 20. Two distinct breaks in the curve can be observed. These breaks correspond to metal ligand ratios of 1:1 and 1:4.

Figure 21 shows the effect of increasing amounts of thiocyanate ion on the absorbance of individual solutions of titanium(III) in dilute hydrochloric acid. The intensity of absorption increases with increasing concentration of thiocyanate ion (see also Figure 22) and the position of maximum absorption shifts from 495 nm to 540 nm. As the concentration is increased to give a large excess of thiocyanate ion i.e. up to about 7 molar, the position of maximum absorbance shifts to 550 nm (see Figure 23) and the absorbance of the solution also increases (see also Appendices 11 and 12).

When these solutions were left to stand in air it was noticed that their color darkened somewhat before fading to a yellow color. At the lower thiocyanate ion concentrations i.e. less than about 2M, a yellow-white precipitate  formed. At the higher concentrations however, no precipitate appeared to form, instead the violet solution was observed to darken in color and change through various shades of brown, eventually forming a dark yellow solution. An example of the change in the titanium (III) concentration with time as oxidation occurs is shown in Figure 24. The spectrum of the solution was also recorded at different stages during the oxidation. These spectra showed that as the total titanium(III) content decreased due to oxidation to titanium(IV) the absorbance peak ( $\lambda_{\text{max}} = 550\text{nm}$ ) similarly decreased, while absorbance in the ultraviolet increased strongly (Figure 25). For the results represented in Figure 25, the ionic strength and total titanium content were constant, and therefore the spectra correspond to a continuous variation of titanium(III) and titanium(IV). Job difference plots of the absorbance data at 450 nm and 470 nm, as obtained in Appendix 13, are shown in Figure 26. These plots indicate the formation of

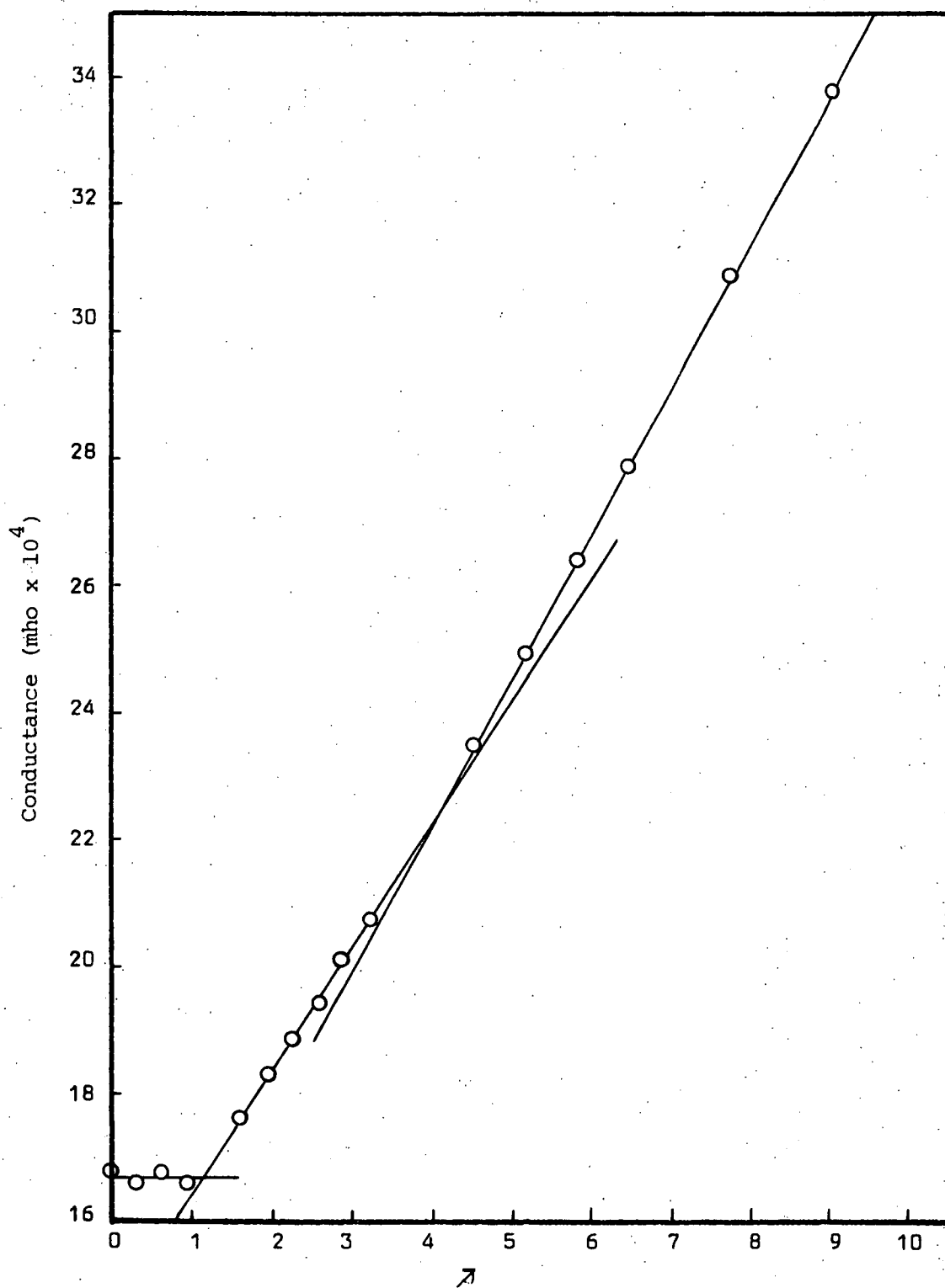


Figure 20. Conductometric titration curve for titanium(III) with thiocyanate ion. Temperature = 20.0°C.

$$\bar{\lambda} = \text{ratio } [\text{NCS}^-] : [\text{Ti(III)}]$$

$$[\text{Ti(III)}] = 0.0920, [\text{Cl}^-] = 0.334\text{M}$$

a 1:1 mixed oxidation state species.

### 3.4 Discussion

The results obtained have enabled the stoichiometry and stability constants of the titanium(III) thiocyanate complexes, formed in solution, to

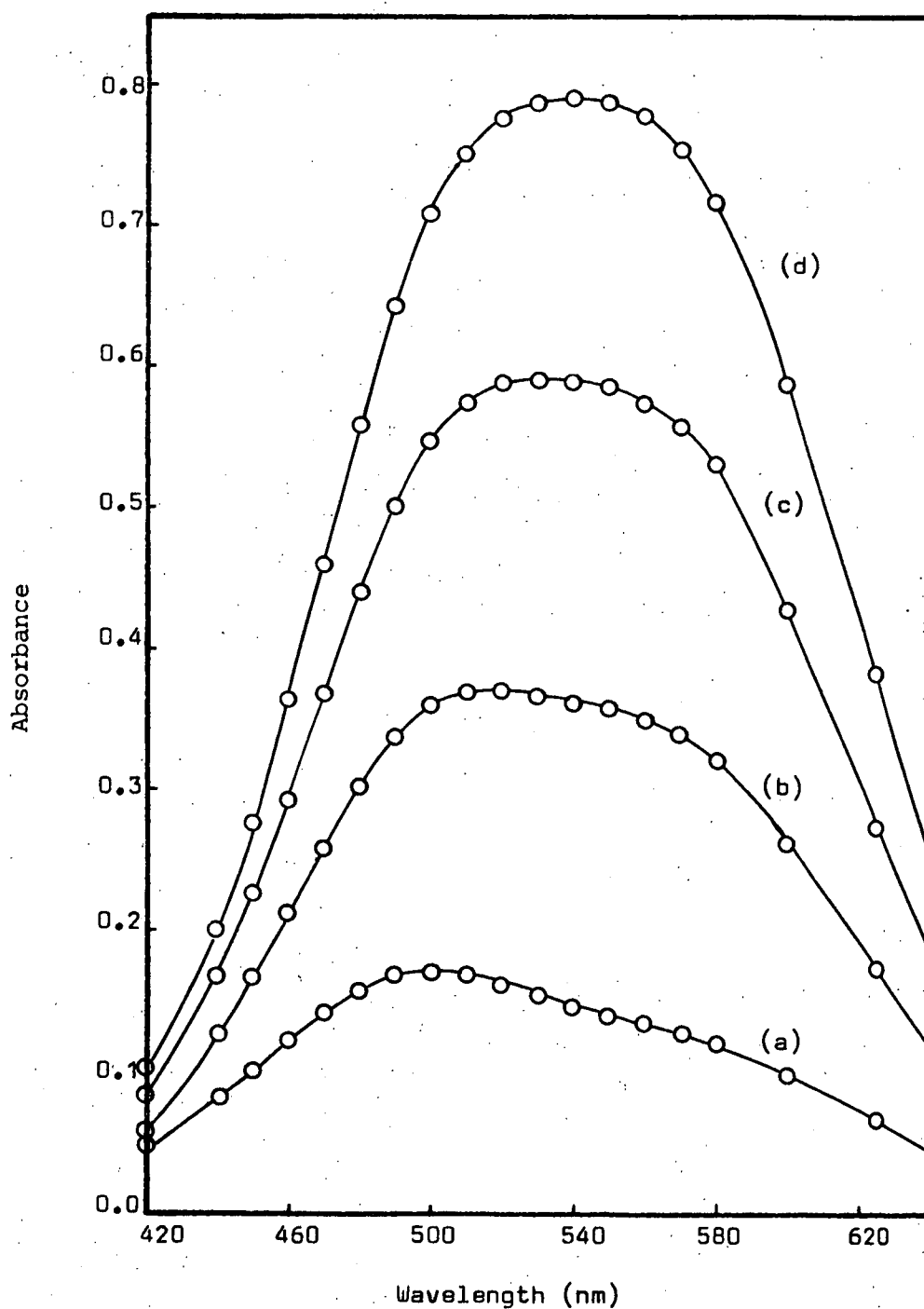


**Figure 21.** Spectra of solutions of titanium(III) where

$\bar{\alpha} = 0.0(a), 1.30(b), 3.26(c), 6.52(d)$ , using 0.5 cm cells.

$[Ti(III)] = 0.092M$ ,  $[Cl^-] = 0.334M$ .  $\bar{\alpha} = \text{ratio } [NCS^-]:[Ti(III)]$ .

be determined.

The two distinct breaks in the conductometric titration curve (Figure 20 can be interpreted as due to the formation of 1:1 and 1:4 species.

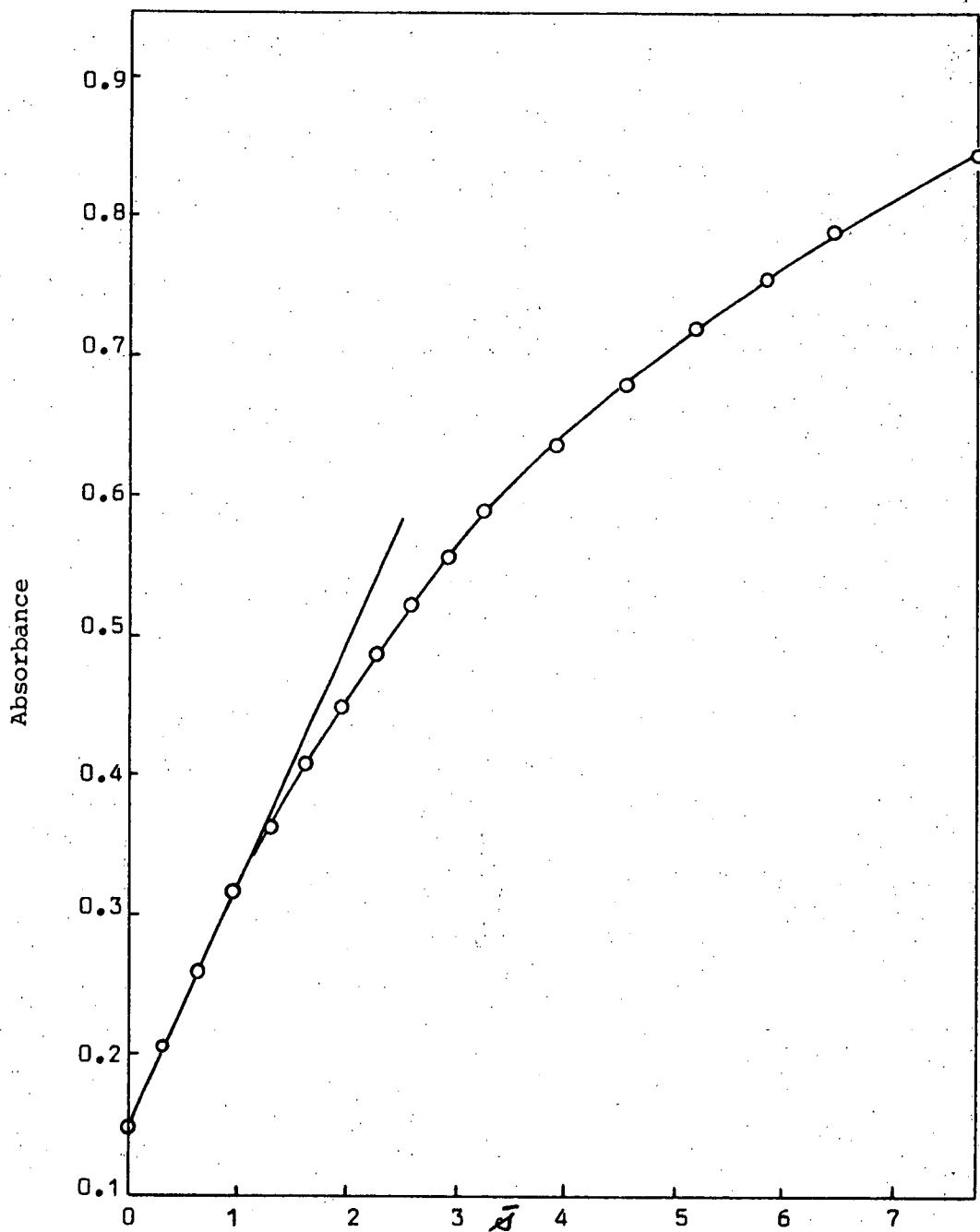


Figure 22. Variation of absorbance at 540 nm with

thiocyanate ion concentration for titanium(III) solutions.

$\bar{A}$  = ratio  $[\text{NCS}^-]: [\text{Ti(III)}]$ . Path length = 0.5 cm.

$[\text{Ti(III)}] = 0.0920\text{M}$ .  $[\text{Cl}^-] = 0.334\text{M}$ .

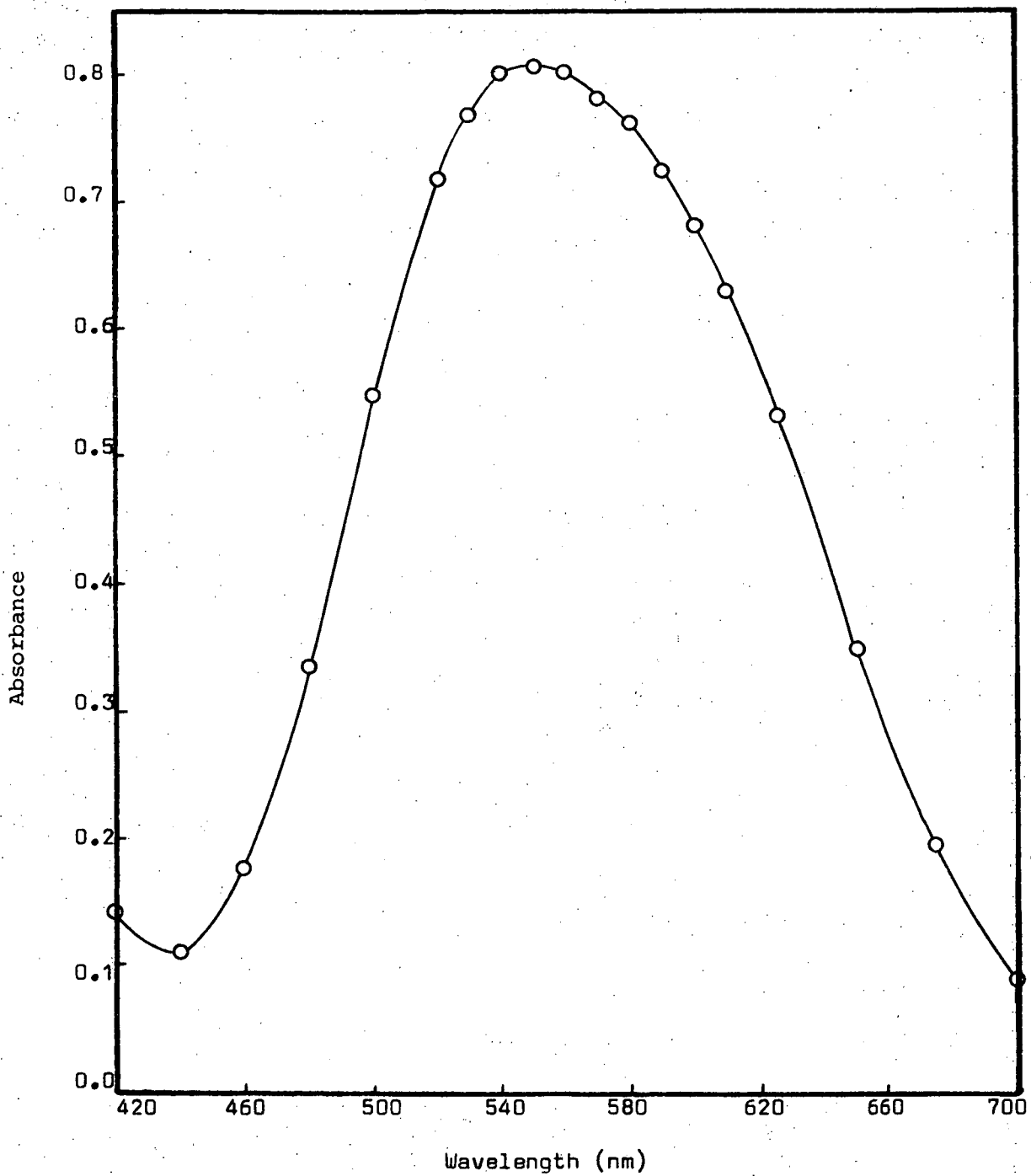
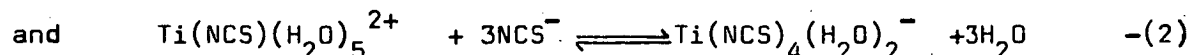
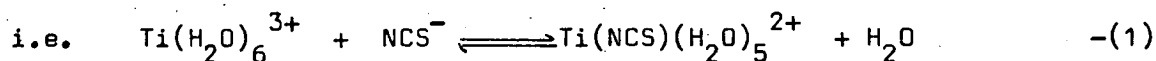


Figure 23. Spectrum of titanium(III) in 7.20M ammonium thiocyanate solution (i.e.  $\lambda_{\text{max}} = 212$ ) using 0.5 cells.

$[\text{Ti(III)}] = 0.034\text{M}$ ,  $[\text{Cl}^-] = 0.263\text{M}$ .





The formation of the former complex (as given by equation (1)) confirms previous work<sup>3,49-51</sup>, while the latter species,  $\text{Ti}(\text{NCS})_4(\text{H}_2\text{O})_2^-$ , has not previously been identified in solution. However the solid complex  $\text{NH}_4\text{Ti}(\text{NCS})_4(\text{H}_2\text{O})_2$  has been isolated from a solution containing 0.25M  $\text{TiCl}_3 \cdot 6\text{H}_2\text{O}$  and 1.50M  $\text{NH}_4\text{NCS}$ <sup>52</sup>. No evidence for the existence in solution of a  $\text{Ti}(\text{NCS})_3(\text{H}_2\text{O})_3$  species suggested by Jorgensen<sup>40</sup> was observed. This is not unexpected as the evidence for the existence of the 1:3 species was based upon the fact that a purple titanium(III) thiocyanate complex could be extracted into ether solution, and it was assumed that this was the neutral species. However, as  $\text{NH}_4\text{Ti}(\text{NCS})_4(\text{H}_2\text{O})_2$  was prepared by an ether extraction process it seems likely that the species reported by Jorgensen in solution was in fact the 1:4 complex. No evidence for the formation of a 1:6 species, reported to have been isolated as  $(\text{K}, \text{NH}_4)_3\text{Ti}(\text{NCS})_6 \cdot 6\text{H}_2\text{O}$  by Van der Pfordten<sup>53</sup>, was observed. Repetition of Van der Pfordten's work by Sutton<sup>52</sup> failed to yield a pure sample of the violet thiocyanate complex from aqueous solution. It seems likely that the complex isolated by Van der Pfordten in 1886 was actually an impure sample of  $\text{NH}_4\text{Ti}(\text{NCS})_4(\text{H}_2\text{O})_2$ . The spectrophotometric results could not be used to confirm the composition of the species formed as a Yoe and Jones molar variation plot<sup>57</sup> gave a smooth curve (Figure 22) rather than intersecting lines.

Sufficient information, however, can be obtained from the spectrophotometric data to enable stability constants for the various titanium(III) complexes to be estimated.

For the 1:1 complex, from equation(1),

$$K_1 = \frac{[\text{Ti}(\text{NCS})(\text{H}_2\text{O})_5^{2+}]}{[\text{Ti}(\text{H}_2\text{O})_6^{3+}][\text{NCS}^-]} \quad -(3)$$

Using the method described in Appendix (11), absorbance data at 500 nm and

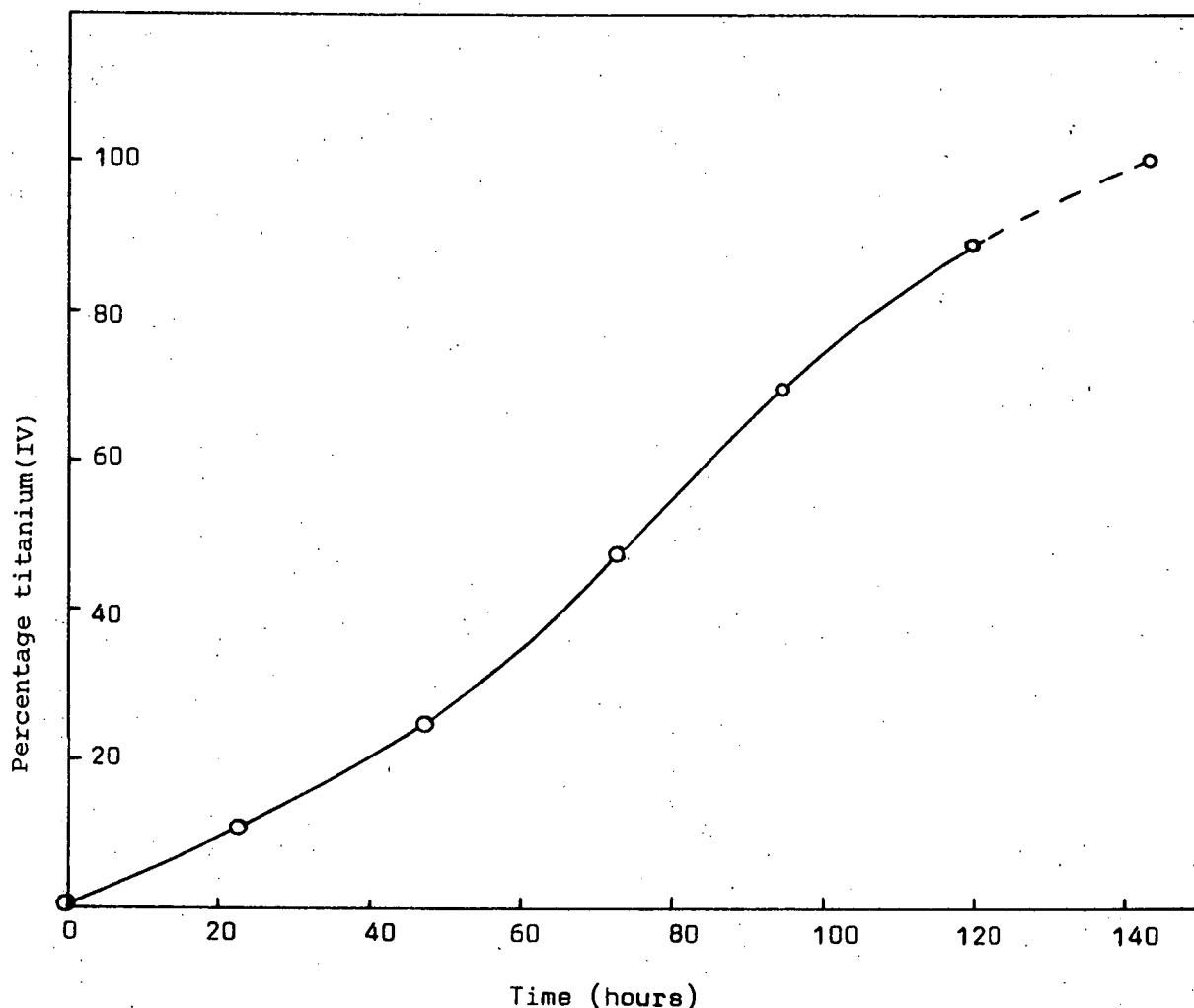


**Figure 24.** Rate of oxidation of titanium(III) to titanium(IV).

$[\text{Ti(III)}]_{\text{initial}} = 0.034\text{M}$ ,  $[\text{Cl}^-] = 0.281\text{M}$ ,  $[\text{NH}_4\text{NCS}] = 6.40\text{M}$ .

600 nm for solutions where the  $\text{NCS}^-:\text{Ti(III)}$  ratio ranged from 0 to 9, gave  $\log K_1$  values of 0.410 and 0.407 and  $\epsilon_{\text{max}}(540 \text{ nm}) = 27.0 \pm 0.3 \text{ moles}^{-1} \text{ l cm}^{-1}$  (temperature  $20^\circ\text{C}$ ). A value of  $\log K_1 = 0.176 \pm 0.030$  for the titanium(III) complex has been calculated by Diebler<sup>50</sup>. However the values obtained in this work are similar to the values of  $\log K_1 = 0.4\text{--}0.5$

found for the mono thiocyanate complexes of aluminium and several of the trivalent "f-block" elements (see Table 4)<sup>25</sup>. Other trivalent transition metal  $M(NCS)(H_2O)_5^{2+}$  complexes e.g. where  $M = V(III)$ ,  $Cr(III)$ ,  $Fe(III)$  and  $Ru(III)$ , are more stable.

Table 4

Stability Constants of some 1:1 metal thiocyanate complexes.

Metal	Temp °C	Ionic Strength (M)	log $K_1$
Pu(III)	25	1	0.46
Am(III)	25	1	0.50
Cf(III)	25	1	0.49
Cm(III)	25	1	0.43
Ti(III)	20	0.5	0.41*
Al(III)	23	0	0.42
V(III)	25	1	2.1
Cr(III)	25	0	3.1
Fe(III)	20	1.2	2.1
Ru(III)	70	1	1.8

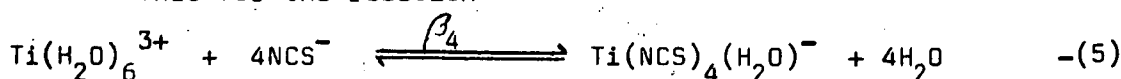
\*This work.

For the 1:4 complex, from equation(2)

$$K_{14} = \frac{[Ti(NCS)_4(H_2O)_2^-]}{[Ti(NCS)(H_2O)_5^{2+}][NCS^-]^3} \quad -(4)$$

Using the method described in Appendix 12, absorbance data at 520 nm and 560 nm from solutions where the  $NCS^-:Ti(III)$  ratio ranged from 47 to 212, gave log  $K_{14}$  values of -1.67 and -1.85, and  $\epsilon_{max}(550) = 50.9 \pm 1.0$  temperature 25°C).

Thus for the reaction



$$\log \beta_4 = \log K_1 + \log K_{14} \quad -(6)$$

$$\text{i.e. } \log \beta_4 = -1.34 \pm 0.10$$

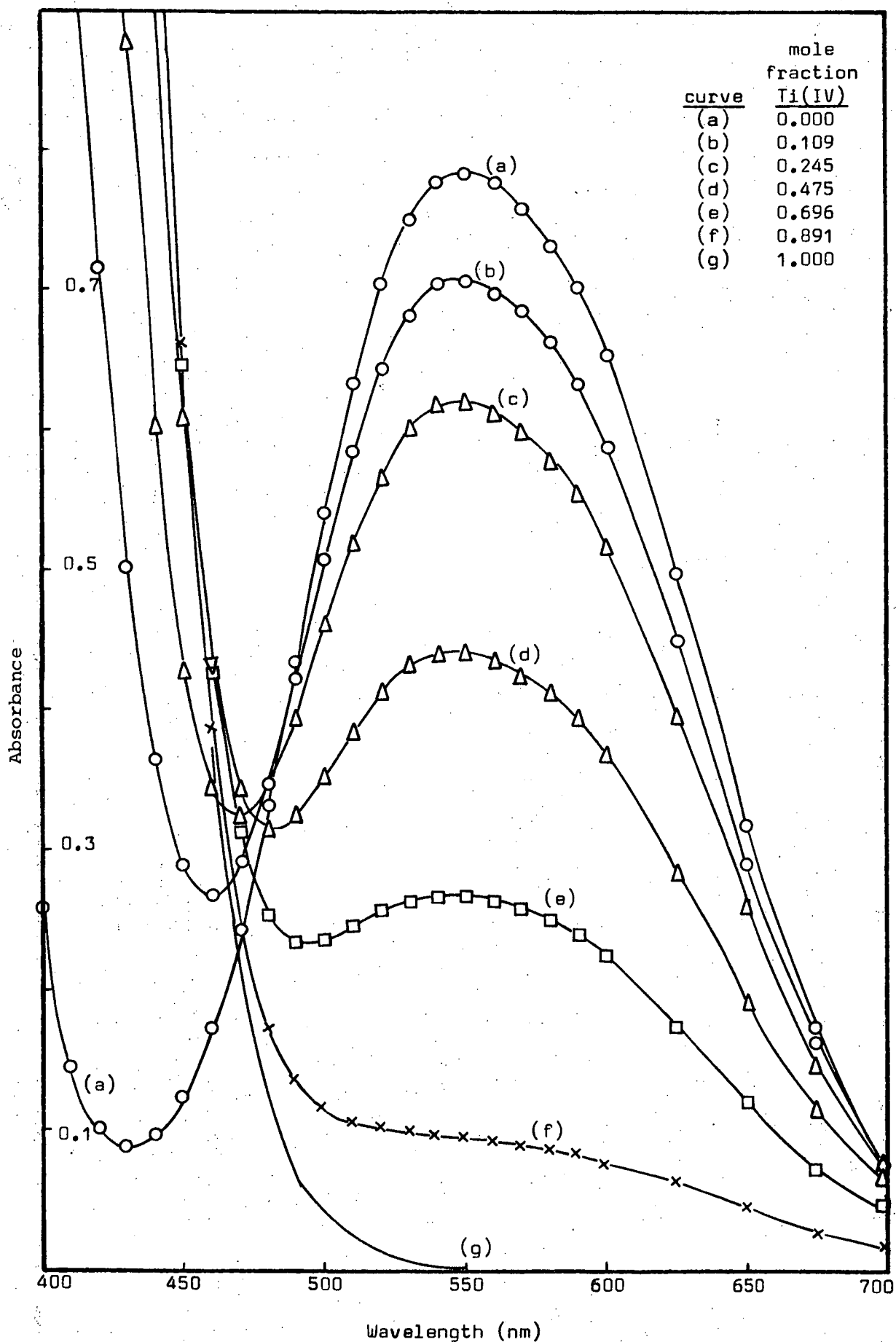


**Figure 25.** Spectra of titanium(III), titanium(IV) continuous variation solutions using 0.5 cm cells.  $[Ti]_{total} = 0.034M$ ,  $[Cl^-] = 0.281M$ ,  $[NH_4NCS] = 6.40M$

No stability constant for this 1:4 complex has been reported previously and the negative  $\log \beta_4$  value shows the low stability of the titanium(III) species compared with reported  $\log \beta_4$  values of 4.71, 6.31, 3.22, 3.40, 0.86 and 0.00 for the tetrathiocyanate complexes of chromium(III), iron(III), indium(III), bismuth(III), europium(III) and americium(III), respectively<sup>25</sup>.

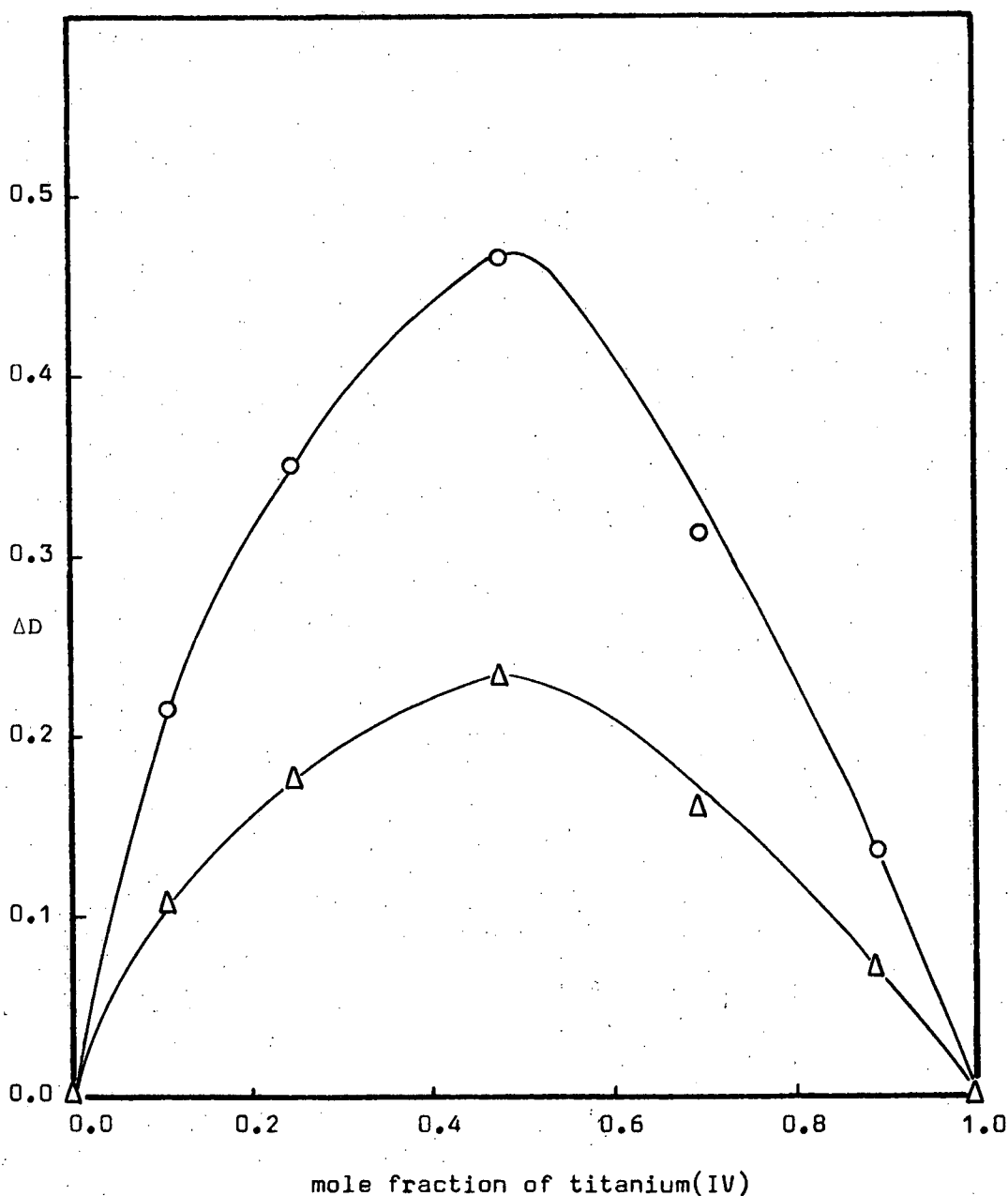
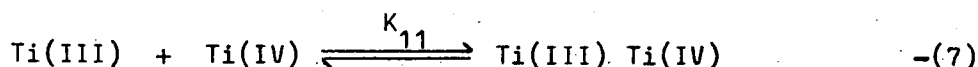


**Figure 26.** Job's continuous variation method, difference plots.

○ ~ 450 nm, △ ~ 470 nm.

For the 1:1 mixed oxidation state species given by the reaction



a value of  $\log K_{11} = 0.9 \left( \begin{smallmatrix} +0.3 \\ -0.9 \end{smallmatrix} \right)$  was calculated (see Appendix 13). Since the titanium(III) in the above equilibrium consists of a mixture of 80%  $\text{Ti(NCS)}_4(\text{H}_2\text{O})_2^-$  and 20%  $\text{Ti(NCS)(H}_2\text{O})_5^{2+}$ , it does not seem worthwhile to speculate on the nature of the mixed oxidation state species except to say that it is presumably a dimer containing either bridging thiocyanate or oxo ions. This type of behaviour for titanium(III) in thiocyanate media has not been reported previously. However the formation of a similar titanium 1:1 mixed oxidation state species has been demonstrated in concentrated chloride media and  $\log K_{11}$  for equation (6) in 12M hydrochloric acid was reported as  $1.08^{40}$ .

### 3.5 Conclusion

Complex formation in the aqueous  $\text{Ti(III)} - \text{NCS}^-$  system can now be clearly understood. New species are formed when  $\text{NCS}^-$  ions are introduced into solutions containing  $\text{Ti(H}_2\text{O)}_6^{3+}$ , by the replacement of either one or four of the water ligands in the hydration shell by  $\text{NCS}^-$  ligands. No stepwise replacement is observed which appears to be characteristic of titanium(III) co-ordination behaviour. In addition, it has been shown for the first time that oxidation of titanium(III) thiocyanate complexes proceeds via the formation of a stable intermediate 1:1  $\text{Ti(III):Ti(IV)}$  mixed oxidation state species.

## CHAPTER 4

### Titanium(III) sulphate complexes formed in aqueous solutions

#### 4.1 Introduction

It is generally assumed that titanium(III) in dilute sulphate solutions exists as the titanium hexaquo ion  $\text{Ti}(\text{H}_2\text{O})_6^{3+}$ <sup>8</sup>. This follows from the work of Hartmann and Schlafer<sup>5</sup> who measured the spectra of 0.117M titanium(III) sulphate solution, 0.100M titanium(III) chloride solution and solid cesium titanium alum  $\text{CsTi}(\text{SO}_4)_2 \cdot 12\text{H}_2\text{O}$ , and found that the absorption maximum fell at 492 nm in each case. It is well known that the trivalent metal ion exists as a hexaquo complex in alums<sup>58</sup> and detailed studies of the behaviour of titanium(III) in aqueous chloride solutions show that in dilute chloride solutions titanium(III) exists predominantly as the hexaquo ion<sup>7</sup>. Thus there is supporting evidence for Hartmann and Schlafer's results on titanium(III) chloride solutions and solid alums. However there is conflicting evidence for titanium(III) sulphate solutions. For example, Arris and Duffy report that the spectrum of titanium(III) in 0.1M  $\text{H}_2\text{SO}_4$  has an absorbance maximum at 510 nm<sup>59</sup>. This suggests that complex formation with sulphate ion does occur even in dilute solutions. No other spectral data for titanium(III) in dilute aqueous sulphate solutions appear to be available in the literature.

In this chapter, results of a detailed study of complex formation between titanium(III) and sulphate ions is presented. Direct evidence for the existence of several species in solution, not previously identified, is given. The species predominating in dilute sulphuric acid solutions has been isolated as the solid complex  $\text{Ti}(\text{HSO}_4)(\text{SO}_4)(\text{H}_2\text{O})_4$ . This solid corresponds to the previously reported<sup>64</sup> salt  $\text{Ti}_2(\text{SO}_4)_3 \cdot \text{H}_2\text{SO}_4 \cdot 8\text{H}_2\text{O}$ .

In addition, the new solid titanium(III) compound  $\text{Ti}(\text{HSO}_4)(\text{SO}_4)$  has been prepared and studied. This latter compound has also been identified as the titanium(III) species present in concentrated sulphuric acid solutions.

Results of an investigation of the oxidation of titanium(III) sulphate solutions are presented. These complement existing studies in this area and confirm the formation of a stable mixed oxidation state intermediate species during the oxidation. Data for the hydrolysis of titanium(III) sulphate solutions are reported for the first time and show that the hydrolysis behaviour observed is, in several respects, quite different from that for titanium(III) chloride solutions reported in Chapter 2. Evidence is presented for the existence of titanium(III) hydroxy sulphate complexes during primary hydrolysis, as well as the formation of a mixed oxidation state hydrolysis species after secondary hydrolysis occurs, as in Chapter 2. The results in this chapter include potentiometric, analytical, spectral and conductometric data for titanium(III) sulphate solutions of varying acid and sulphate ion concentrations.

## 4.2 Titanium(III) - sulphate complexes formed in acidic aqueous solutions

### 4.2.1 Experimental

#### (a) Solution studies

In aqueous sulphuric acid solutions, the hydrogen-sulphate ion is the main anionic species at all concentrations below  $\sim 16$  molar<sup>60</sup>. However, from reported evidence<sup>61</sup>, in ammonium sulphate solutions the sulphate ion predominates. Thus in this work ammonium sulphate was used to adjust the sulphate ion concentration. Titanium(III) in dilute hydrochloric acid was used as the source of hexaquotitanium(III) ion, enabling studies to be made at sulphate ion concentrations ranging down to zero.

The variation of absorbance with sulphate ion concentration was used to determine the metal:ligand ratios of the species present in solution. Series of individual solutions containing a fixed quantity of titanium(III) with a varying amounts of sulphate ion were prepared. Absorbance measurements over a range of wavelength values were made. These spectra were also used to provide information about the nature of the species present. Some

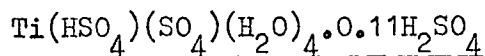


spectra of titanium (III) in strong sulphuric acid solutions were also recorded for comparison.

Conductometric titrations were used to confirm the metal: ligand ratios obtained above. The procedure used was identical to that used for the thiocyanate system described in Chapter 3.2.

Again, as in the work described in the previous two chapters, it was necessary to take precautions against aerial oxidation of titanium (III) and all solutions used were presaturated with nitrogen.

#### (b) Solid Complexes

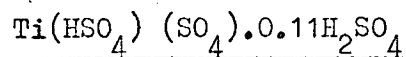


100 mls of 15% weight per volume  $\text{Ti}_2(\text{SO}_4)_3$  solution in 23% weight per volume  $\text{H}_2\text{SO}_4$  (see Appendix 1) was heated slowly under nitrogen with 60 mls of concentrated sulphuric acid until crystals started to form. The solution was then allowed to cool slowly. The small pale violet crystals were filtered through sintered glass and washed sparingly with acetone before being dried under vacuum over KOH.

Found Ti (III), 14.71, 14.72, 14.88%

Found  $\text{SO}_4^{2-}$ , 63.0, 62.6 %

Calculated for  $\text{Ti}(\text{HSO}_4)(\text{SO}_4)(\text{H}_2\text{O})_4 \cdot 0.11\text{H}_2\text{SO}_4$ ;      Ti(III) 14.78%,  
 $\text{SO}_4^{2-}$  62.7%



The compound  $\text{Ti}(\text{HSO}_4)(\text{SO}_4)(\text{H}_2\text{O})_4 \cdot 0.11\text{H}_2\text{SO}_4$  was heated to  $98^\circ\text{C}$  under nitrogen under vacuum using the apparatus shown in Figure 27. Water was given off leaving a pale blue powder.

( Found Ti(III), 18.88, 19.11, 19.09%

$\text{Ti}(\text{HSO}_4)(\text{SO}_4) \cdot 0.11\text{H}_2\text{SO}_4$  requires Ti(III) 19.01%

The compounds were analysed for titanium (III) by dissolving in 5 molar hydrochloric acid and titrating with standard ferric ammonium sulphate solution. (see Chapter 2.2. Solid UV-visible reflectance spectra were recorded using undiluted samples mounted in an airtight holder having a silica window. I.R. spectra were run using conventional nujol mulls. Sulphate

analyses were done by the filter crucible method<sup>91</sup>,  $\text{Ti}^{3+}$  having been previously precipitated from solution with  $\text{NH}_4\text{OH}$  and filtered off.

#### 4.2.2 Results

Figure 28 shows the shift in the position of maximum absorbance for a series of solutions where the sulphate ion concentration was increased

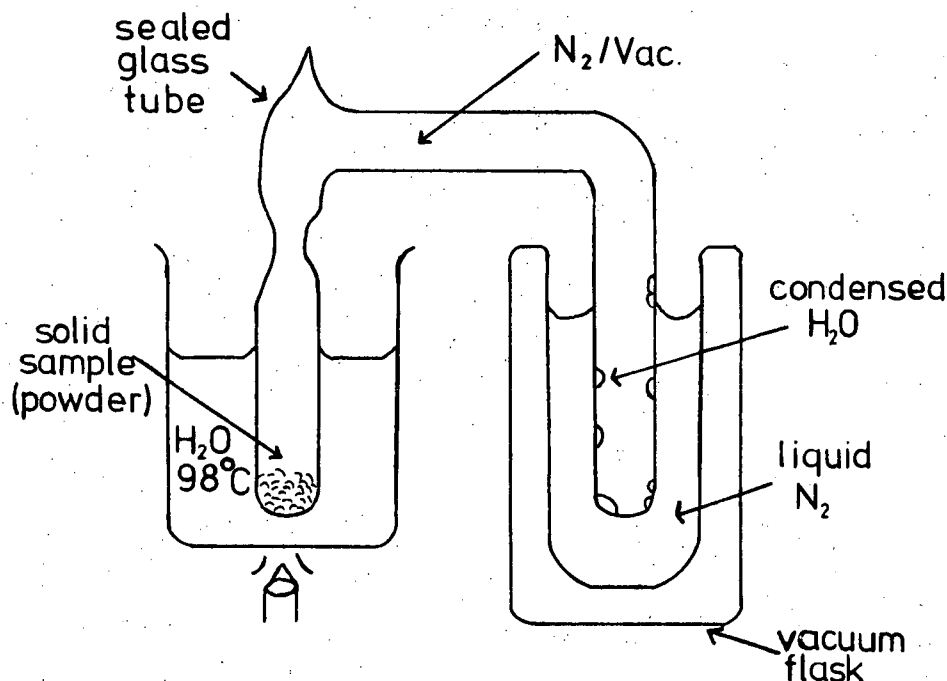
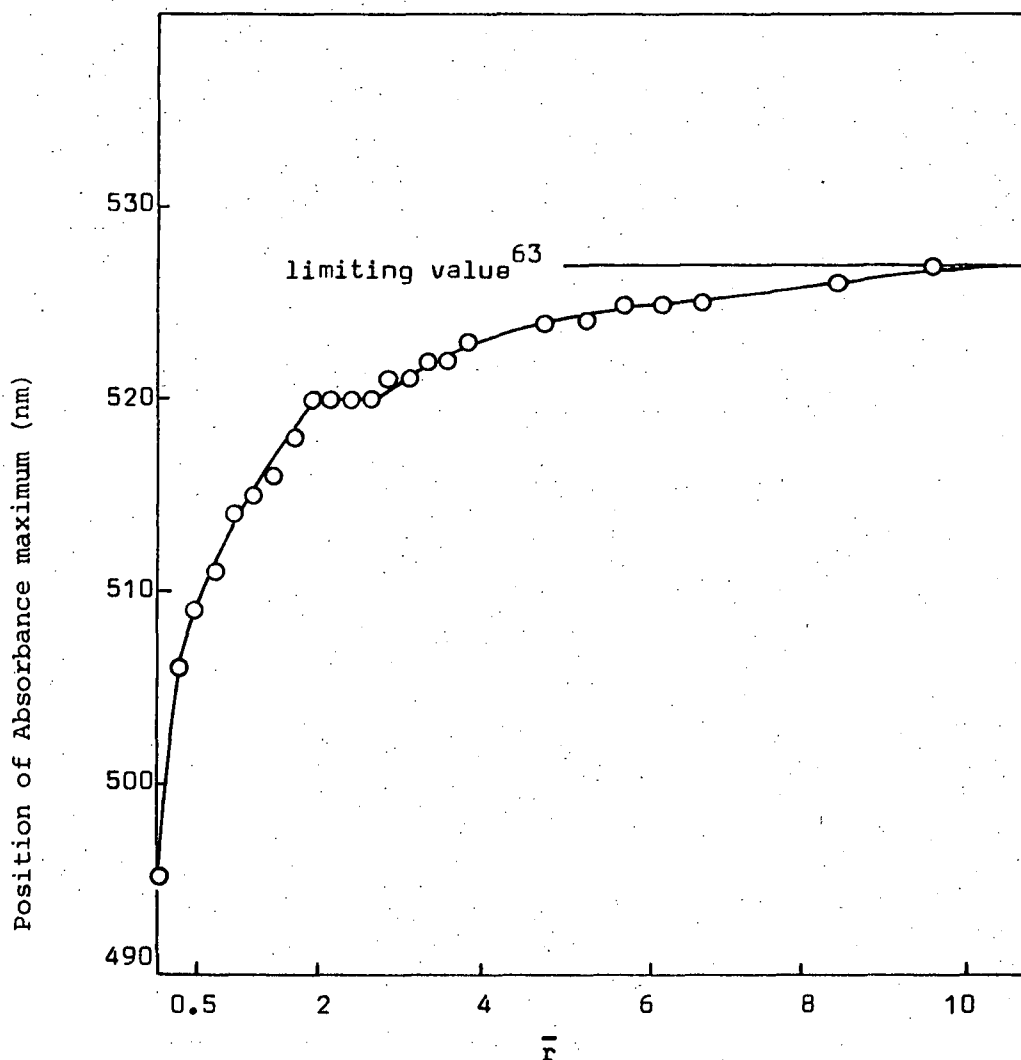


Figure 27. Dehydration apparatus.

with respect to a constant amount of titanium(III). The peak maximum rapidly shifts from 495 nm to about 509 nm, then less rapidly to 520 nm where it levels off before slowly increasing towards 527 nm. Some of the solution spectra are shown in Figure 29. A molar variation plot of the absorbance at 520 nm (Figure 30) gave intersecting lines corresponding to the formation of 2:1 and 1:2,  $\text{Ti(III):SO}_4^{2-}$  complexes. A similar plot at 540 nm (Figure 31) over an extended range of sulphate ion concentrations confirmed the formation of the 2:1 and 1:2 species and demonstrated the existence of a 1:4 species.

The results of the conductometric titration studies for series of solutions containing two ranges of sulphate ion concentrations are shown in Figures 32 and 33. Breaks in the curves corresponding to



**Figure 28.** Variation of peak position with sulphate ion concentration for titanium(III) solutions.

$$\bar{r} = \text{ratio } [\text{SO}_4^{2-}] : [\text{Ti(III)}]$$

$$[\text{Ti(III)}] = 0.0928\text{M}, [\text{Cl}^-] = 0.478\text{M}.$$

metal:ligand ratios of 1:2 and 1:4 were observed, confirming the spectrophotometric evidence for the formation of these species.

When a series of solutions containing 2 mls of 0.5M Ti(III) in dilute  $\text{H}_2\text{SO}_4$  (see Appendix 1) and x mls of concentrated  $\text{H}_2\text{SO}_4$  (where  $x = 0, 1, 2, 3, \dots, 23$ ) made to 25 mls with distilled water, were allowed to stand for some time (4 days) small pale violet crystals of  $\text{Ti}(\text{HSO}_4)(\text{SO}_4)(\text{H}_2\text{O})_4$  settled out of solutions where  $x = 9$  to 17. / solutions

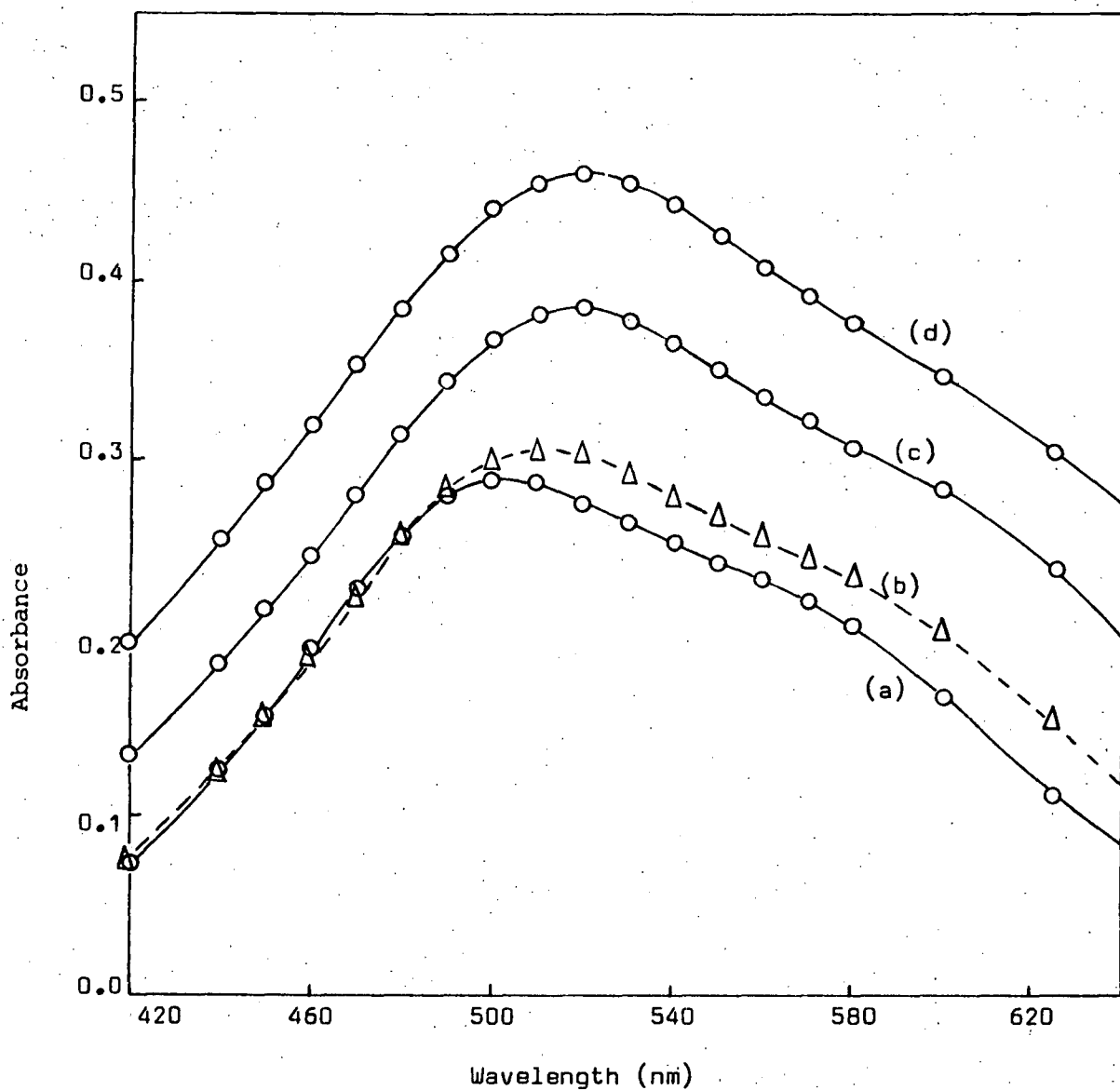


**Figure 29.** Spectra of titanium(III) solutions containing varying amounts of sulphate ion, using 1 cm cells.

$[\text{SO}_4^{2-}] : [\text{Ti(III)}] = 0.000(\text{a}), 0.516(\text{b}), 1.852(\text{c}), 3.611(\text{d}).$

$[\text{Ti(III)}] = 0.0756\text{M}, [\text{Cl}^-] = 0.357\text{M}.$

where  $x = 11$  to  $15$  were colorless, there being a considerable quantity of crystals present, suggesting that virtually all the titanium(III) was precipitated under these conditions. The solutions where  $x = 20$  to  $23$  were a characteristic blue color and an example of the visible spectrum of these solutions is shown in Figure 34.

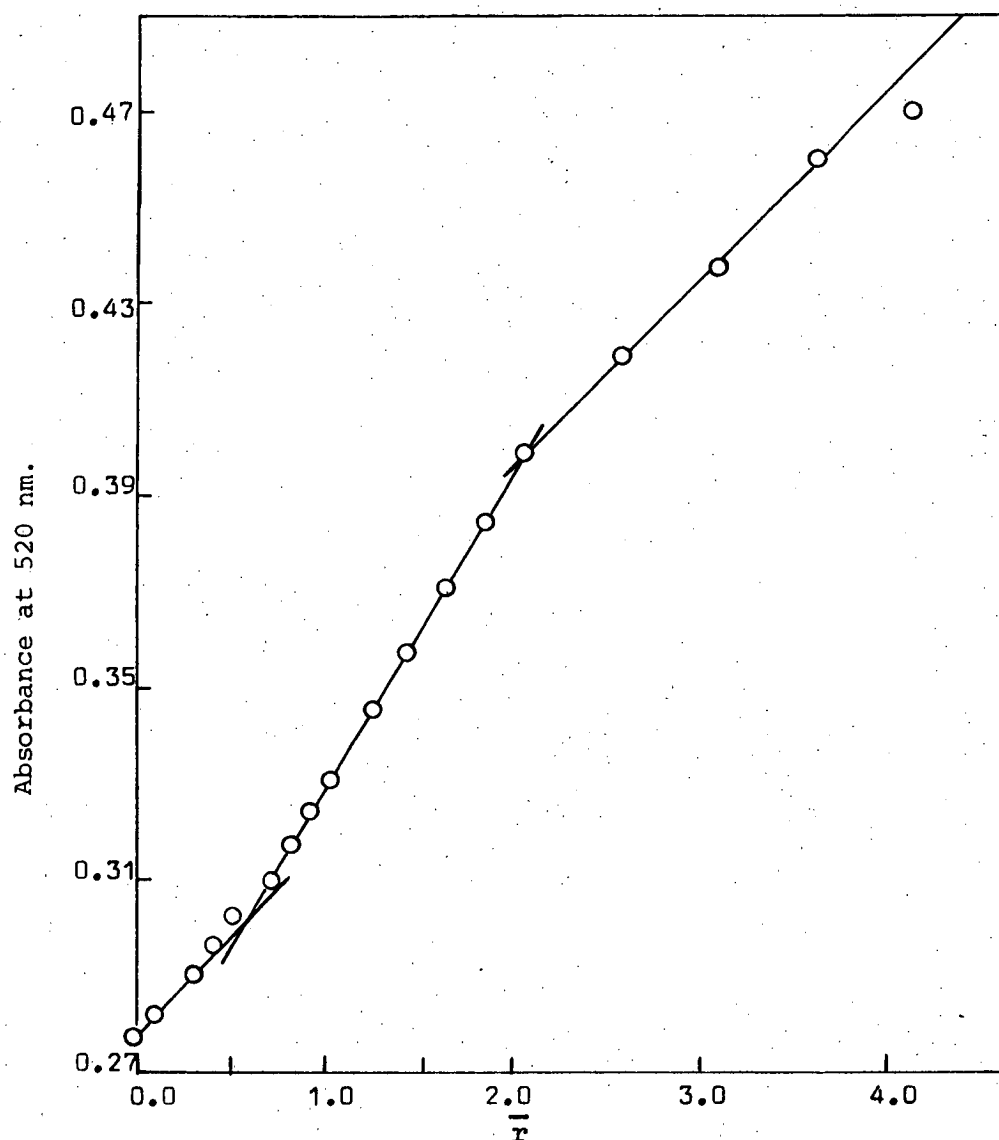


Figure 30. Absorbance values at 520 nm for titanium(III) solutions containing varying amounts of sulphate ion.

$$\bar{r} = [\text{SO}_4^{2-}] : [\text{Ti(III)}].$$

$$[\text{Ti(III)}] = 0.0756\text{M}, [\text{Cl}^-] = 0.357\text{M}. \text{ Path length} = 1 \text{ cm}.$$

Reflectance spectra for the solid compounds are shown in Figure 34 and infrared absorption data are summarised in Table 5.

Table 5

Peak Positions (1200-600 $\text{cm}^{-1}$ region)	
$\text{Ti}(\text{HSO}_4)_4(\text{SO}_4)_4(\text{H}_2\text{O})_4$	$\text{Ti}(\text{HSO}_4)_4(\text{SO}_4)_4$
665	660
1015	1020
1040(s)	1050(b)
1180(b)	1130(b)

#### 4.2.3 Discussion

From the molar variation absorbance data (Figures 30 and 31) evidence for the existence in solution of 2:1, 1:2 and 1:4 titanium (III): sulphate, complexes is clearly presented. Other workers have also reported evidence for the existence of three titanium (III) sulphate species<sup>93</sup>, however the stoichiometry of each complex was not identified. Because the molar variation plots give straight lines for the 2:1 and 1:2 species, the complexes are quite stable and their formation constants cannot be obtained from absorbance data<sup>62</sup>. The 1:4 complex is less stable, however, as there are two other species competing in equilibrium, the system is very complicated and again the formation constant cannot be determined.

The conductometric titration results (Figures 32 and 33) confirm the spectrophotometric data that 1:2 and 1:4 titanium (III) sulphate complexes are formed. No break corresponding to the formation of the 2:1 species is observed, which implies that this species has similar ionic mobility and stability to the 1:2 complex. This is consistent with the spectrophotometric evidence that both these complexes are very stable. No evidence for the existence of higher complexes or intermediate 1:1 or 1:3 species is observed, again in agreement with the spectrophotometric data.

By comparing Figures 30 and 31 with 28, it can be seen that the 2:1 complex would probably have an absorbance maximum at about 509 nm. This spectrum, being similar to that for the hexaquo ion, suggests that the complex contains a high degree of aquation and could probably be assigned the structure  $\text{Ti}(\text{H}_2\text{O})_5(\text{SO}_4)\text{Ti}(\text{H}_2\text{O})_5^{4+}$  containing a bridging sulphate group, unidentate with respect to each titanium (III) atom. The plateau at 520 nm

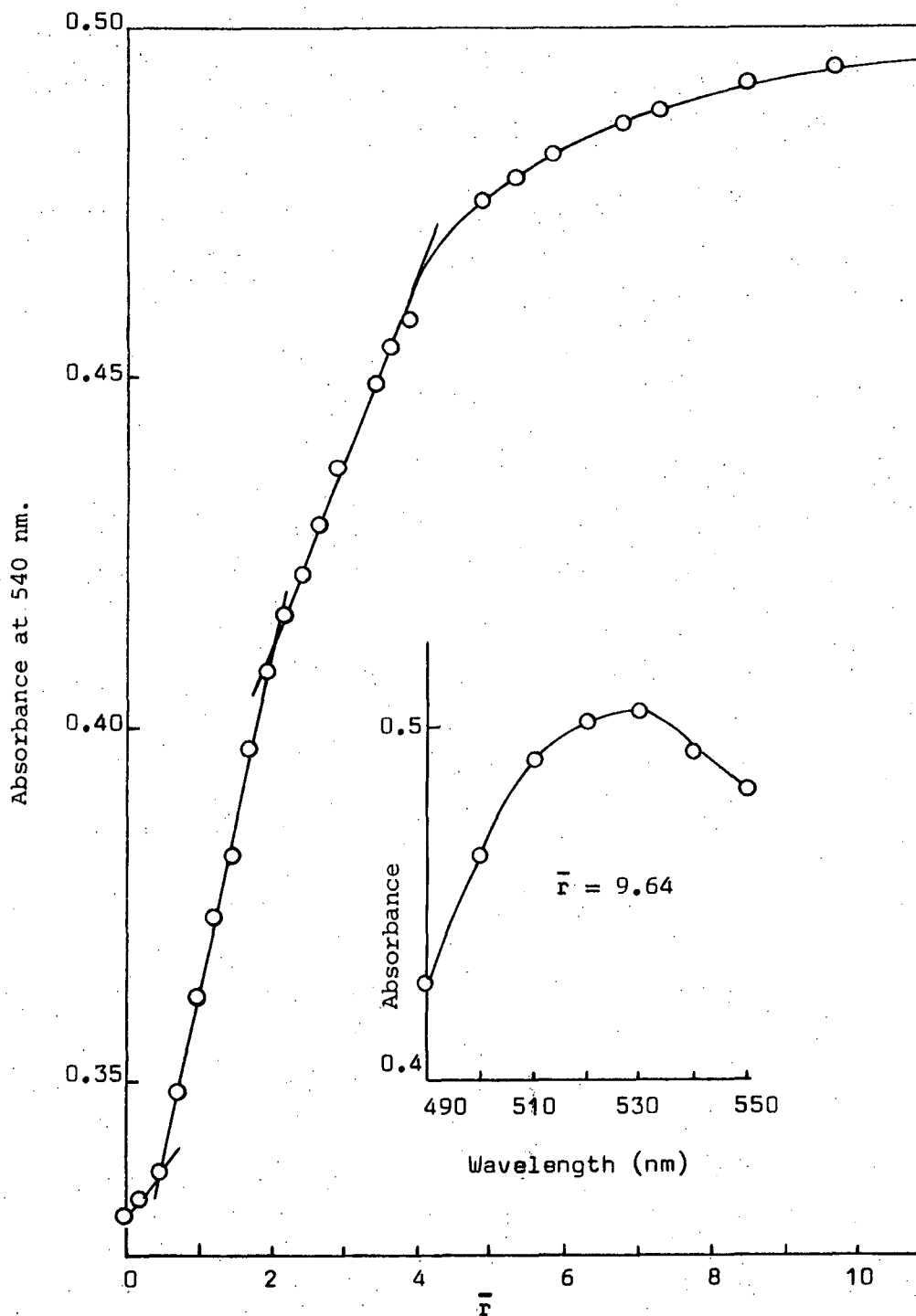
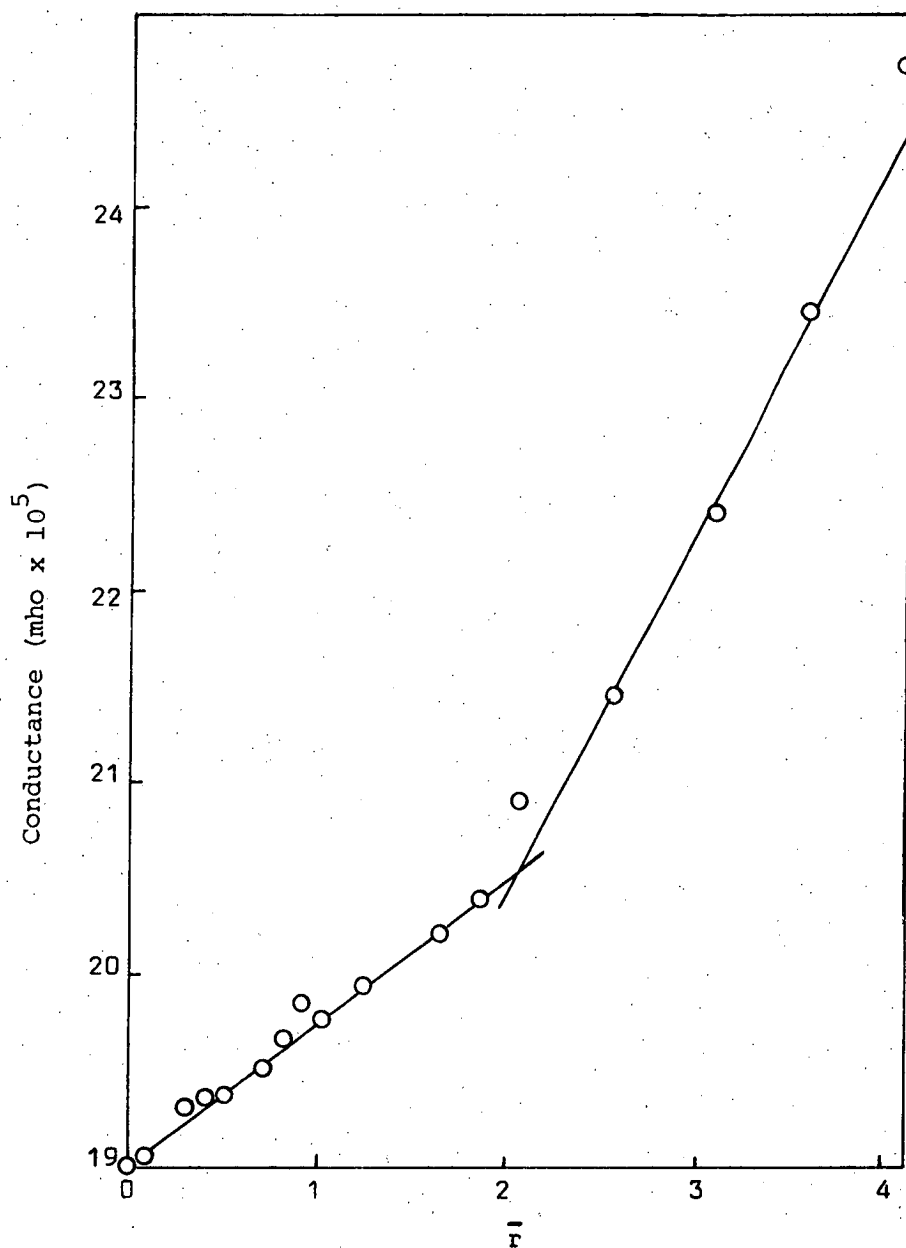


Figure 31. Absorbance values at 540 nm for titanium(III) solutions containing varying amounts of sulphate ion.

$$\bar{r} = [\text{SO}_4^{2-}] : [\text{Ti(III)}]$$

$[\text{Ti(III)}] = 0.0928\text{M}$ ,  $[\text{Cl}^-] = 0.478\text{M}$ . Path length = 1 cm.



**Figure 32.** Conductometric titration curve for titanium(III) with sulphate ion.

$\bar{r}$  = ratio  $[\text{SO}_4^{2-}] : [\text{Ti(III)}]$ . Temperature =  $20.0^\circ\text{C}$   
 $[\text{Ti(III)}] = 0.0756\text{M}$ ,  $[\text{Cl}^-] = 0.357\text{M}$ .

in Figure 28 clearly demonstrates that this is the position of the absorbance maximum for the 1:2 species. For the 1:4 species, being less stable, the position of the peak moves much more slowly towards its



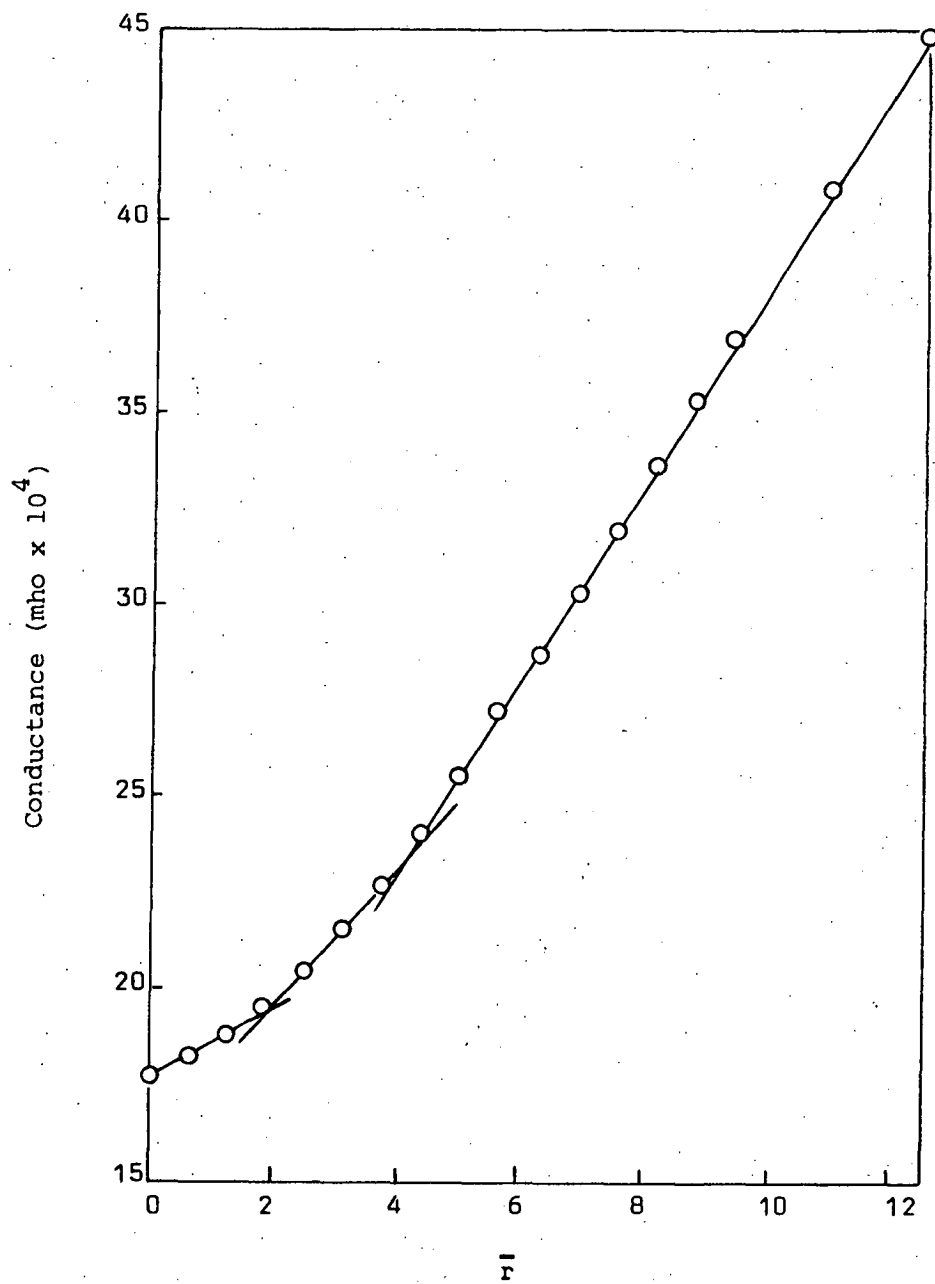


**Figure 33.** Conductometric titration curve for titanium(III) with sulphate ion.

$\bar{r}$  = ratio  $[\text{SO}_4^{2-}] : [\text{Ti(III)}]$  . Temperature =  $29.8^\circ\text{C}$   
 $[\text{Ti(III)}] = 0.0799\text{M}$ ,  $[\text{Cl}^-] = 0.334\text{M}$ .

characteristic value of 527 nm. This complex most likely contains four unidentate sulphate groups with two molecules of water completing the octahedral co-ordination. The peak position of the latter species corresponds with that reported by Goroshchenko and Godneva<sup>63</sup> who made spectrophotometric studies of titanium(III) in sulphuric acid solutions over the range 10-100%  $\text{H}_2\text{SO}_4$ . They observed that in the region 10-40%  $\text{H}_2\text{SO}_4$  (i.e. approximately 1.8 to 7.2M) the titanium(III) solutions have an absorbance maximum at 527 nm. The variation in absorbance at 527 nm over this concentration range (taken from their reported spectra) is plotted in Figure 35 and shows that the gradual increase in absorbance which would be expected, begins to increase quite rapidly at high concentrations (greater than about 4M). This behaviour suggests that the 1:4 species forms polymers at these high concentrations.

At higher sulphuric acid concentrations, i.e. up to approximately 70%  $\text{H}_2\text{SO}_4$ , observations in this work show that a pale violet titanium(III) salt crystallises from solution. In the solutions containing 44% to 60% almost all the titanium(III) appears to be precipitated after several days. A similar observation has been made by other workers<sup>64</sup> who found that 90-97% precipitation occurred in solutions containing 38%-54%  $\text{H}_2\text{SO}_4$ . As the salt crystallises from concentrated sulphuric acid solutions, removal of traces of sulphuric acid solvent are difficult. Consequently the composition of the salt has been reported as  $3\text{Ti}_2(\text{SO}_4)_3 \cdot \text{H}_2\text{SO}_4 \cdot 25\text{H}_2\text{O}$ <sup>65</sup> and  $3\text{Ti}_2(\text{SO}_4)_3 \cdot 2\text{H}_2\text{SO}_4 \cdot 26\text{H}_2\text{O}$ <sup>66</sup> reflecting the difficulty in obtaining a pure compound. However it seems that the salt would be better formulated as  $\text{Ti}_2(\text{SO}_4)_3 \cdot \text{H}_2\text{SO}_4 \cdot 8\text{H}_2\text{O}$ <sup>63,64</sup>. The salt prepared in this work gave a mean titanium(III) analysis of 14.77% corresponding to a Formula weight of 648 compared with 626 for pure  $\text{Ti}_2(\text{SO}_4)_3 \cdot \text{H}_2\text{SO}_4 \cdot 8\text{H}_2\text{O}$  suggesting, as expected, since the compound was precipitated from a strong  $\text{H}_2\text{SO}_4$  solution, that a small amount of  $\text{H}_2\text{SO}_4$  (calculated 0.22 mole) was occluded in the crystals.

The peak position for the violet salt, i.e. 520 nm, (see Figure 34) corresponds with the peak for the 1:2 species in solution. This

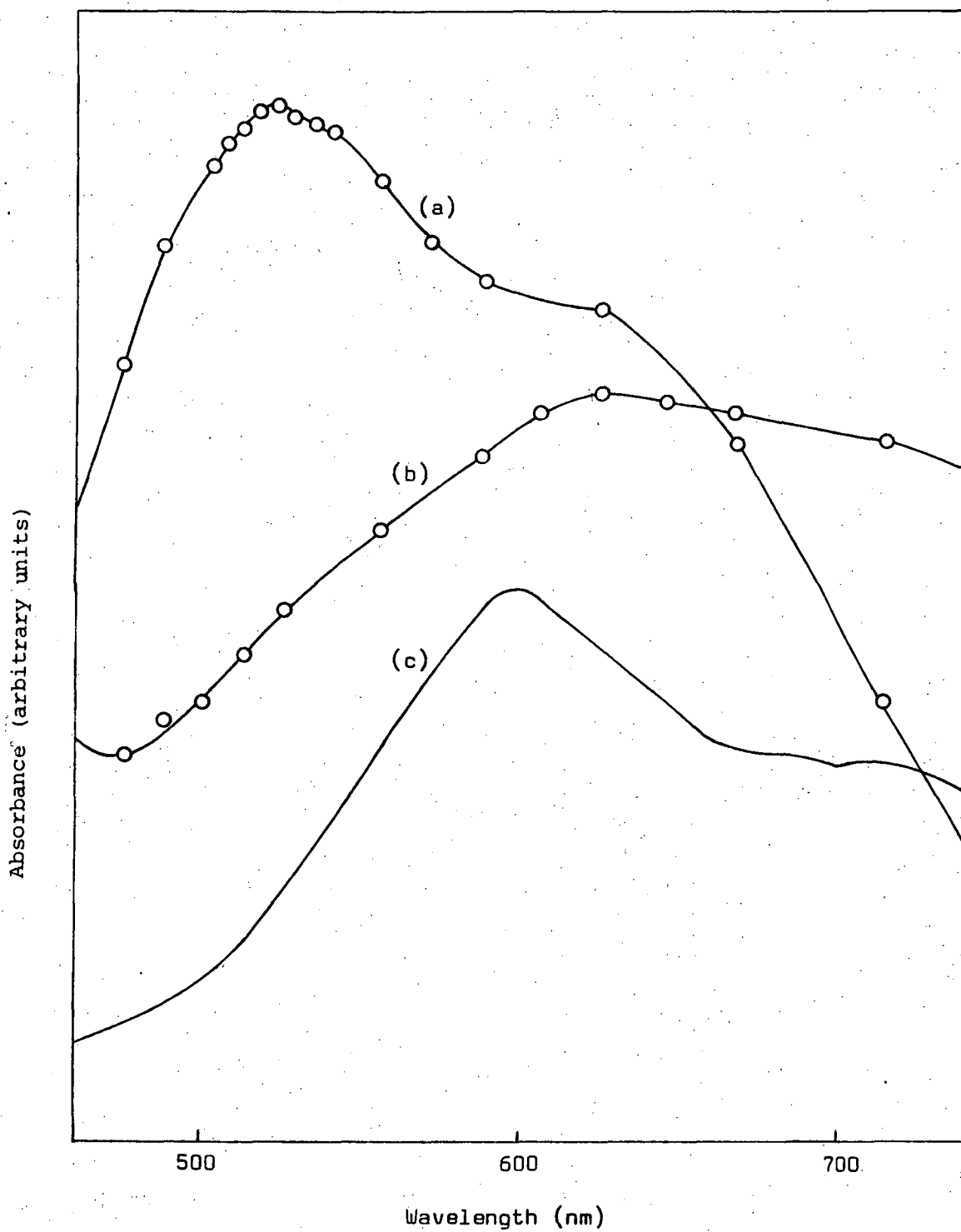


**Figure 34.** Visible spectra for

(a) solid  $\text{Ti}(\text{HSO}_4)(\text{SO}_4)(\text{H}_2\text{O})_4 \cdot 0.11\text{H}_2\text{SO}_4$

(b) solid  $\text{Ti}(\text{HSO}_4)(\text{SO}_4) \cdot 0.11\text{H}_2\text{SO}_4$

(c) 0.042M  $\text{Ti}(\text{III})$  in 92%  $\text{H}_2\text{SO}_4$  ( $\epsilon_{598} \approx 5$ ).

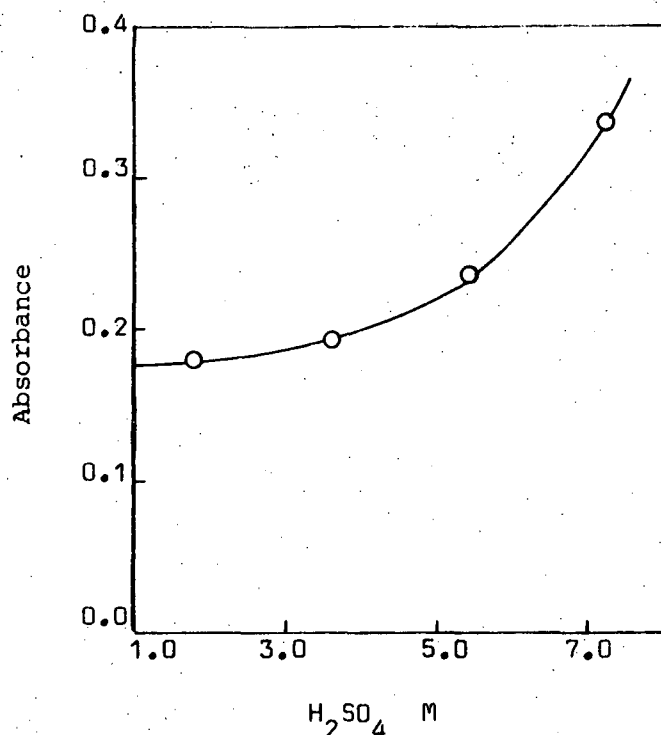


Figure 35. Absorbance data at 527 nm for titanium(III) in sulphuric acid solutions  $[\text{Ti(III)}] = 0.01\text{M}$ . Path length = 5.017 cm. Values taken from reported spectra<sup>63</sup>.

correlation becomes more obvious when the formula of the salt is rearranged and factorised by 2 giving  $\text{H}[\text{Ti}(\text{SO}_4)_2(\text{H}_2\text{O})_4]$ . i.e. The violet compound is the acid salt of the 1:2 complex.

Since sulphate ion can act as a uni-, bi- and tri-dentate ligand<sup>67</sup> and the degree of the hydration does not always reflect the number of water molecules co-ordinated<sup>68</sup>, the actual bonding arrangement around the central titanium(III) ion must be considered carefully. As no evidence for the loss of only  $2\text{H}_2\text{O}$  on heating, forming a  $\text{HTi}(\text{SO}_4)_2(\text{H}_2\text{O})_2$  species, or the uptake of only  $2\text{H}_2\text{O}$  hygroscopically by the anhydrous salt was observed,

it seems very likely that all 4 waters are co-ordinated. That is, the sulphate ion is acting as a unidentate ligand. Infrared studies supported this. Both compounds gave three SO stretching/ frequencies in the region  $1200-1000\text{ cm}^{-1}$ , and studies of other metal sulphate compounds suggest that three SO stretching/ frequencies are observed for unidentate sulphate groups with four stretchings being observed in the bidentate case<sup>69</sup>. As well the salts show some characteristics of the spectra reported for bisulphate salts<sup>70</sup>. This is not surprising as in sulphuric acid at the concentrations which the salt precipitates, bisulphate ion and sulphate ion are the main anionic species in solution<sup>60,61</sup>. Thus the proton in the salt is most probably located on a sulphate ion giving the structure  $\text{Ti}(\text{HSO}_4)(\text{SO}_4)(\text{H}_2\text{O})_4$ . This leaves little doubt that the structure of the 1:2 species both in solution and as a solid contains 4 waters co-ordinated.

The formation of 1:2 metal sulphate complexes in solution has been reported for Sc(III), many of the lanthanides and actinides, Cr(III), Fe(III), Co(III), Ru(III), Al(III) and In(III)<sup>25</sup>. Vanadium(III) and iron(III) salts corresponding to the violet tetrahydrate have also been reported i.e.  $\text{V}(\text{HSO}_4)(\text{SO}_4)(\text{H}_2\text{O})_4$ <sup>71</sup> and  $\text{Fe}(\text{HSO}_4)(\text{SO}_4)(\text{H}_2\text{O})_4$ <sup>72</sup>. However this is the first time that titanium(III) sulphate species have been identified in dilute sulphate solutions, and also the first time that the nature of the pale violet salt has been determined. It is worth noting that this latter compound is stable in air (a sample having been stored in air in a vacuum desiccator over KOH for about 12 months without decomposition being observed) and may be a convenient way of storing a water soluble source of titanium(III).

Dehydration of the pale violet salt causes it to change to pale blue and analysis shows that this blue compound has a titanium(III) content of 19.03% corresponding to a formula weight of 252. By comparing this formula weight with that for the violet salt i.e. 324, the difference is 72 atomic weight units. i.e. The loss of exactly  $4\text{H}_2\text{O}$  had occurred confirming that the pale blue compound is the anhydrous salt  $\text{Ti}(\text{HSO}_4)(\text{SO}_4)$ . This

blue compound has an absorption maximum at 630 nm (see Figure 34). Solutions with a very high sulphuric acid concentration containing titanium(III) have a similar blue color. The spectrum of 0.04M titanium(III) in 92% sulphuric acid is given in Figure 34. Similar observations have been reported by other workers<sup>59,63</sup>. The variation of the position of maximum absorbance with sulphuric acid concentration for titanium(III) in concentrated sulphuric acid solutions is shown in Figure 36. Extrapolation of the curve to 100% sulphuric acid gives the position of maximum absorbance at about 630 nm, corresponding to that for the anhydrous 1:2 complex. This is consistent with the behaviour of concentrated sulphuric acid as a desiccant. The structure of this blue anhydrous 1:2 complex could involve tridentate sulphate groups (as in other anhydrous 1:2 metal sulphate complexes<sup>67</sup>) or a polymeric structure involving bidentate or even possibly unidentate, sulphate groups. However as the position of maximum absorbance has shifted considerably (630 nm compared with 520 nm) and the extinction coefficient of the species in solution is relatively low  $\sim 3^{59,63}$ , it is not likely to be a polymeric species but rather to contain tridentate sulphate groups.

This is the first time that the nature of the blue titanium(III) species present in concentrated sulphuric acid solutions has been understood and also the first time that the anhydrous blue titanium(III) sulphate compound has been prepared and characterised.

#### 4.3 Oxidation Studies

##### 4.3.1 Experimental

No data on the formation of mixed oxidation state titanium species in dilute sulphate solutions appears to be available, so a spectrophotometric study was made of the behaviour of titanium(III) during its oxidation by air in 0.9M  $(\text{NH}_4)_2(\text{SO}_4)$  solution. This sulphate ion concentration was used to avoid the precipitation of white titanium(IV) hydrated oxide which was observed to occur when solutions containing titanium(III) and low sulphate ion concentrations (less than about 0.6M) were oxidised by air. The

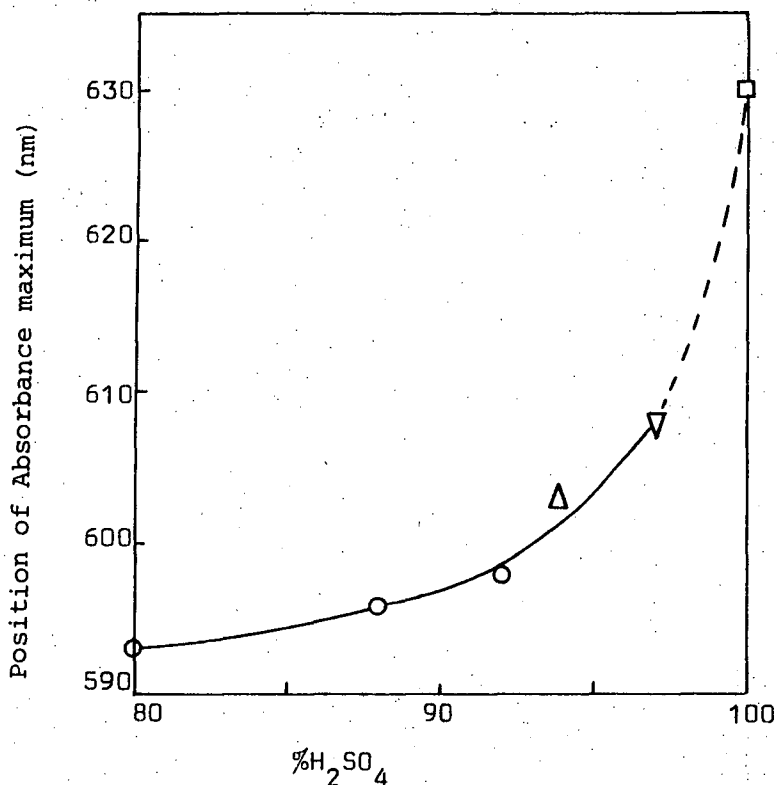


**Figure 36.** Variation of peak position with sulphuric acid concentration for titanium(III) in strong sulphuric acid solutions.

O ~ This work, Δ ~ Arris and Duffy<sup>59</sup>,

▽ ~ Goroshchenko and Godneva<sup>63</sup>

□ ~ solid  $\text{Ti}(\text{HSO}_4)(\text{SO}_4)$  (anhydrous).

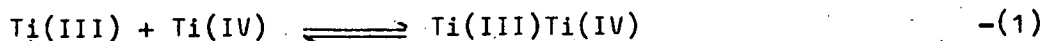
procedure used involved following the changes in the spectra of solutions with time as they were allowed to equilibrate in air. The titanium(III) content of the solution was determined by direct titration (see Chapter 2.2) immediately following the absorbance measurements.

#### 4.3. 2 Results

When solutions containing titanium(III) ions and sulphate ions were allowed to stand in air they were observed to change slowly in color from blue to reddish brown, then brown, then fade gradually to eventually become colorless. An example of the change of the titanium(III) content (% oxidation) with time for a solution, is shown in Figure 37. Some of the solution spectra at various stages during the oxidation are given in Figure 38 (also see absorbance data tables 18 and 19, Appendix 14). These show that as the titanium(III) content decreases due to oxidation to titanium(IV), the absorbance of the solution increases strongly in the first part and then gradually decreases back to zero, corresponding to the colorless clear fully oxidised solution. During the oxidation process the position of the absorbance maximum gradually shifts from 530 nm towards 480 nm.

#### 4.3. 3 Discussion

The dark color of sulphuric acid solutions containing titanium(III) and titanium(IV) has been known for some time<sup>40,48</sup> and examination of early spectrophotometric data<sup>48</sup> shows that approximately a 1:1 titanium(III):titanium(IV) complex is formed. A detailed study<sup>63</sup> of the formation of mixed oxidation state species in 1.8 to 10.8M H<sub>2</sub>SO<sub>4</sub> confirmed the formation of a 1:1 species with a characteristic absorbance maximum of 472 nm. No formation constant was determined. However, by replotting the reported absorbance data (see Figure 39) and using the method outlined in Appendix 13, the formation constant for the reaction



was calculated to be  $9.5 \pm 0.7$  i.e.  $\log K = 1.0$ . This is the first time that the formation constant for the titanium mixed oxidation state species in sulphuric acid solutions has been reported.



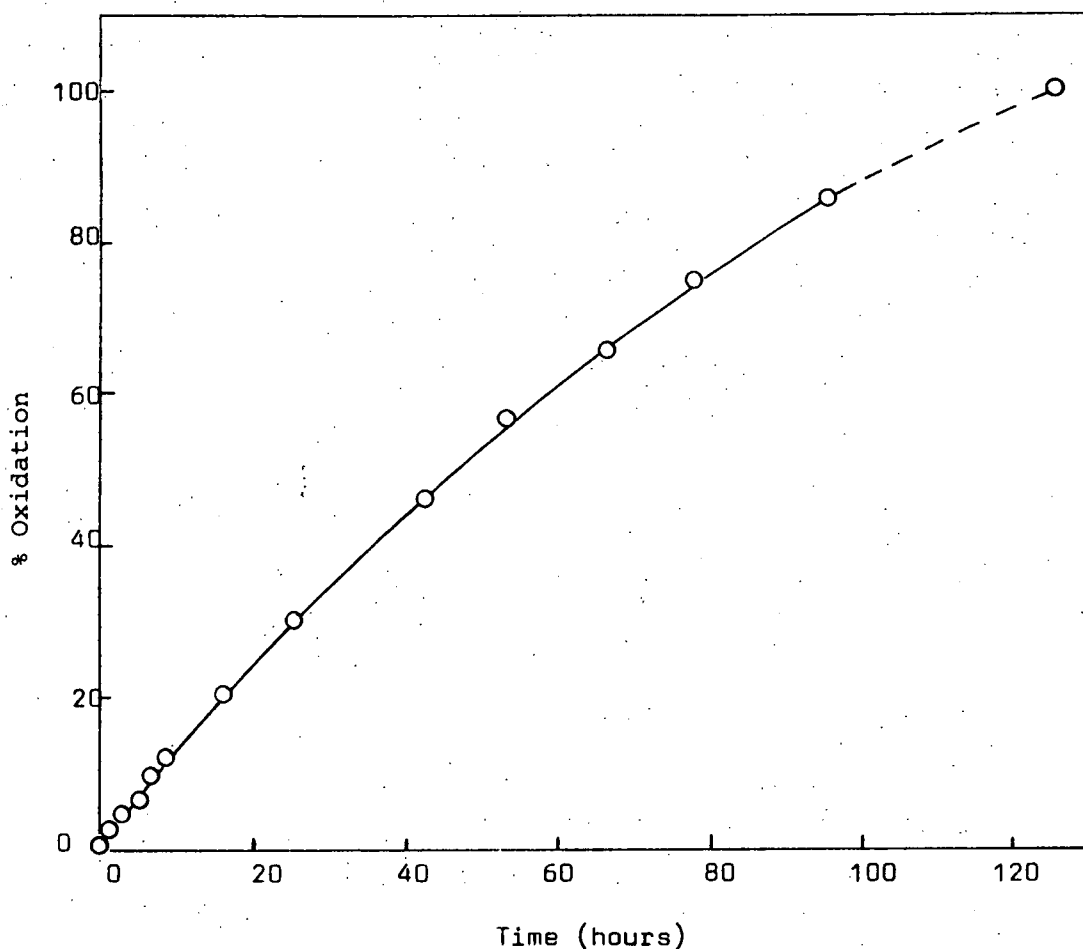
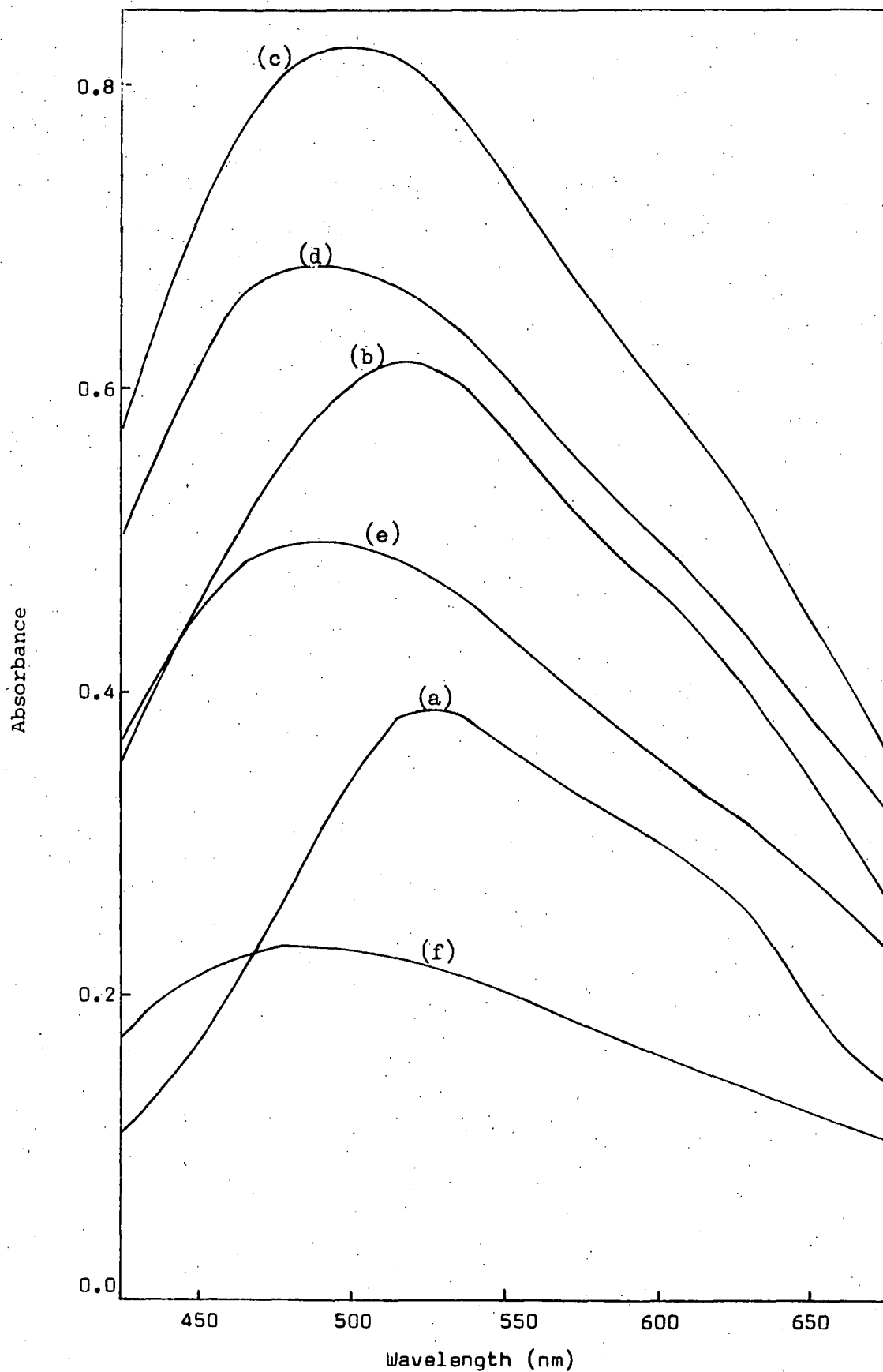


Figure 37. Rate of oxidation (in air) of titanium(III) in sulphate media. Temperature  $\sim 25^{\circ}\text{C}$

$$[\text{Ti(III)}] = 0.0826\text{M}, [\text{Cl}^-] = 0.478\text{M}, [(\text{NH}_4)_2\text{SO}_4] = 0.894\text{M}.$$

The results of the study, in this work, of the oxidation of titanium(III) show that a mixed oxidation state species is also formed in dilute sulphate media. Since the ionic strength and total titanium concentration were constant during the study, the spectra Figure 38 correspond to a continuous variation of titanium(III) and titanium(IV). Job difference plots of the data (Appendix 14) at 530 nm and 476 nm (Figure 40) suggest the formation of a 4:1 titanium (III):titanium(IV) mixed oxidation state species. The ratio of the



**Figure 38.** Spectra of titanium(III) solutions at different

stages of oxidation. Mole fraction of titanium(IV) was

0.000(a), 0.045(b), 0.203(c), 0.460(d), 0.656(e), 0.856(f).

$[\text{Ti}]_{\text{total}} = 0.0826\text{M}$ ,  $[\text{Cl}^-] = 0.478\text{M}$ ,  $[(\text{NH}_4)_2\text{SO}_4] = 0.894\text{M}$

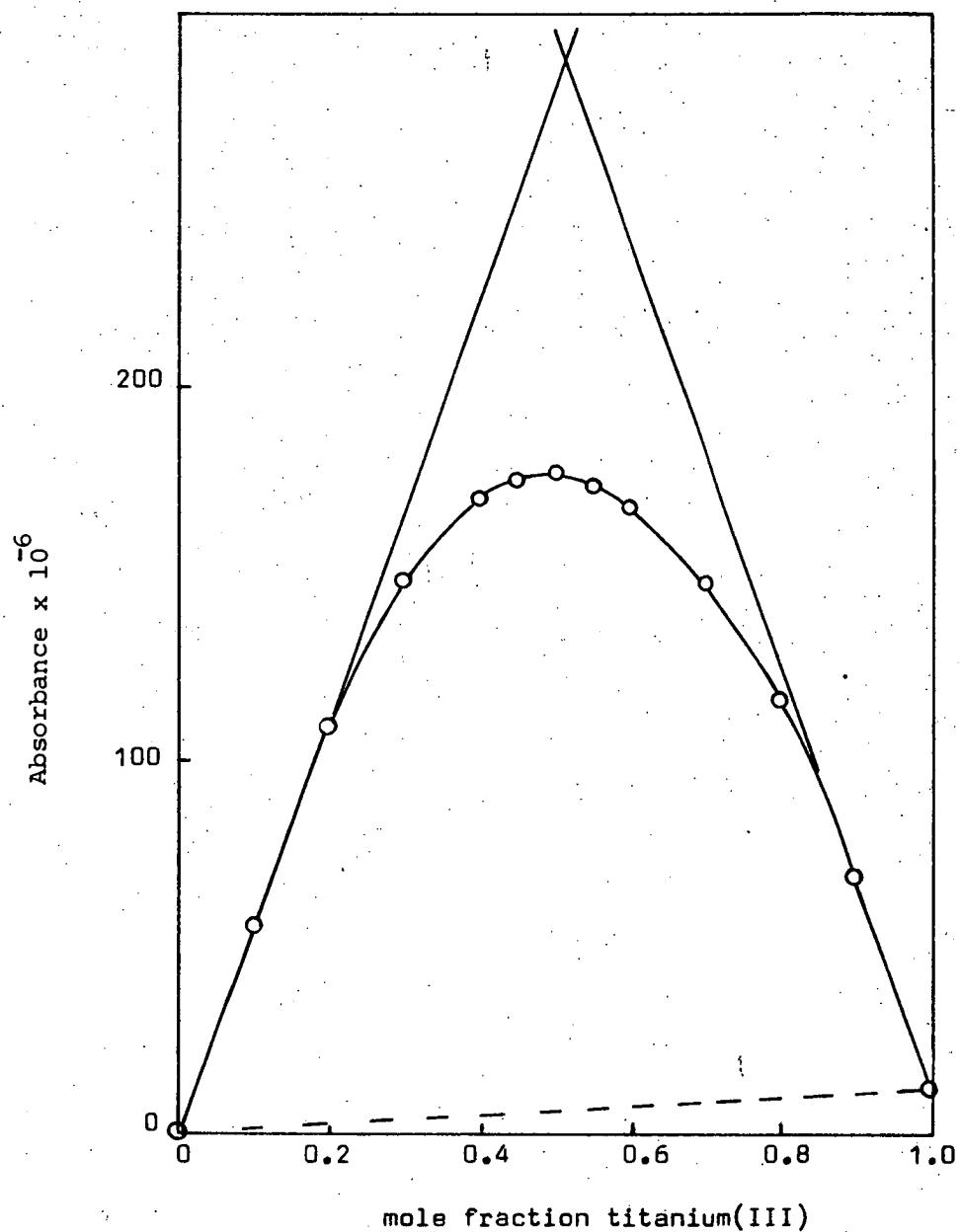
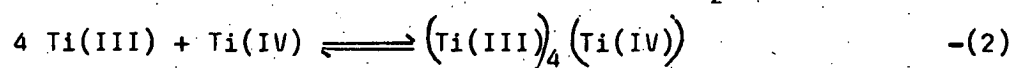


Figure 39. Reported absorbance data for titanium(III) titanium(IV) continuous variation solutions in 20% sulphuric acid<sup>63</sup>. (1 cm cells).

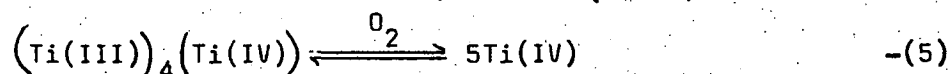
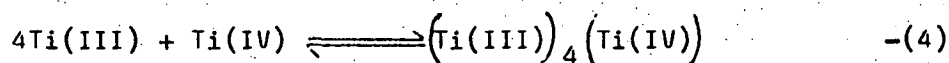
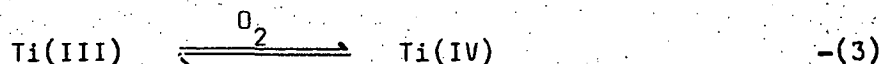
$$[\text{Ti}]_{\text{total}} = 0.001094\text{M.}$$

slope of the tangents drawn in Figure 40 is 4:1 and  $\Delta D_{\text{max}}$  occurs at  $\sim 20\%$  Ti(IV). From the Job plot data the value of  $K_2$  for the reaction



was calculated to be  $18 \pm 5$  i.e.  $\log K = 1.3$  (see Appendix 14). Thus in dilute sulphate solutions the mixed valence titanium species formed is of a different nature and more stable than the corresponding species formed in strong sulphuric acid solutions.

A simple mechanism for the oxidation process is given by equations 3-5



since the percentage oxidation versus time curve (Figure 37) shows that the rate of oxidation decreases uniformly, reaction(3) probably predominates with the mixed valence species being more stable to oxidation. Thus the initial rate (initial slope of curve Figure 37) is indicative of the rate of oxidation of titanium(III), (reaction(3)), which is faster in sulphate solutions than in thiocyanate solutions (compare Figure 24).

This is in agreement with other workers who have observed that the presence of thiocyanate ions reduces the rate of oxidation by oxygen of titanium(III) chloride solutions<sup>3</sup>, while dilute sulphuric acid catalyses the oxidation<sup>73</sup>.

Also in this study it was noticed that the presence of only a small amount of titanium(IV), i.e. during the early stages of oxidation, caused the absorbance of the solution to increase quite considerably (see Figures 38 and 40). The effect of a small amount of oxidation on the extinction coefficient of titanium(III) is given in Figure 41, and shows that after 5% oxidation the extinction coefficient has almost doubled due to the formation of the mixed oxidation state species. Consequently only a fraction of a percent of oxidation results in large errors in extinction coefficient. By comparing the percent oxidation versus time data given in Figure 37, with data in Figure 41, the observed extinction coefficient of a fresh titanium(III) sulphate solution exposed to air, would increase by 1% every 2.2 minutes. This explains the difficulty in obtaining accurately

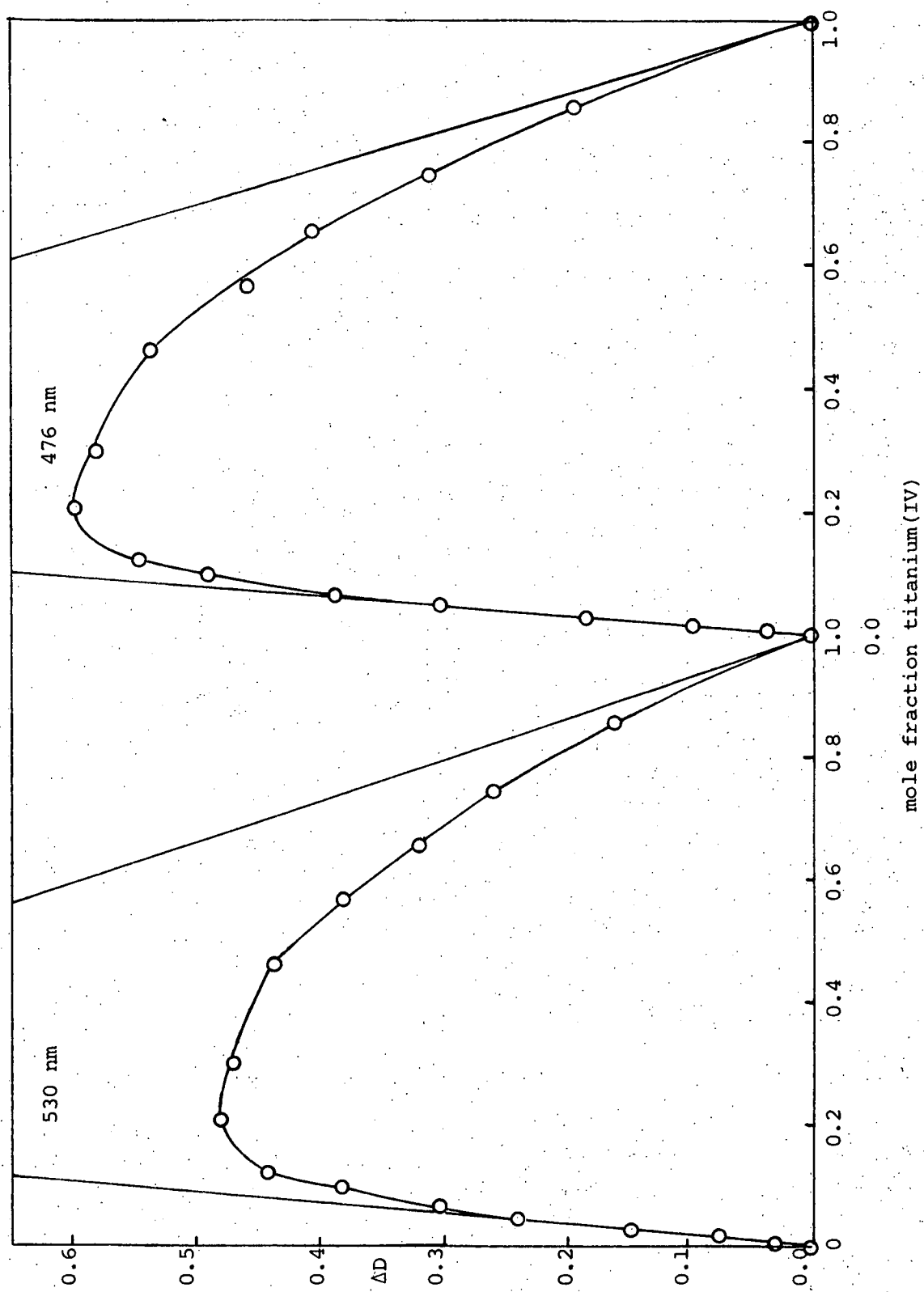


**Figure 40.** Job difference plots for titanium(III) titanium(IV) continuous variation solutions.

$$[\text{Ti}]_{\text{total}} = 0.0826\text{M}, [\text{Cl}^-] = 0.478\text{M}, [(\text{NH}_4)_2 \text{SO}_4] = 0.894\text{M}$$

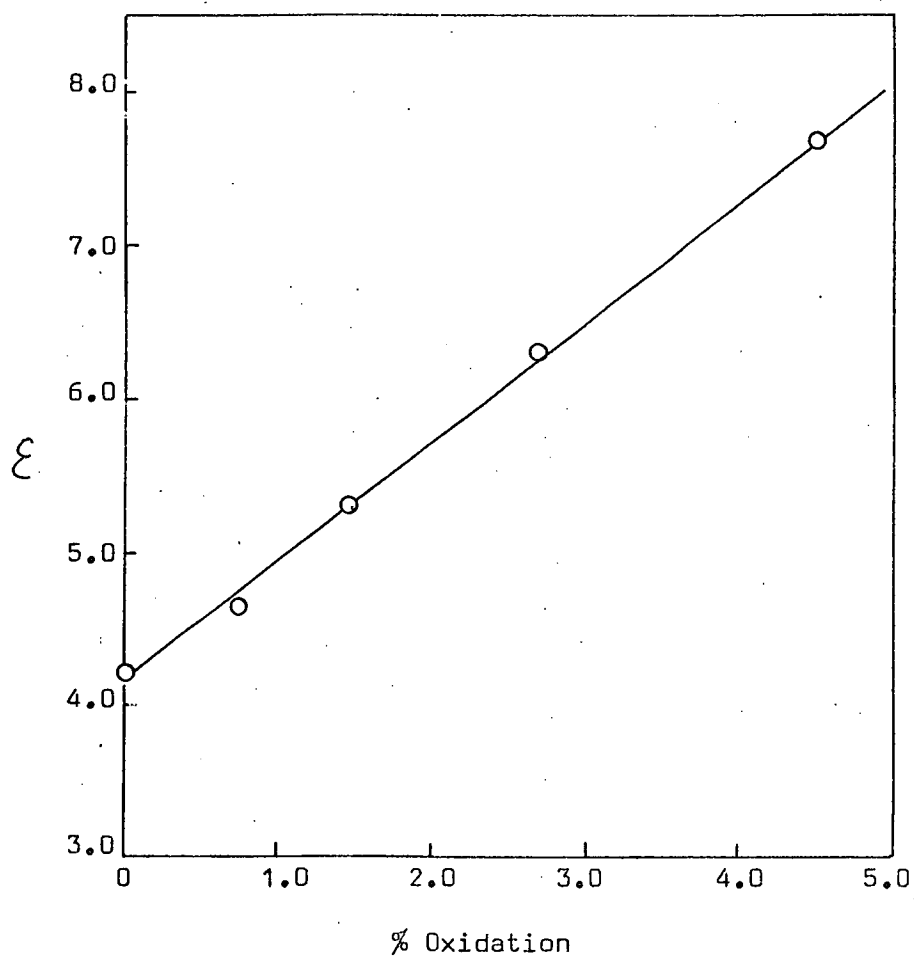


**Figure 41.** Variation of the apparent extinction coefficient of titanium(III) ( $\epsilon$ ) during the early stages of the oxidation of titanium(III) in sulphate media.

$$\epsilon = \frac{(\text{absorbance at } 500.5 \text{ nm})}{(\text{Ti (III) content of solution (moles l}^{-1}\text{)})}$$

$$[\text{Ti}]_{\text{total}} = 0.826\text{M}, [\text{Cl}^{-}] = 0.478\text{M}, [(\text{NH}_4)_2\text{SO}_4] = 0.894\text{M}.$$

reproducible spectral data when studying titanium(III) sulphate systems.

Because a straight line relationship between absorbance and

percent oxidation is observed during the early stages of oxidation (see Figures 40 and 41) this phenomena could have a useful analytical application. That is, a single absorbance measurement on a titanium(III) sulphate solution of known titanium(III) content could be used to give the amount of oxidation which had occurred (i.e. the amount of titanium(IV) present) providing a calibration curve had been prepared for the particular sulphate concentration of the solution used (such as in Figure 41). This is a much simpler, faster and more accurate method than the alternative methods<sup>74</sup> available.

The results presented in this section have shown that titanium mixed oxidation state species form in dilute sulphate solutions, as well as in strong sulphuric acid solutions. For the first time stability constants for these mixed valence species have been determined. Also it has been demonstrated that the formation of these species must be considered when making accurate spectrophotometric measurements of aqueous titanium(III) sulphate systems.

#### 4.4 Hydrolysis Studies

##### 4.4.1 Experimental

As no data on the hydrolysis of titanium(III) in aqueous sulphate media has been reported, a study of this system was carried out. The hydrolysis behaviour at high and low sulphate ion concentrations under both initial and equilibrium conditions were investigated. Ammonium sulphate was again used to vary the sulphate ion concentration. The maximum workable concentration was limited to less than 4 molar.

Rapid potentiometric titrations were used to study the species initially formed. To determine the metal:hydroxide ion ratio at different sulphate ion strengths, titanium(III) solutions containing sulphate ion concentrations ranging from 0 to 4M were titrated with  $\text{NH}_4\text{OH}$ . The procedure used for the titrations was the same as that described earlier

in Chapter 2.2. To determine the number of sulphate groups present in the titanium(III) hydroxy sulphate species formed, a series of solutions containing a range of sulphate ion concentrations were titrated with increasing aliquots of base, the pH being quickly measured immediately after each addition.

For studies of the hydrolysis species present under equilibrium conditions, series of individual solutions containing fixed titanium(III) and sulphate ion concentrations and varying concentrations of base were prepared and equilibrated. The procedure used was the same as that described in Chapter 2.2 for the equilibrium studies of the hydrolysis in chloride media. pH measurements were again made to determine the metal:hydroxide ion ratio for the hydrolysis species. The variation of the titanium(III) content of the solutions was noted to check the stoichiometry of the hydrolysis reaction. Also, visible spectra for some of the solutions were recorded to provide additional information about the hydroxy sulphate species present.

#### 4.4. 2 Results

##### (a) Initial hydrolysis behaviour

Some rapid pH titration curves (total time 3 minutes) for titanium(III) solutions containing different sulphate ion concentrations are shown in Figure 42. The presence of a small amount of sulphate ion caused significant changes in pH values and the shape of the titration curve. As the sulphate ion concentration was increased further the pH values slowly increased. The variation of pH with sulphate ion concentration is shown in more detail in Figure 43.

##### (b) Equilibrium hydrolysis behaviour

The equilibrium potentiometric titration curve for titanium(III) in dilute sulphate media is given in Figure 44. Each pH value shown was obtained from individually equilibrated solutions. The corresponding



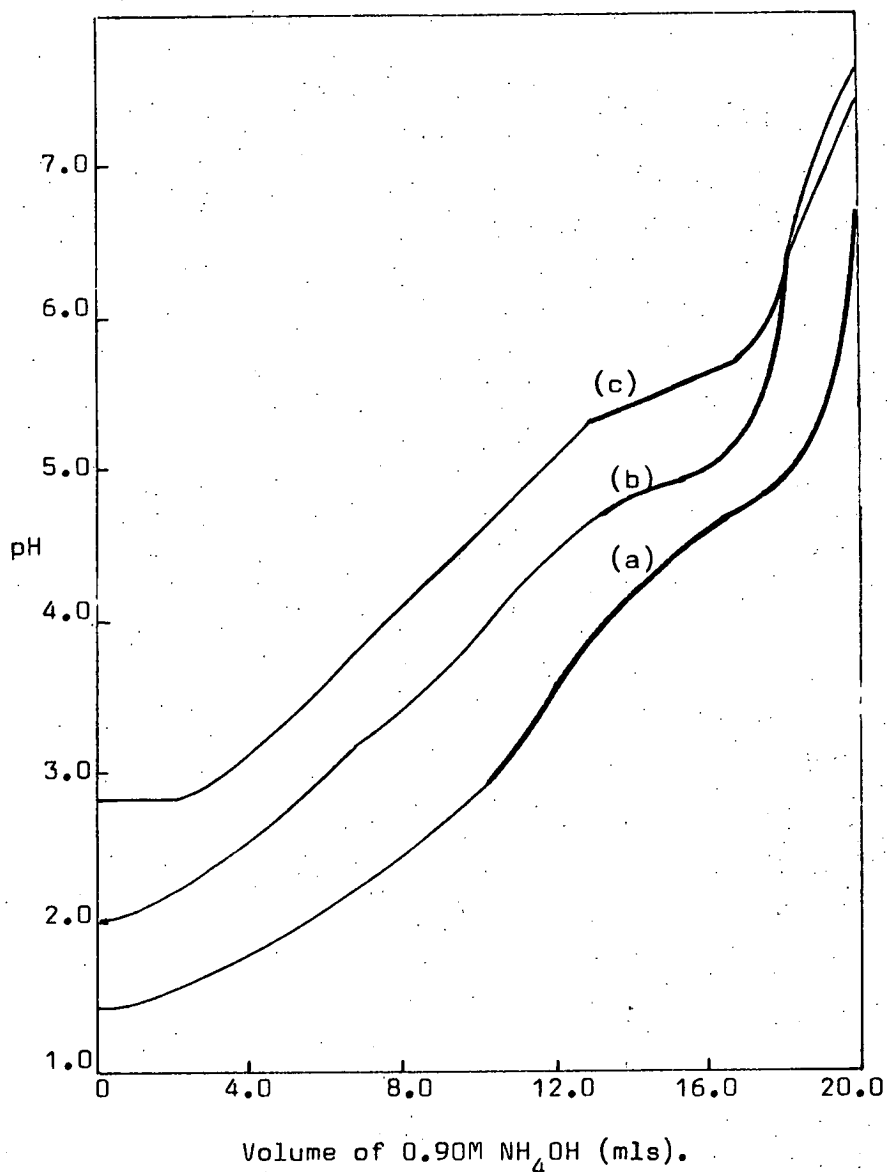


**Figure 42.** Rapid titration curves for titanium(III) solutions containing varying sulphate ion concentrations.

$[\text{Ti(III)}] = 0.0573\text{M}$ ,  $[\text{Cl}^-] = 0.241\text{M}$ ,

$[(\text{NH}_4)_2\text{SO}_4] = 0.00\text{M(a)}, 0.53\text{M(b)}, 3.73\text{M(c)}.$

Initial volume = 75 mls.

$1.0 \bar{n} = 4.775 \text{ mls.}$  ————— = apparent region of precipitation.

variation of the titanium(III) concentration in solution is also plotted.

In region (a) a purple solution was present; in region (b) the solution was

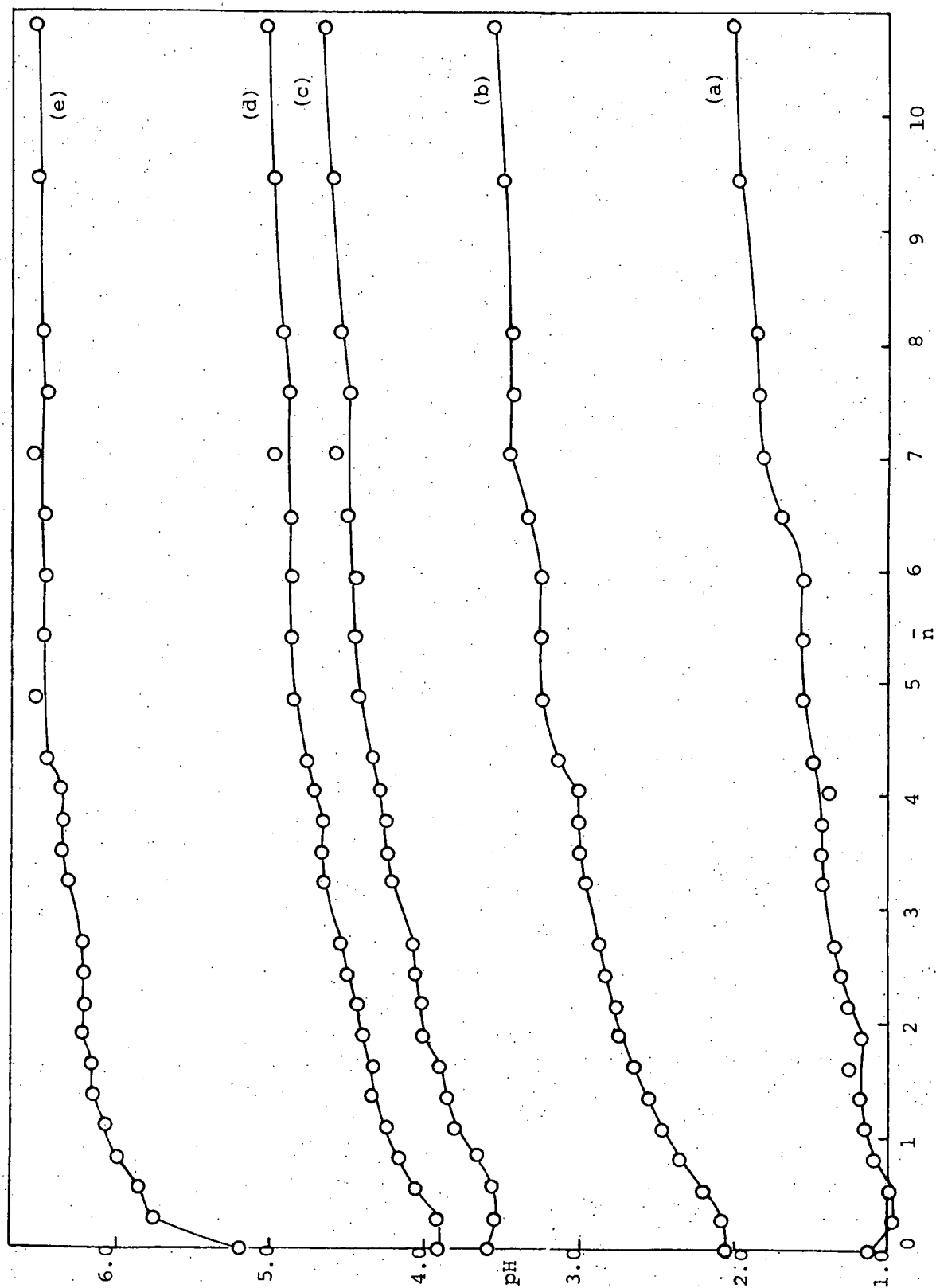


**Figure 43.** pH of titanium(III) solutions, containing varying amounts of sulphate ion, immediately after the addition of 0.0(a), 2.0(b), 3.0(c), 4.0(d), 5.0(e) mls of 1.79M  $\text{NH}_4\text{OH}$ .  $\bar{n}$  = ratio  $\left[ \text{SO}_4^{2-} \right] : \left[ \text{Ti(III)} \right]$ .  $\left[ \text{Ti(III)} \right] = 0.0928\text{M}$ ,  $\left[ \text{Cl}^- \right] = 0.478\text{M}$  Initial volume = 25 mls.

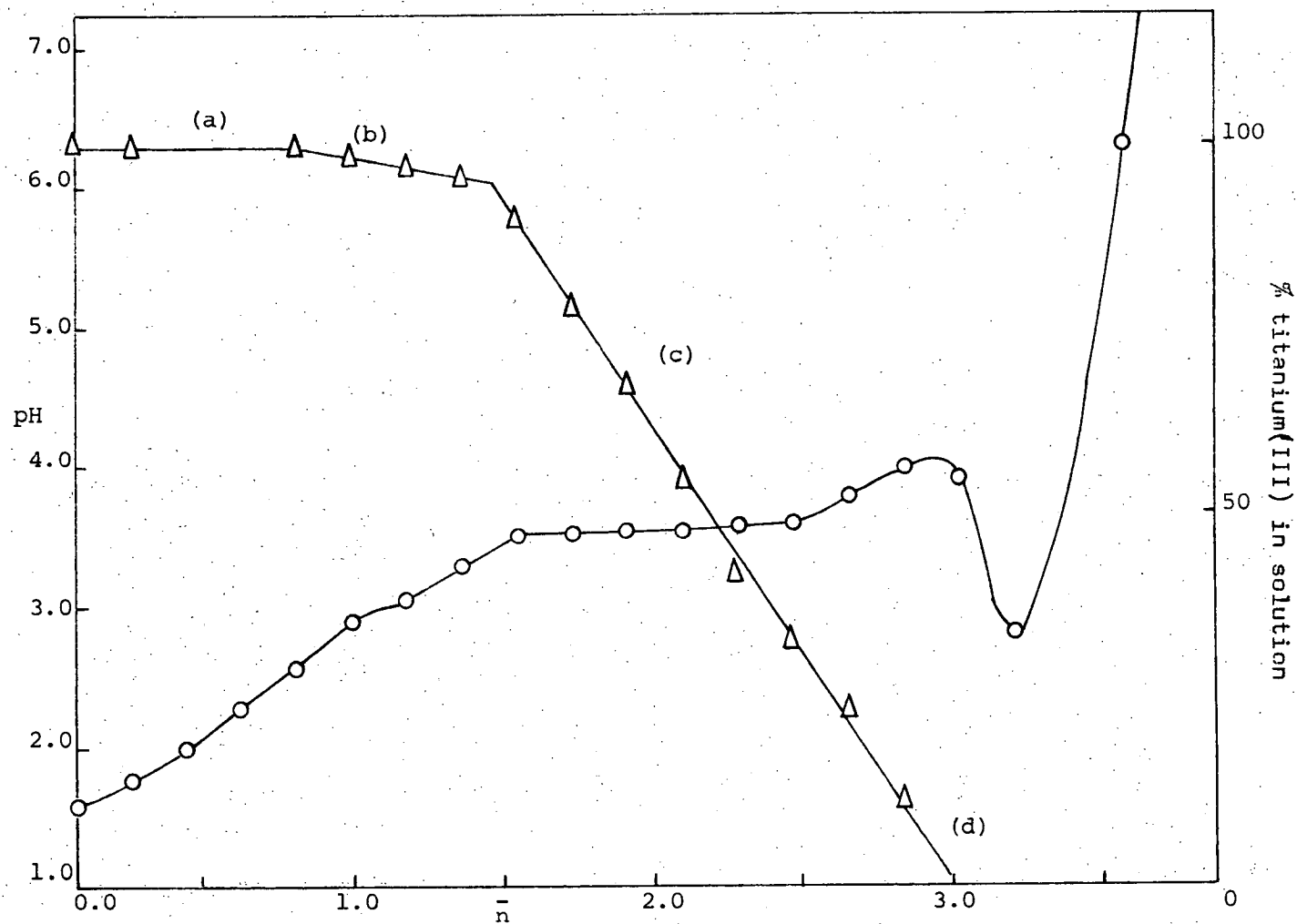


**Figure 44.** Equilibrium pH data and titanium(III) concentration values for titanium(III) sulphate solutions containing varying amounts of sodium hydroxide.  $\bar{n}$  = ratio  $[\text{OH}^-] : [\text{Ti(III)}]$   
 $[\text{Ti(III)}]_{\text{Total}} = 0.0848\text{M}$ ,  $[\text{SO}_4^{2-}] = 0.148\text{M}$ . O~ pH value,  $\Delta$ ~ concentration value.

darker and a small amount of a dark precipitate was present; in region (c) a reddish brown solution was present above a brown precipitate. The intensity of the color of the solution uniformly decreased to zero in this latter region. No hydrogen evolution was observed. In region (d) a clear solution was present above a dark blue precipitate and slow hydrogen evolution was observed. Spectra of the solutions at various stages of the hydrolysis are shown in Figure 45.

The equilibrium potentiometric titration curve and titanium (III) analysis data for solutions containing a high sulphate ion concentration are shown in Figure 46. In region (a) two stepwise primary hydrolysis equilibria were observed suggesting the formation of a soluble  $1:2 \text{ OH}^-:\text{Ti(III)}$  species and a soluble  $1:1 \text{ OH}^-:\text{Ti(III)}$  species. In solutions where  $\bar{n} > 1.0$  secondary hydrolysis occurred and hydrogen evolution was also observed resulting in the formation of the dark blue species. In region (c) a dark blue precipitate had settled but in region (b) no precipitate was present, there being instead an intensely dark blue solution. The rate of decrease in the titanium(III) concentration in this region was 1.0 Ti(III) per 4.0  $\text{OH}^-$  added. When excess hydrochloric acid was added to an aliquot of the dark blue solution a cloudy white precipitate formed indicating the presence of titanium(IV). Spectra of the solutions at various stages of the hydrolysis are shown in Figure 47.

#### 4.4.3 Discussion

The study of the initial hydrolysis behaviour of titanium(III) in sulphate solutions has shown that quite different reactions occur compared with that in chloride media. The change in the shape of the potentiometric titration curves in the presence of sulphate ion (see Figure 42) is indicative of the formation of hydroxy sulphate complexes. The hydrolysis of the hexaquo titanium(III) ion proceeds via the formation of a soluble  $1:1 \text{ Ti:OH}^-$  species followed by the precipitation of  $\text{Ti(OH)}_3$ .

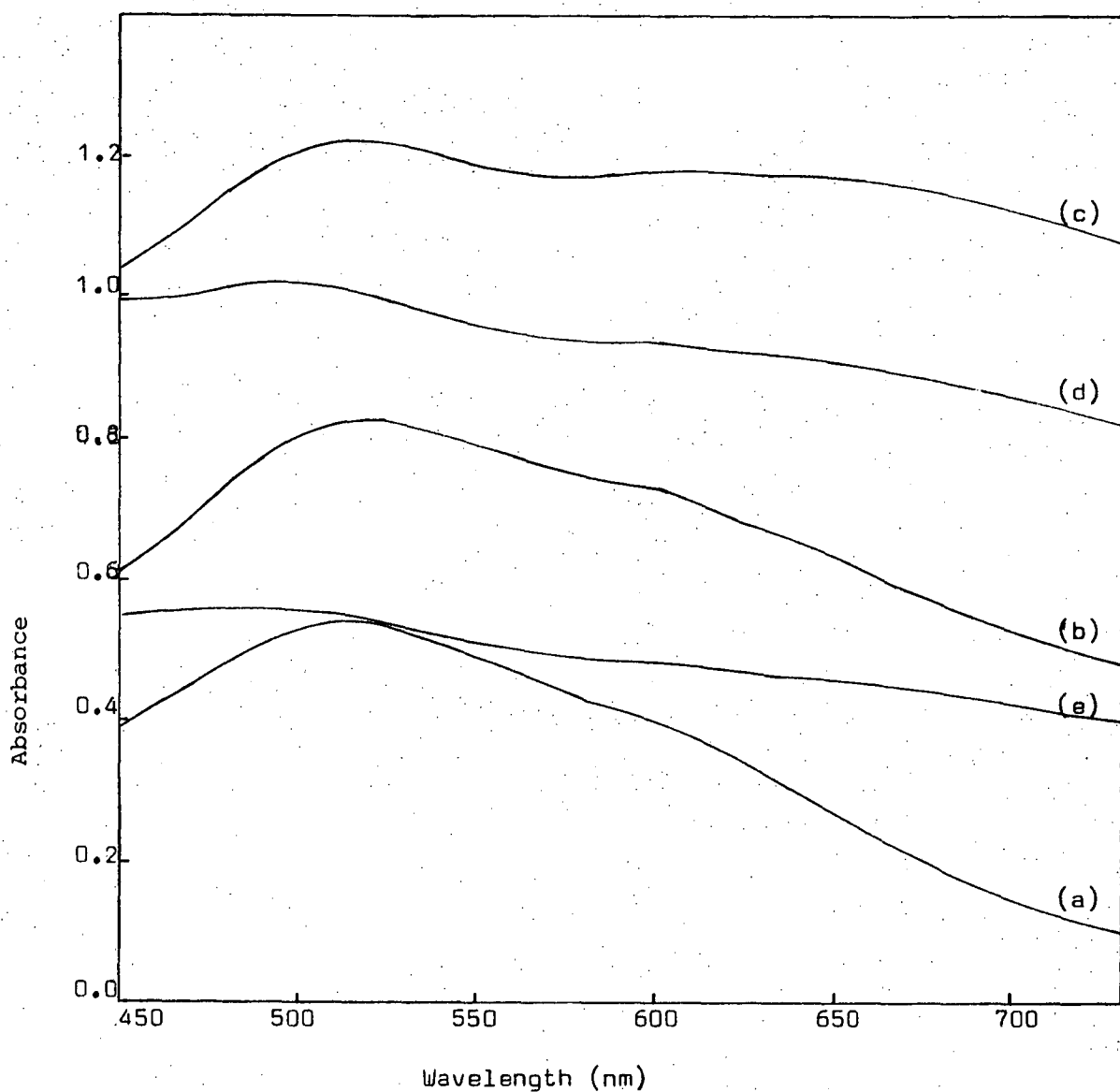


**Figure 45.** Spectra of titanium(III) sulphate solutions at different stages during hydrolysis, using 1 cm cells.  $\bar{n} = 0.08(a)$ ,  $0.81(b)$ ,  $1.19(c)$ ,  $2.10(d)$ ,  $2.48(e)$ .  $[Ti(III)] = 0.082M$ ,  $[SO_4^{2-}] = 0.148M$ .

as further base is added in the region  $1 < \bar{n} < 3$ . In dilute sulphate solutions, providing sufficient sulphate ion is present to complex with all the titanium(III), the hydrolysis firstly proceeds via the formation of a soluble 1:2  $Ti:OH^-$  species. Because of the very dark color of the

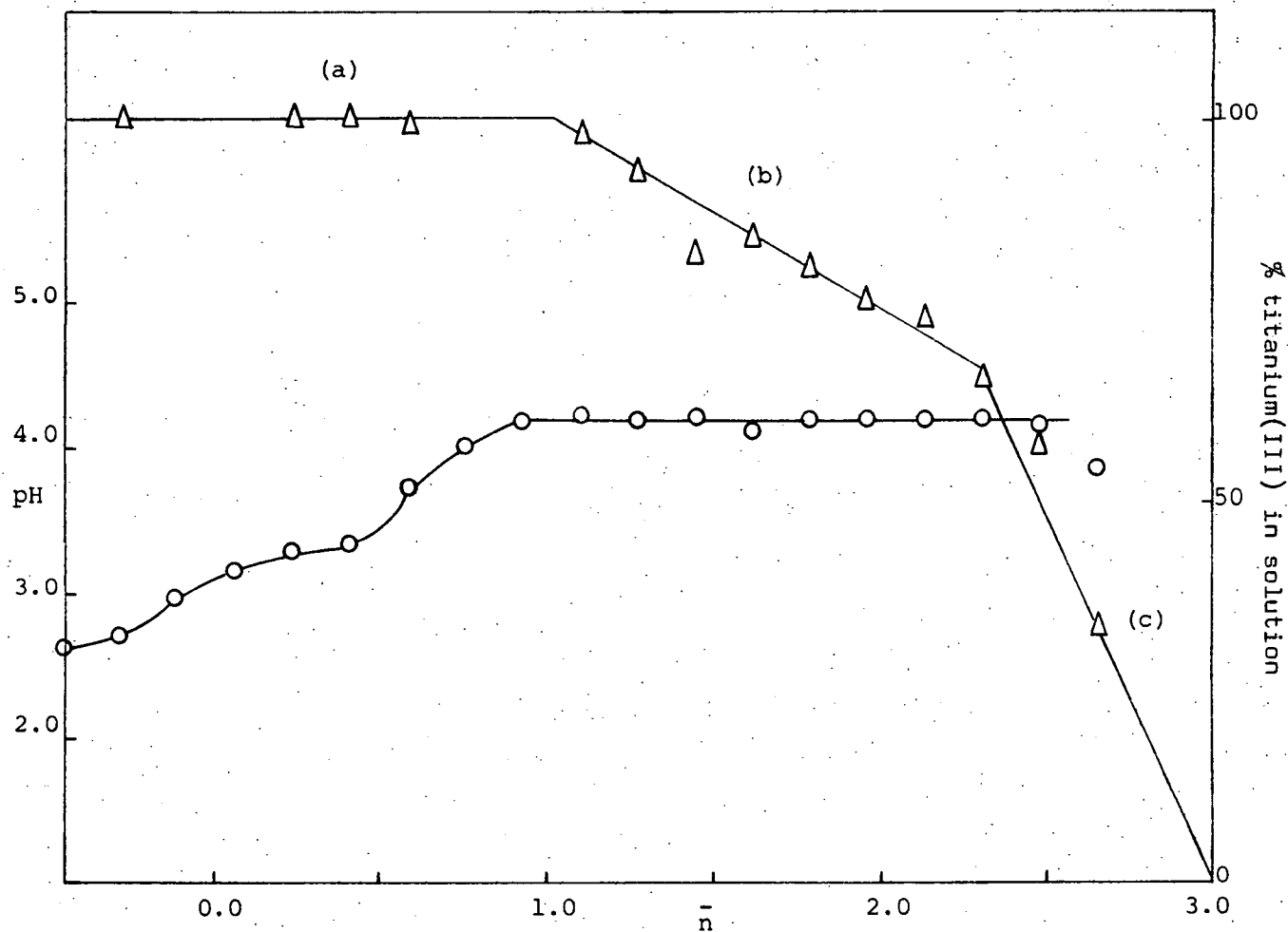


Figure 46. Equilibrium pH data and titanium(III) concentration values for titanium(III) sulphate solutions containing varying amounts of ammonium hydroxide.

$[\text{Ti}]_{\text{Total}} = 0.0840\text{M}$ ,  $[\text{SO}_4^{2-}] = 3.04\text{M}$ . O~ pH value, Δ~ concentration value.

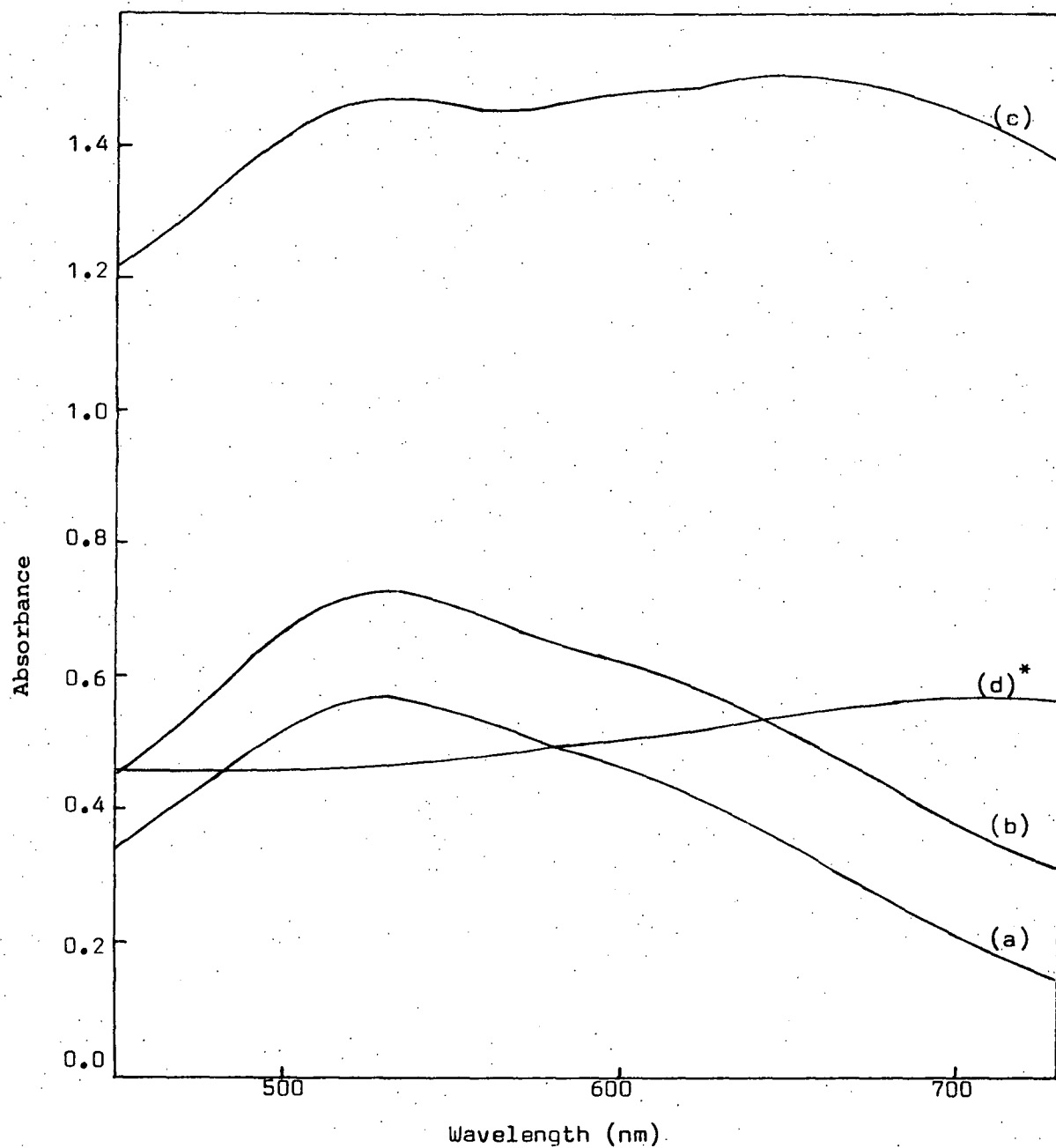


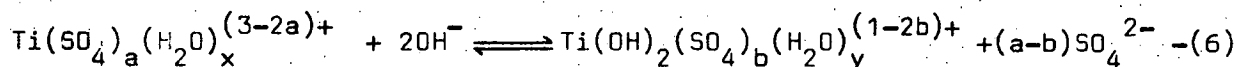
Figure 47. Spectra of titanium(III) sulphate solutions at different stages during hydrolysis, using 1 cm cells.  $\bar{n} = 0.00(a), 0.24(b), 0.59(c), 1.10(d)^*$ .  $[Ti(III)] = 0.084M$ ,  $[SO_4^{2-}] = 3.04M$

\* ~ 0.1 cm cells.

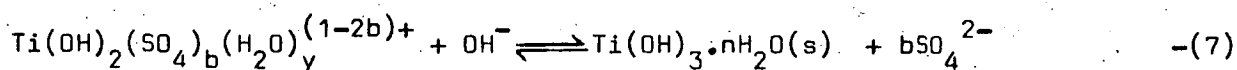
solutions it is very difficult to tell exactly when precipitation begins during these rapid titrations. However it appears that precipitation of brown  $Ti(OH)_3$  does not begin in the sulphate solutions until  $\bar{n} > 2$ .

Increasing the sulphate ion concentration does not change the shape of the titration curve i.e. there is no change in the overall stoichiometry of the hydrolysis reaction, but merely increases the pH values as higher concentrations of base are required for hydrolysis in lieu of the increased stability of the titanium sulphate complexes under these conditions.

Thus initially, when base is added to titanium(III) solutions containing sulphate ions, primary hydrolysis involves the formation of a soluble 1:2 Ti:OH<sup>-</sup> species



followed by secondary hydrolysis resulting from the uptake of another OH<sup>-</sup> group to form a brown precipitate of titanium(III) hydroxide



The attempt to determine the number of sulphate ligands involved in the primary hydrolysis hydroxy sulphate species, by studying in more detail the effect of sulphate ion concentration on the initial pH values was not successful. The relative changes in pH with respect to the change in sulphate ion concentration is quite small (see Figure 43) and tended to be gradual rather than stepwise. As a result, interpretation of the data is quite difficult and inconclusive. Also, because of the lack of stability data for titanium(III) sulphate species, and the complex nature of the system, no attempts were made to estimate hydrolysis constants.

Under equilibrium conditions, the hydrolysis behaviour was quite different.

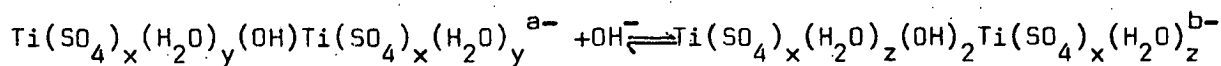
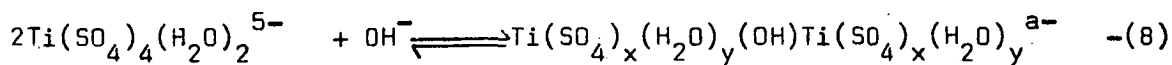
At low sulphate ion concentrations, the final hydrolysis behaviour was both unusual and complex. Firstly, two types of precipitate were observed to form, a brown precipitate and a small amount of black precipitate. Secondly, no hydrogen evolution was observed until after all the titanium(III) had been precipitated i.e. excess base was present. From the potentiometric titration curve Figure 44, the predominant primary hydrolysis reaction involves the formation of a soluble 2:3 Ti:OH<sup>-</sup> species



(up to  $\bar{n} = 1.5$ ) which requires  $1.5 \text{ OH}^-$  to precipitate brown titanium(III) hydroxide. However, because a small amount of a black precipitate (probably  $\text{TiO}(\text{OH}) \cdot n\text{H}_2\text{O}$ ) begins to form after  $\bar{n} = 1.0$ , this indicates that a lesser hydrolysis reaction is also taking place involving the formation of a soluble  $1:1 \text{ Ti}:\text{OH}^-$  primary hydrolysis species which requires  $2.0 \text{ OH}^-$  to precipitate the titanium. This type of mixed hydrolysis behaviour is not unexpected as titanium(III) forms several sulphate species in solution. Consequently the observed amount of base required for precipitation during secondary hydrolysis was  $1.62 \text{ OH}^-$ , compared with  $1.50 \text{ OH}^-$  for the predominant reaction and  $2.00 \text{ OH}^-$  for the lesser reaction.

Spectra of the solutions (see Figure 45) showed that in the primary hydrolysis region the absorbance increased with each additional aliquot of base added but only a very slight shift in the position of the absorbance maximum was observed. This suggests that the  $\text{OH}^-$  groups are simply replacing water molecules in the co-ordination sphere of the titanium(III) sulphate complex, probably forming an hydroxy bridged species e.g.,  $\text{Ti}_2(\text{OH})_3(\text{SO}_4)_x(\text{H}_2\text{O})_y$ . As the predominant titanium(III) sulphate complex is  $\text{Ti}(\text{SO}_4)_2(\text{H}_2\text{O})_4^-$  in dilute solutions,  $x$  is probably equal to 4. For the secondary hydrolysis region, the spectra confirmed that none of the dark blue mixed oxidation state hydroxy species was present. This is in agreement with the observation that no hydrogen was evolved.

Still different hydrolysis behaviour was observed in solutions high in sulphate ion concentration. The titanium(III) sulphate species present, prior to hydrolysis, in these solutions is  $\text{Ti}(\text{SO}_4)_4(\text{H}_2\text{O})_2^{5-}$ . From Figure 46 it can be seen that the primary hydrolysis of this titanium(III) sulphate complex involves the formation of two soluble species related by a stepwise equilibria i.e.



-(9)

The spectra of solutions in the primary hydrolysis region (Figure 47) show that significant changes in absorbance occur as the hydroxy species forms. However no noticeable peak shift was observed suggesting that again, as in dilute sulphate solutions, hydrolysis involves the replacement of co-ordinated water by bridging hydroxyl groups. Thus for equations (8) and (9) the most likely values for x, y and z would be 4, 1 and 0 respectively. In solutions where the second primary hydrolysis species forms, as in equation (9), very high absorbance values were obtained with a second peak appearing at approximately 640 nm. This suggests that a small amount of the dark blue secondary hydrolysis species may be in equilibrium, masking the spectrum of the latter primary hydrolysis species.

Where  $\bar{n} > 1$  the presence of the dark blue species having an intense absorption band in the 700-750 nm region (see Figure 47) and the evolution of hydrogen from these solutions show that a mixed oxidation state hydrolysis species is formed. The variation of the titanium(III) content of the solutions (see Figure 46) shows that under these conditions 1.0 Ti(III) is removed as Ti(IV) per 4.0  $\text{OH}^-$  added. This rate is the same as that observed for the secondary hydrolysis of titanium(III) in chloride media (Chapter 2) and thus confirms the formation of the 1:1 Ti(III):Ti(IV) hydroxy species.

Very few other trivalent metal hydroxy sulphate systems in solution have been investigated. Vanadium(III) has been shown to form a 1:2 V(III): $\text{OH}^-$  complex in the presence of sulphate ions<sup>75</sup> and the di-hydroxy bridged chromium(III) species  $\text{Cr}_2(\text{OH})_2\text{SO}_4^{2+}$  and  $\text{Cr}_2(\text{OH})_2(\text{SO}_4)_3^{2-}$  have been reported<sup>76,77</sup>. Scandium is also known to form an hydroxy sulphate complex,  $\text{Sc}(\text{OH})(\text{SO}_4)_2^{2-}$ , over a range of sulphate ion concentrations<sup>25</sup>.

The results in this work have shown for the first time that similar titanium(III) hydroxy sulphate complexes are formed. Several different complexes were detected and the type of complexes formed are a function of time, pH and sulphate ion concentration.

#### 4. 5 Conclusion

The results presented in this chapter have shown that complex formation between titanium(III) and sulphate ion does occur in dilute solutions. The complexes formed have been identified and characterised and this has led to the identification of the titanium(III) species present in concentrated sulphuric acid solutions as well.

It has also been shown that as a result of the formation of these titanium(III) sulphate complexes, the hydrolysis of titanium(III) in sulphate solutions is quite different <sup>from</sup> that in chloride solutions.

The studies of the oxidation of titanium(III) sulphate solutions have given for the first time stability data for mixed valence Ti(III):Ti(IV) sulphate complexes and the importance of the formation of these species in titanium(III) sulphate systems has been shown.

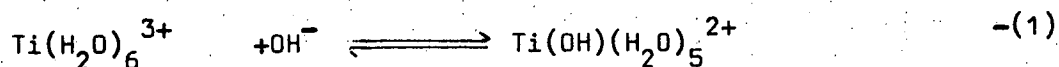
## CHAPTER 5

### Some aspects of the solution chemistry of titanium(III)

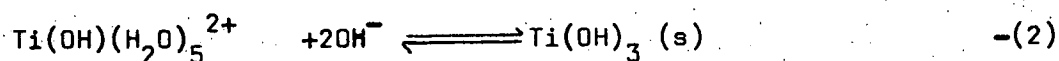
#### 5.1 Summary

As discussed in the preceding chapters, several aspects of the chemistry of titanium(III) in aqueous solutions have been studied. This involved investigating the nature of the hydroxide species formed at different pH values and the type of complexes formed in the presence of thiocyanate ions and sulphate ions.

The hydrolysis of hexaquotitanium(III) ion in dilute chloride solutions takes place in two stages. At low pH values primary hydrolysis occurs as given by the equation



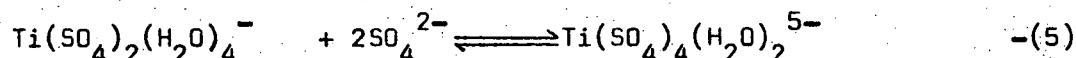
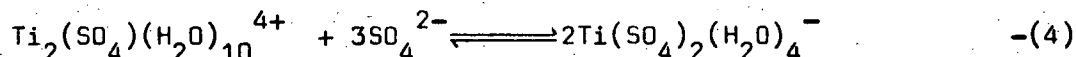
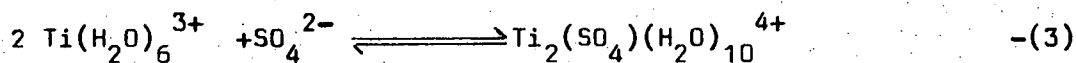
At slightly higher pH values secondary hydrolysis occurs given by the equation



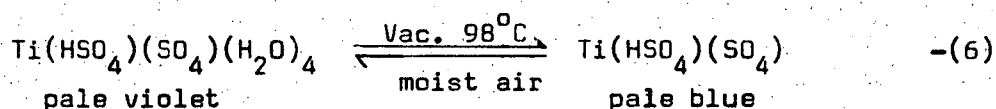
Both the primary and secondary hydrolysis products dimerise on standing to form hydroxy-bridged and oxy-bridged species respectively. This behaviour is fairly common in hydrolytic equilibria<sup>24</sup>. Under certain conditions the secondary hydrolysis products oxidise with the evolution of hydrogen to form a dark blue 1:1 mixed oxidation state species. The pH range over which the respective hydrolysis reactions occur depends on the total chloride ion concentration. On increasing the chloride ion concentration (over the range 0.4 to 4M) the  $\log \beta$  values increase approximately as the square root of the total chloride ion concentration.

Titanium(III) forms two complexes in aqueous thiocyanate solutions; a 1:1 cationic species  $\text{Ti}(\text{NCS})(\text{H}_2\text{O})_5^{2+}$  and a 1:4 anionic species  $\text{Ti}(\text{NCS})_4(\text{H}_2\text{O})_2^-$ . A 1:1 titanium(III):titanium(IV) mixed oxidation state species is formed during the oxidation of titanium(III) thiocyanate solutions.

In dilute sulphate solutions, titanium(III) forms a series of complexes given by equations (3) - (5)



The latter 1:4 complex persists in sulphate solutions up to about 4 molar and at higher concentrations forms polymers. At very high sulphuric acid concentrations i.e. about 15-18 molar, these polymers collapse to form the anhydrous species  $\text{Ti}(\text{HSO}_4)(\text{SO}_4)$ . The relatively stable pale violet 1:2 tetrahydrate can be crystallised from solution and readily converted to the anhydrous form.



Hydroxy sulphate species are formed during the hydrolysis of the above complexes and mixed oxidation state titanium(III) titanium(IV) species are formed when solutions containing the above complexes are allowed to oxidise in air.

## 5.2 Titanium(III) co-ordination complexes.

The titanium(III) complexes investigated in this work showed characteristic co-ordination behaviour. The hydroxide thiocyanate and sulphate ligands studied all appeared to behave as unidentate ligands with respect to each titanium atom, and formed complexes containing 2:4; 1:5 or 0:6 octahedral co-ordination. This trend is even more distinct when other aquo titanium(III) complex ions are compared. Table 6 clearly illustrates this. Generally 2:4

Table 6

Titanium(III) complexes formed in aqueous solutions

2:4 Co-ordination      1:5 Co-ordination      0:6 Co-ordination

$\text{TiF}_2(\text{H}_2\text{O})_4^+$	$\text{TiF}(\text{H}_2\text{O})_5^{2+}$	$\text{Ti}(\text{H}_2\text{O})_6^{3+}$
$\text{TiCl}_2(\text{H}_2\text{O})_4^+$	$\text{TiCl}(\text{H}_2\text{O})_5^{2+}$	$\text{TiF}_6^{3-}$
$\text{Ti}(\text{SO}_4)_2(\text{H}_2\text{O})_4^- *$	$\text{Ti}(\text{NCS})(\text{H}_2\text{O})_5^{2+} *$	$\text{Ti}(\text{CN})_6^{3-}$
$\text{Ti}_2(\text{OH})_2(\text{H}_2\text{O})_8^{4+} *$	$\text{Ti}(\text{OH})(\text{H}_2\text{O})_5^{2+} *$	$\text{Ti}(\text{OH})_3 \text{ polymer} *$
$\text{TiF}_4(\text{H}_2\text{O})_2^-$	$\text{Ti}_2(\text{SO}_4)(\text{H}_2\text{O})_{10}^{4+} *$	$\text{Ti}(\text{C}_2\text{O}_4)_2^-$
$\text{Ti}(\text{NCS})_4(\text{H}_2\text{O})_2^- *$	$\text{TiCl}_5(\text{H}_2\text{O})^{2-}$	$\text{Ti}(\text{SO}_4)_2^- *$
$\text{Ti}(\text{SO}_4)_4(\text{H}_2\text{O})_2^{5-} *$		

\* Investigated in this work.

co-ordination species tend to form, the 1:5 species being usually less stable, while 0:6 co-ordination only occurs with ligands that complex strongly or under extreme conditions <sup>where</sup> a very large excess of one ligand is present.

This characteristic co-ordination behaviour also appears to apply to reactions in non-aqueous solvents. For example, in liquid ammonia the titanium(III) complexes  $\text{Ti}(\text{NH}_3)_6^{3+}$  <sup>8</sup> and  $\text{Ti}(\text{CN}_4)(\text{NH}_3)_2^-$  <sup>78</sup> are reported to form. Acetic acid complexes  $\text{TiCl}_4(\text{AcOH})_2^-$  and  $\text{TiCl}_5(\text{AcOH})^{2-}$  have been prepared in non-aqueous solvents <sup>79</sup>. And when  $\text{TiCl}_3$  is dissolved in alcohols such as ethanol, i-propanol, s-butanol and cyclohexanol, complexes of the type  $\text{TiCl}_2(\text{alcohol})_4^+$  are formed <sup>8</sup>.

Where 2:4 and 1:5 co-ordination occurs distortion of the octahedral environment around the titanium(III) atom also exists. This distortion is directly accommodating the energy requirements of the Jahn-Teller effect for  $d^1$  systems.

### 5.3 Titanium(III) mixed oxidation state complexes

The formation of mixed oxidation state compounds i.e. containing the same element in different valence states, has been known for a long time.

A review of mixed valence chemistry by Robin and Day<sup>80</sup> has shown that almost all the transition metals are known to form mixed oxidation state compounds.

Titanium(III) is easily oxidised to titanium(IV) and because of this titanium(III) and titanium(IV) are often present together in solution. A careful examination of the literature for titanium(III) systems reveals that a surprising number of mixed valence titanium species have been reported. For example, in concentrated chloride solutions e.g. 12M hydrochloric acid, a dark binuclear titanium species containing equal amounts of titanium(III) and titanium(IV) has been reported to exist<sup>40</sup>. A dark blue 1:1 titanium(III):titanium(IV) hydrolysis species has been identified in this work (see Chapter 2) and the studies in Chapter 3 have shown the formation of a 1:1 titanium(III):titanium(IV) species in concentrated aqueous thiocyanate media. Evidence for the formation of a 1:1 hexacyano-complex  $K_5[Ti^{(III)}(CN)_6Ti^{(IV)}(CN)_6]$  has been reported by Heintz<sup>81</sup>. In sulphuric acid media, the dark color of solutions containing titanium(III) and titanium(IV) has been known for some time<sup>40,48</sup> and detailed studies of the behaviour in 1.8M to 10.8M sulphuric acid has again shown the formation of a 1:1 mixed valence complex. An interesting E.S.R. study of the oxidation of tris (acetylacetonato)titanium(III) has been made by Lo and Brubaker<sup>82</sup>. Their data also suggest the formation of a mixed oxidation state acetylacetonate species.

From these reported instances of the existence of titanium mixed oxidation state species, it is clear that during oxidation reactions in solution the occurrence of mixed valence intermediate complexes is the rule rather than the exception. However the formation of these species has been overlooked in most investigations of titanium(III) systems. For example, studies of the kinetics of the oxidation of titanium(III) in solution in the presence of fluoride ions<sup>13,15</sup>, chloride ions<sup>3,73,83-85</sup>, iodide ions<sup>86</sup>, perchlorate ions<sup>84,87</sup>, nitrate ions<sup>85</sup> and sulphate ions<sup>2,4,84,88</sup> have been made but in none of these studies has the possible effect

of the formation of mixed oxidation state species on the oxidation mechanism been mentioned. However, definite kinetic effects related to the formation of mixed oxidation state species are known. Observations by Heintz<sup>81</sup> on the oxidation of  $K_3Ti(CN)_6$  showed that once a 1:1 ratio of titanium(III) to titanium(IV) was attained the oxidation proceeded more slowly. A similar observation has been made in this work in relation to the auto-oxidation of titanium(III) hydroxide in solution (see Figure 12). Hydrogen evolution proceeds until the dark-blue 1:1 mixed oxidation state species is formed, and thereafter proceeds only slowly in the presence of excess base. i.e. Uniform oxidation through to white titanium(IV) hydrated oxide is not observed. A similar curve has been obtained for the oxidation of molybdenum(II) acetate in 12M hydrochloric acid<sup>89</sup>. Again, once a mean oxidation number of 2.5 was obtained, corresponding to the formation of the 1:1 molybdenum(II):molybdenum(III) species, the rate of oxidation decreased.

The evidence discussed above illustrates the importance of the formation of mixed valence species in understanding the chemistry of titanium. As well, the need to ensure that no oxidation takes place during the study of titanium(III) systems is emphasised.

#### 5.4 Conclusion

The application of a combination of physico-chemical techniques namely potentiometric, conductometric and spectrophotometric methods has enabled successful elucidation of the titanium(III) hydroxide, thiocyanate and sulphate systems. This approach to studying the solution chemistry of titanium(III) would also be applicable to studying the titanium(III) phosphate and titanium(III) fluoride systems which to date have not been systematically investigated.

The additional information about titanium(III) systems obtained as a result of this work has enabled some characteristic trends in the



co-ordination behaviour of octahedral titanium(III) complexes to be distinguished. Evidence that titanium(III) reduces hydroxide ion has been presented and the extent of titanium(III) titanium(IV) mixed oxidation state complexes in titanium chemistry has been demonstrated.

Appendix 1Chemicals and solutions used

Titanium(III) solutions were prepared from the following B.D.H. solutions:-

- (i) Titanium trichloride solution (technical, about 12.5% weight per volume  $\text{TiCl}_3$  and containing about 15% weight per volume  $\text{HCl}$  (total)).
- (ii) Titanium trichloride solution (low in iron, contains zinc chloride, about 15% weight per volume  $\text{TiCl}_3$ ).
- (iii) Titanium(III) sulphate solution (technical, 15% weight per volume  $\text{Ti}_2(\text{SO}_4)_3$  and containing about 23% weight per volume  $\text{H}_2\text{SO}_4$  (total)).

Ferric ammonium sulphate solutions were prepared from Hopkin and Williams A.R. ammonium ferric sulphate (assay not less than 99.0%). 9.645g was dissolved in about 500 mls of nitrogenated distilled water to which 5 mls of 50% sulphuric acid had been added. This was then made to 1 litre with nitrogenated distilled water.

Sodium chloride solution, 0.200M was prepared by dissolving dry B.D.H. A.R. sodium chloride (2.923g) in distilled water and making to 250 mls.

Silver nitrate solutions were standardised against standard sodium chloride solution using  $\text{K}_2\text{CrO}_4$  indicator.

Thiocyanate solutions (dilute) were standardised against standard silver nitrate solution using saturated ferric alum solution as indicator.

Ammonium sulphate solution (0.390M) was standardised by sulphate ion analysis (gravimetric  $\text{BaSO}_4$  method).

Hydrochloric acid solution (1.800M) was standardised by chloride ion analysis (Volhard's method).

Sodium hydroxide solutions were standardised against standard hydrochloric acid using bromothymol blue indicator.

Ammonium hydroxide solutions were standardised against standard hydrochloric acid using bromo-cresol-green indicator.

The pH meters were standardised using 0.050M potassium hydrogen phthalate solution (pH 4.00 at 20°C, 4.01 at 25°C)<sup>90</sup>.

Appendix 2Equipment

Optical density measurements of solutions were made using Unicam SP500 and Perkin Elmer 4000A Spectracord spectrophotometers. A Zeiss PMQ-II spectrophotometer was used for reflectance spectra measurements.

Infra-red spectra were run on a Perkin Elmer 221 spectrophotometer.

Rapid potentiometric titration curves were recorded on a "Heath Built" pH Recording Electrometer, while individual pH measurements were made with Horriba and Pye Potentiometric pH meters.

Conductance measurements were made using a research A.C. conductance bridge.

Appendix 3pH titration data(i) pH titration results

Run 1

80 ml solution containing 0.113M Ti(III) and 0.450M Cl<sup>-</sup>

titrated rapidly with 1.97M NaOH.

Vol. NaOH (mls)	pH	Vol. NaOH (mls)	pH	Vol. NaOH (mls)	pH	Vol. NaOH (mls)	pH
0.00	1.63	5.11	2.52	9.71	4.18	14.31	4.70
1.02	1.68	5.62	2.59	10.22	4.34	14.82	4.76
1.53	1.75	6.13	2.72	10.73	4.45	15.33	4.83
2.04	1.79	6.64	2.81	11.24	4.52	15.84	4.88
2.56	1.91	7.15	2.94	11.75	4.59	16.35	5.01
3.07	2.02	7.67	3.07	12.26	4.61	16.86	5.16
3.58	2.15	8.18	3.31	12.78	4.62	17.37	5.40
4.09	2.27	8.69	3.60	13.29	4.62	17.89	5.63
4.60	2.38	9.20	3.96	13.80	4.64	18.40	5.83

Run 2

80 ml solution containing 0.113M Ti(III) and 0.450M Cl<sup>-</sup>

titrated rapidly with 1.97M NaOH.

Vol. NaOH (mls)	pH	Vol. NaOH (mls)	pH	Vol. NaOH (mls)	pH	Vol. NaOH (mls)	pH
0.00	1.70	5.27	2.55	10.01	4.28	14.75	4.77
1.06	1.75	5.80	2.68	10.54	4.38	15.28	4.86
1.59	1.78	6.32	2.80	11.06	4.51	15.80	4.88
2.11	1.89	6.85	2.93	11.59	4.60	16.33	5.00
2.64	2.00	7.38	3.06	12.12	4.63	16.86	5.14
3.17	2.04	7.90	3.20	12.64	4.65	17.38	5.38
3.69	2.21	8.43	3.45	13.17	4.69	17.91	5.58
4.22	2.30	8.96	3.80	13.70	4.74	18.43	5.80
4.74	2.44	9.48	4.10	14.22	4.75	18.96	6.06

## Run 3

75 ml solution containing 0.0573M Ti(III) and 2.26M Cl<sup>-</sup>titrated rapidly with 1.08M NH<sub>4</sub>OH.

Vol.NH <sub>4</sub> OH (mls) <sup>4</sup>	pH	Vol.NH <sub>4</sub> OH (mls) <sup>4</sup>	pH	Vol.NH <sub>4</sub> OH (mls) <sup>4</sup>	pH	Vol.NH <sub>4</sub> OH (mls) <sup>4</sup>	pH
0.00	1.13	4.92	1.78	9.83	3.38	14.75	4.33
0.61	1.14	5.53	1.90	10.45	3.65	15.36	4.40
1.23	1.19	6.15	2.03	11.06	3.85	15.98	4.49
1.84	1.27	6.76	2.17	11.68	4.00	16.59	4.58
2.46	1.35	7.37	2.33	12.29	4.10	17.21	4.92
3.07	1.42	7.99	2.49	12.90	4.18	17.82	5.90
3.69	1.54	8.60	2.69	13.52	4.24	18.44	6.66
4.30	1.66	9.22	3.02	14.13	4.29	19.05	7.02

## Run 4

75 ml solution containing 0.0573M Ti(III) and 3.59M Cl<sup>-</sup>titrated rapidly with 1.08M NH<sub>4</sub>OH.

Vol.NH <sub>4</sub> OH (mls) <sup>4</sup>	pH	Vol.NH <sub>4</sub> OH (mls) <sup>4</sup>	pH	Vol.NH <sub>4</sub> OH (mls) <sup>4</sup>	pH	Vol.NH <sub>4</sub> OH (mls) <sup>4</sup>	pH
0.00	0.97	5.28	1.71	10.57	3.57	15.85	4.38
0.66	0.99	5.95	1.86	11.23	3.77	16.52	4.50
1.32	1.04	6.61	2.00	11.89	3.94	17.18	4.86
1.98	1.13	7.27	2.16	12.55	4.03	17.84	5.95
2.64	1.21	7.93	2.34	13.21	4.13	18.50	6.60
3.30	1.32	8.59	2.57	13.87	4.20	19.16	6.92
3.96	1.44	9.25	2.88	14.53	4.23		
4.62	1.58	9.91	3.28	15.19	4.30		

Run 5

75 ml solution containing 0.0573M  $\text{Ti(III)}$  and 4.93M  $\text{Cl}^-$ titrated rapidly with 1.08M  $\text{NH}_4\text{OH}$ .

Vol. $\text{NH}_4\text{OH}$ (mls) <sup>4</sup>	pH	Vol. $\text{NH}_4\text{OH}$ (mls) <sup>4</sup>	pH	Vol. $\text{NH}_4\text{OH}$ (mls) <sup>4</sup>	pH	Vol. $\text{NH}_4\text{OH}$ (mls) <sup>4</sup>	pH
0.00	0.75	5.41	1.57	10.82	3.49	16.22	4.29
0.68	0.79	6.08	1.71	11.49	3.70	16.90	4.50
1.35	0.86	6.76	1.87	12.17	3.84	17.58	5.25
2.03	0.94	7.44	2.04	12.84	3.95	18.25	6.16
2.70	1.04	8.11	2.22	13.52	4.02	18.93	6.58
3.38	1.17	8.79	2.46	14.20	4.07	19.60	6.87
4.06	1.29	9.46	2.83	14.87	4.13		
4.73	1.42	10.14	3.23	15.55	4.19		

(ii) calculated primary hydrolysis data i.e.  $0 < \bar{n} < 1$ 

Run 1

pH	$\bar{n}$	$\log \frac{\bar{n}}{1-\bar{n}}$	$\log \beta_1$	$[\text{Cl}^-]$
2.52	0.148	-0.759	-3.28	0.422
2.59	0.259	-0.456	-3.05	0.420
2.72	0.370	-0.231	-2.95	0.417
2.81	0.481	-0.033	-2.84	0.415
2.94	0.592	0.162	-2.78	0.413
3.07	0.704	0.376	-2.65	0.410
3.31	0.815	0.644	-2.67	0.408

$$\text{mean } \log \beta_1 = -2.89 \pm 0.20^*$$

$$\text{mean } [\text{Cl}^-] = 0.415 \pm 0.007\text{M} \text{ i.e. } \sqrt{I} = 0.644$$

\*see (\*) p105

Run 2

pH	$\bar{n}$	$\log \frac{\bar{n}}{1-\bar{n}}$	$\log \beta_1$	$[Cl^-]$
2.55	0.195	-0.616	-3.17	0.422
2.68	0.310	-0.248	-3.03	0.420
2.80	0.425	-0.131	-2.93	0.417
2.93	0.540	0.070	-2.86	0.415
3.06	0.655	0.279	-2.78	0.412
3.20	0.770	0.525	-2.67	0.410

$$\text{mean } \log \beta_1 = -2.91 \pm 0.17^*$$

$$\text{mean } [Cl^-] = 0.416 \pm 0.006M \text{ i.e. } \sqrt{I} = 0.645$$

\* Standard deviation calculated using equation (1)

$$S.D. = \frac{3 \sum R}{t \sqrt{t}} \quad (1)$$

where  $\sum R$  = sum of residuals from mean-value.

t = number of values

Run 3

pH	$\bar{n}$	$\log \frac{\bar{n}}{1-\bar{n}}$	$\log \beta_1$	$[Cl^-]$
2.03	0.098	-0.963	-2.99	2.089
2.17	0.251	-0.475	-2.65	2.073
2.33	0.405	-0.167	-2.50	2.058
2.49	0.560	0.105	-2.38	2.042
2.69	0.714	0.397	-2.30	2.028
3.02	0.869	0.822	-2.40	2.013

$$\text{mean } \log \beta_1 = -2.50 \pm 0.20$$

$$\text{mean } [Cl^-] = 2.05 \pm 0.04M \text{ i.e. } \sqrt{I} = 1.43$$



## Run 4

pH	$\bar{n}$	$\log \frac{\bar{n}}{1-\bar{n}}$	$\log \beta_1$	$[Cl^-]$
2.00	0.214	-0.565	-2.57	3.299
2.16	0.379	-0.215	-2.38	3.273
2.34	0.545	0.079	-2.26	3.247
2.57	0.711	0.391	-2.18	3.221
2.88	0.877	0.853	-2.03	3.196

$$\text{mean } \log \beta_1 = -2.28 \pm 0.20$$

$$\text{mean } [Cl^-] = 3.25 \pm 0.05M \text{ i.e. } \sqrt{I} = 1.80$$

## Run 5

pH	$\bar{n}$	$\log \frac{\bar{n}}{1-\bar{n}}$	$\log \beta_1$	$[Cl^-]$
1.17	0.080	-1.060	-2.77	4.560
1.87	0.251	-0.475	-2.35	4.522
2.04	0.422	-0.137	-2.18	4.485
2.22	0.591	0.160	-2.06	4.449
2.46	0.761	0.503	-1.96	4.413
2.83	0.930	1.235	-1.59	4.378

$$\text{mean } \log \beta_1 = -2.15 \pm 0.34$$

$$\text{mean } [Cl^-] = 4.47 \pm 0.09M \text{ i.e. } \sqrt{I} = 2.11$$

(iii) calculated secondary hydrolysis data i.e.  $1 < \bar{n} < 3$ , i.e.  $0 < \bar{m} < 1$ .

Run 1

pH	$(1-\bar{m})$	$[\text{Ti(III)}]$	$\log (1-\bar{m}) [\text{Ti(III)}]$	$\log \beta_3$	$[\text{Cl}^-]$
4.45	0.815	0.0998	-1.090	-7.81	0.397
4.52	0.757	0.0992	-1.124	-7.92	0.394
4.59	0.701	0.0987	-1.160	-8.02	0.393
4.61	0.644	0.0981	-1.199	-8.02	0.390
4.62	0.589	0.0977	-1.240	-8.00	0.388
4.62	0.533	0.0970	-1.286	-7.95	0.386
4.64	0.478	0.0966	-1.335	-7.94	0.384
4.70	0.422	0.0960	-1.392	-8.01	0.381
4.76	0.375	0.0955	-1.446	-8.07	0.380
4.83	0.310	0.0949	-1.532	-8.13	0.377
4.88	0.255	0.0945	-1.618	-8.14	0.375
5.01	0.200	0.0940	-1.726	-8.29	0.373

$$\text{mean } \log \beta_3 = -8.02 \pm 0.08$$

$$\text{mean } [\text{Cl}^-] = 0.385 \pm 0.012M \text{ i.e. } \sqrt{I} = 0.62$$

Run 2

pH	$(1-\bar{m})$	$[\text{Ti(III)}]$	$\log (1-\bar{m}) [\text{Ti(III)}]$	$\log \beta_3$	$[\text{Cl}^-]$
4.38	0.828	0.1001	-1.081	-7.68	0.398
4.51	0.770	0.0995	-1.116	-7.90	0.395
4.60	0.713	0.0989	-1.152	-8.05	0.393
4.63	0.655	0.0983	-1.191	-8.07	0.391
4.65	0.598	0.0978	-1.233	-8.07	0.389
4.69	0.540	0.0972	-1.280	-8.10	0.386
4.74	0.483	0.0967	-1.331	-8.15	0.384
4.75	0.425	0.0962	-1.388	-8.11	0.382
4.77	0.368	0.0956	-1.454	-8.09	0.380
4.86	0.310	0.0951	-1.530	-8.19	0.378
4.88	0.253	0.0946	-1.622	-8.14	0.376
5.00	0.195	0.0941	-1.738	-8.26	0.374

$$\text{mean } \log \beta_3 = -8.07 \pm 0.80$$

$$\text{mean } [\text{Cl}^-] = 0.386 \pm 0.012M \text{ i.e. } \sqrt{I} = 0.62$$

Run 3

pH	(1-m)	[Ti(III)]	$\frac{\log}{(1-m)[Ti(III)]}$	$\log \beta_3$	[Cl <sup>-</sup> ]
3.85	0.834	0.0499	-1.381	-6.32	1.970
4.00	0.756	0.0496	-1.426	-6.57	1.955
4.10	0.680	0.0492	-1.475	-6.72	1.942
4.18	0.603	0.0489	-1.530	-6.83	1.928
4.24	0.525	0.0485	-1.593	-6.89	1.915
4.29	0.449	0.0482	-1.665	-6.91	1.902
4.33	0.371	0.0479	-1.750	-6.91	1.889
4.40	0.294	0.0476	-1.854	-6.95	1.876
4.49	0.216	0.0472	-1.991	-6.99	1.863
4.58	0.140	0.0469	-2.182	-6.98	1.851

$$\text{mean } \log \beta_3 = -6.81 \pm 0.15$$

$$\text{mean } [\text{Cl}^-] = 1.91 \pm 0.06\text{M} \quad \text{i.e. } \sqrt{I} = 1.38$$

Run 4

pH	(1-m)	[Ti(III)]	$\frac{\log}{(1-m)[Ti(III)]}$	$\log \beta_3$	[Cl <sup>-</sup> ]
3.77	0.813	0.0498	-1.392	-6.15	3.122
3.94	0.730	0.0495	-1.442	-6.44	3.099
4.03	0.647	0.0491	-1.498	-6.56	3.075
4.13	0.564	0.0487	-1.561	-6.70	3.052
4.20	0.481	0.0484	-1.633	-6.77	3.030
4.23	0.398	0.0480	-1.719	-6.74	3.007
4.30	0.315	0.0476	-1.824	-6.78	2.985
4.38	0.233	0.0473	-1.959	-6.80	2.964
4.50	0.148	0.0470	-2.157	-6.84	2.942

$$\text{mean } \log \beta_3 = -6.64 \pm 0.17$$

$$\text{mean } [\text{Cl}^-] = 3.03 \pm 0.09\text{M} \quad \text{i.e. } \sqrt{I} = 1.74$$

Run 5

pH	(1-m)	[Ti(III)]	(1-m) <sup>log</sup> [Ti(III)]	log $\beta_3$	[Cl <sup>-</sup> ]
3.49	0.864	0.0501	-1.363	-5.62	4.308
3.70	0.780	0.0497	-1.411	-5.99	4.275
3.84	0.695	0.0493	-1.465	-6.21	4.242
3.95	0.611	0.0489	-1.524	-6.38	4.209
4.02	0.525	0.0485	-1.593	-6.45	4.177
4.07	0.440	0.0482	-1.674	-6.47	4.145
4.13	0.356	0.0478	-1.770	-6.49	4.114
4.19	0.270	0.0475	-1.893	-6.49	4.083
4.29	0.186	0.0471	-2.057	-6.52	4.053
4.50	0.101	0.0468	-2.326	-6.67	4.023

$$\text{mean log } \beta_3 = -6.33 \pm 0.22$$

$$\text{mean } [\text{Cl}^-] = 4.16 \pm 0.14\text{M} \quad \text{i.e. } \sqrt{I} = 2.04$$

#### Appendix 4

#### Calculated $\log \beta_{12}$ values

Values of  $\beta_{12}$  calculated from equilibrium pH data Figure 4 using equation (15) of Chapter 2 are shown below. Each solution contained 0.0906M Ti(III), 0.352M  $\text{Cl}^-$  and varying amounts of 2.06M NaOH. Total volume of each solution was 50 mls.

Note  $\frac{1}{2} \log [\text{Ti(III)}] = -0.52$

pH	$\bar{n}$	$\log\left(\frac{\bar{n}}{2}\right)$	$\log(1-\bar{n})$	$\log \beta_{12}$
1.78	0.182	-1.0410	-0.0872	-1.69
1.99	0.364	-0.7399	-0.1965	-1.64
2.20	0.545	-0.5638	-0.3420	-1.62
2.46	0.727	-0.4389	-0.5638	-1.60

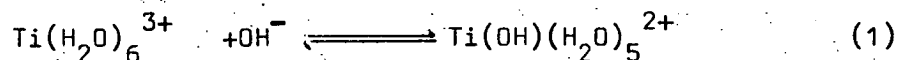
$$\text{mean } \log \beta_{12} = -1.64 \pm 0.04^*$$

\* Standard deviation calculated using equation(1) of

Appendix 3.

Appendix 5Calculation of extinction coefficients for the  
primary hydrolysis species.

For the reaction



from Beer's Law

$$A = \sum b c \quad (2)$$

$$\text{where } A = A_{\text{Ti}(\text{H}_2\text{O})_6^{3+}} + A_{\text{Ti}(\text{OH})(\text{H}_2\text{O})_5^{2+}} \quad (3)$$

= measured absorbance of the solution

$\sum$  = molar extinction coefficient

b = path length = 1 cm in this work

c = concentration, moles litre<sup>-1</sup>

$$\text{Thus } A = a b \quad (4)$$

where a = coefficient of absorbance per concentration of titanium(IV) present.

$$\text{i.e. } \sum = \frac{a}{[\text{Ti(III)}]} \quad (5)$$

where [Ti(III)] is the total concentration of titanium(III) in solution.

Since  $\text{Ti}(\text{OH})(\text{H}_2\text{O})_5^{2+}$  has a relatively high formation constant (see Chapter 2)

$$[\text{Ti}^{3+}] = (1-\bar{n}) [\text{Ti(III)}] \quad (6)$$

where  $\bar{n}$  represents the ratio of hydroxyl ion added to titanium(III) ion initially present. From equation (4)

$$A_{\text{Ti}(\text{H}_2\text{O})_6^{3+}} = (1-\bar{n}) a_{\text{Ti}(\text{H}_2\text{O})_6^{3+}} \quad (7)$$

and substituting in equation (3) gives

$$A = (1-\bar{n}) a_{\text{Ti}(\text{H}_2\text{O})_6^{3+}} + A_{\text{Ti}(\text{OH})(\text{H}_2\text{O})_5^{2+}} \quad (8)$$

$$\text{i.e. } A_{\text{Ti}(\text{OH})(\text{H}_2\text{O})_5^{2+}} = A - (1-\bar{n}) a_{\text{Ti}(\text{H}_2\text{O})_6^{3+}} \quad (9)$$

The results obtained are shown in Table 7.

Table 7

Absorbance data\* at 480 nm for initial solutions  
containing 0.0892M Ti(III) and 0.334M Cl<sup>-</sup>

$\bar{n}$	$(1-\bar{n})$	A	$(1-\bar{n})a_{\text{Ti}(\text{H}_2\text{O})_6^{3+}}$	$A_{\text{Ti}(\text{OH})(\text{H}_2\text{O})_5^{2+}}$
0.00	1.00	0.320	0.320	0.000
0.12	0.88	0.368	0.282	0.086
0.31	0.69	0.379	0.221	0.158
0.50	0.50	0.450	0.160	0.290
0.69	0.31	0.566	0.099	0.467

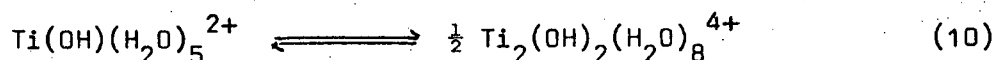
\* Path length = 1 cm.

A plot of  $A_{\text{Ti}(\text{OH})(\text{H}_2\text{O})_5^{2+}}$  versus  $\bar{n}$  should be a straight line of slope  $a_{\text{Ti}(\text{OH})(\text{H}_2\text{O})_5^{2+}}$ , see Figure 48. Thus from Figure 48 and using equation(5)

$$\Sigma_{\text{Ti}(\text{OH})(\text{H}_2\text{O})_5^{2+}} = \frac{0.60}{0.0892}$$

i.e.  $\Sigma_{\text{Ti}(\text{OH})(\text{H}_2\text{O})_5^{2+}} = 6.7 \pm 1.0 \text{ moles}^{-1} \text{ litre cm}^{-1} \text{ at } 480 \text{ nm.}$

For the reaction



one mole of monomer gives  $\frac{1}{2}$  mole of dimer. However, for the dimeric species the extinction coefficient is given as absorbance per mole of titanium(III), not per mole of dimer. Thus the theory outlined by equations (2) - (9) for calculating  $A_{\text{Ti}(\text{OH})(\text{H}_2\text{O})_5^{2+}}$  can be applied similarly to calculate  $A_{\text{Ti}_2(\text{OH})_2(\text{H}_2\text{O})_8^{4+}}$ . The results obtained are shown in Table 8.

Table 8

Absorbance data at 480 nm for equilibrated solutions  
containing 0.0892M Ti(III) and 0.334M Cl<sup>-</sup>, for 1 cm cells.

$\bar{n}$	$(1-\bar{n})$	A	$(1-\bar{n})a_{\text{Ti}(\text{H}_2\text{O})_6^{3+}}$	$A_{\text{Ti}_2(\text{OH})_2(\text{H}_2\text{O})_8^{4+}}$
0.00	1.00	0.320	0.320	0.000
0.12	0.88	0.394	0.282	0.112
0.31	0.69	0.466	0.221	0.245
0.50	0.50	0.630	0.160	0.470
0.69	0.31	0.846	0.099	0.747

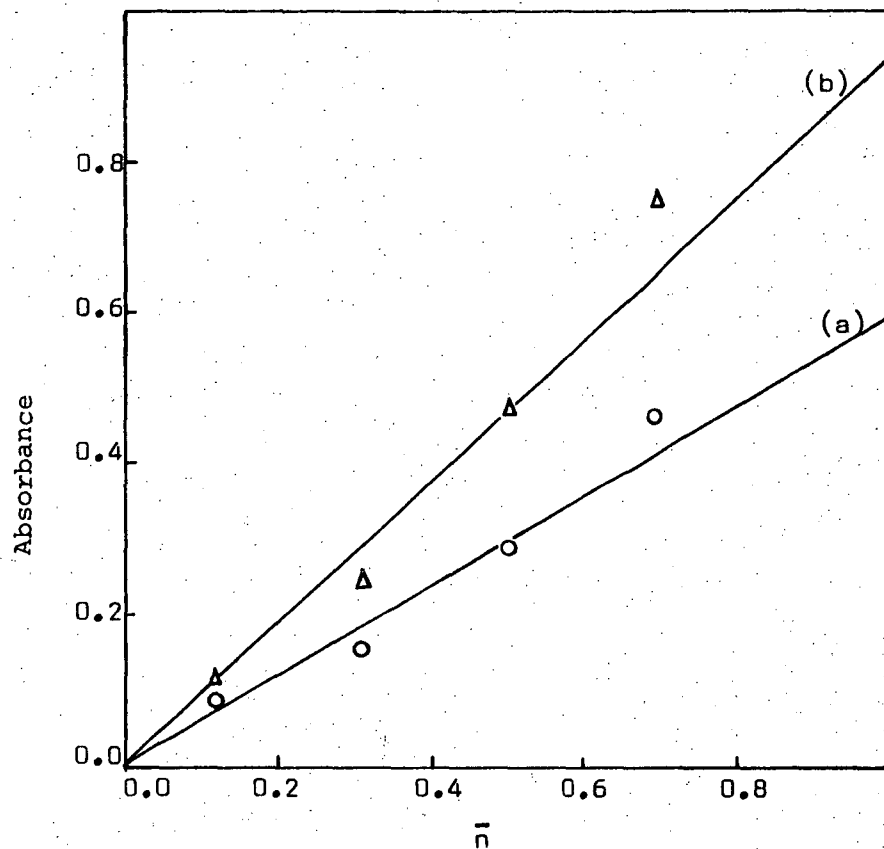


Figure 48.

o ~ initial,  $\Delta$  ~ equilibrated

slope (a) = 0.60, slope(b) = 0.94

A plot of  $A_{\text{Ti}_2(\text{OH})_2(\text{H}_2\text{O})_8^{4+}}$  versus  $\bar{n}$  should be a straight line

slope =  $a_{\text{Ti}_2(\text{OH})_2(\text{H}_2\text{O})_8^{4+}}$  (see Figure 48). Thus from Figure 48 and

using equation (5)  $\epsilon_{\text{Ti}_2(\text{OH})_2(\text{H}_2\text{O})_8^{4+}} = \frac{0.94}{0.0892}$

i.e.  $\epsilon_{\text{Ti}_2(\text{OH})_2(\text{H}_2\text{O})_8^{4+}} = 10.5 \pm 1.0 \text{ moles}^{-1} \text{ l cm}^{-1} \text{ at } 480 \text{ nm.}$



Appendix 6Evolution of hydrogen - kinetic results(i) Summary of results

Each solution contained 0.0920M Ti(III) and 0.334M  $\text{Cl}^-$  and varying amounts of 2.100M NaOH. Total volume of each solution was 50 mls.  $\bar{n} = 2.19$  mls of base.

Run No	Vol NaOH (mls)	Corrected* Vol NaOH	log(corrected ‡ Vol NaOH)	Rate(1)	log Rate(1)	Rate(2)
1	20	15.3	1.1847	0.964	-0.0159	1.236
2 †	20			0.34		0.505
3 ‡	40			5.17		6.00
4	45	40.3	1.6053	3.14	0.4969	3.69
5	40	35.3	1.5478	1.983	0.2974	3.396
6	35	30.3	1.4814	1.682	0.2258	2.073
7	35	30.3	1.4814	1.596	0.2031	2.253
8	30	25.3	1.4031	0.677	-0.1694	1.441
9	25	20.3	1.3075	0.333	-0.4776	1.472
10	20	15.3	1.1847	0.629	-0.2013	1.300
11	15	10.3	1.0128	0.352	-0.4535	0.733
12	10	5.3	0.7243	0.119	-0.9245	0.588
13	40	35.3	1.5478	2.088	0.3198	2.878
14	45	40.3	1.6053	2.425	0.3847	3.063

\* Zero correction; hydrogen evolution occurs when  $\bar{n} > 1.5$ ; i.e. after 4.67 mls of base have been added (including allowance for neutralization of free acid initially present). See also Appendix 7.

†  $[\text{Ti(III)}] = 0.0391\text{M}$ ,  $[\text{Cl}^-] = 0.142\text{M}$ , total volume = 47 mls.

‡  $[\text{Ti(III)}] = 0.1840\text{M}$ ,  $[\text{Cl}^-] = 0.668\text{M}$ .

(ii) Kinetic data

Time values in minutes, pressure refers to height reading of water manometer in cm. Temperature constant at  $30.0^\circ\text{C}$ .

‡ Data plotted as "log  $\text{OH}^-$  concentration" in Figure 14, ( $\text{OH}^-$  concentration is proportional to volume of NaOH added, for constant volume solutions)

Run 1 air pressure 75.50 cm Hg.

time	pressure	time	pressure	time	pressure	time	pressure
0.0	5.0	5.0	10.60	15.0	22.47	35	47.50
0.5	5.88	6.0	11.70	16.0	23.74	40	53.47
1.25	6.00	7.0	12.85	17.0	25.00	45	58.90
1.50	6.10	8.0	14.06	18.0	26.25	50	64.70
2.0	6.20	9.0	15.25	20.0	28.80	55	70.60
-	6.30	10.0	16.46	22.0	31.20	60	76.00
3.0	8.6	11.0	17.66	24.0	33.75	65	81.25
3.5	9.16	12.0	18.81	26.0	36.18	70	86.50
4.0	9.65	13.0	20.05	28.0	38.76	75	92.00
4.5	10.11	14.0	21.30	30.0	41.20	82	98.5

Run 2 air pressure 75.04 cm Hg.

time	pressure	time	pressure	time	pressure	time	pressure
0	10.25	90	50.88	182	70.21	322	80.42
2	11.08	95	52.40	187	70.80	333	80.99
5	11.96	100	54.08	192	71.30	362	81.01
10	13.78	105	55.70	197	71.75	375	81.61
15	16.35	110	57.10	202	72.40	382	82.05
20	19.59	115	58.46	207	73.00	392	82.06
25	22.07	120	59.56	212	73.50	402	82.50
30	24.80	125	60.49	217	74.25	412	82.50
35	27.50	130	62.01	222	74.48	422	82.85
40	30.01	135	62.95	227	75.15	434	83.11
45	32.51	140	63.80	237	76.10	443	83.11
50	35.03	145	64.50	242	76.50	454	83.71
55	37.36	150	65.19	247	76.80	462	83.71
60	39.65	155	65.90	252	77.25	472	83.74
65	41.60	160	66.70	262	77.82	482	83.74
70	43.78	165	67.54	272	78.32	622	85.29
75	45.63	170	68.14	282	78.80	652	85.84
80	47.48	175	69.26	292	79.35	682	86.20
85	49.14	180	69.90	302	79.38		

Run 3 air pressure 75.16 cm Hg.

time	pressure	time	pressure	time	pressure	time	pressure
0.0	6.0	3.5	24.38	8.0	50.55	12.0	74.95
0.5	9.18	4.0	27.20	8.5	53.58	13.0	80.85
1.0	11.15	4.5	29.50	9.0	56.60	14.0	86.80
1.5	13.55	5.0	32.80	9.5	59.82	15.0	92.60
2.5	18.85	6.0	38.60	10.0	62.82	16.2	99.0
3.0	21.80	7.0	44.55	11.0	68.8		

Run 4 air pressure 75.24 cm Hg.

time	pressure	time	pressure	time	pressure	time	pressure
0.0	5.10	4.5	20.30	9.5	38.65	18	67.40
0.5	6.90	5.0	22.00	10.0	40.45	19	70.35
1.0	8.35	5.5	23.7	11	44.12	20	73.28
1.5	9.66	6.0	25.68	12	47.54	22	79.00
2.0	10.38	6.5	27.6	13	50.95	24	84.98
2.5	13.25	7.0	29.28	14	54.27	26	90.85
3.0	14.88	7.5	31.12	15	57.85	28	95.50
3.5	16.17	8.0	32.95	16	60.96	30	99.48
4.0	17.60	8.5	34.90	17	64.05		

Run 5 air pressure 75.37 cm Hg.

time	pressure	time	pressure	time	pressure	time	pressure
0.0	5.0	5.0	20.52	10.0	37.44	22	71.45
0.5	7.10	5.5	22.12	11	40.67	24	76.06
1.0	8.11	6.0	23.75	12	44.00	26	80.46
1.5	9.15	6.5	25.40	13	47.26	28	84.79
2.0	10.38	7.0	27.18	14	50.40	30	88.96
2.5	11.72	7.5	28.88	15	53.35	32	92.80
3.0	13.50	8.0	30.65	16	56.55	34	96.17
3.5	15.23	8.5	32.20	18	62.00	36	99.23
4.0	17.10	9.0	33.98	19	64.39		
4.5	19.00	9.5	35.70	20	66.75		

Run 6      air pressure 75.38 cm Hg.

time	pressure	time	pressure	time	pressure	time	pressure
0.0	6.0	6.0	17.80	14	34.45	26	56.95
0.5	7.88	6.5	18.80	15	36.56	27	58.90
1.0	8.85	7.0	19.80	16	38.56	28	60.55
1.5	9.50	7.5	10.84	17	40.70	29	62.85
2.0	10.26	8.0	21.88	18	42.65	30	64.55
2.5	11.30	8.5	22.88	19	44.70	32	68.20
3.0	12.08	9.0	23.93	20	46.68	34	71.60
3.5	12.92	9.5	24.94	21	48.63	36	75.10
4.0	13.89	10.0	25.97	22	50.65	38	77.80
4.5	14.83	11	28.07	23	52.49	40	80.95
5.0	15.77	12	30.25	24	53.51	45	88.00
5.5	16.80	13	32.36	25	54.95		

Run 7      air pressure 75.08 cm Hg.

time	pressure	time	pressure	time	pressure	time	pressure
0.0	5.0	5.5	15.40	12	30.30	26	60.63
0.5	6.80	6.0	16.75	13	32.44	28	64.49
1.0	7.53	6.5	17.90	14	34.69	30	68.49
1.5	8.25	7.0	19.23	15	36.94	32	72.25
2.0	9.09	7.5	20.18	16	39.29	34	75.90
2.5	9.88	8.0	21.10	17	41.44	36	79.60
3.0	10.74	8.5	22.30	18	43.69	38	83.08
3.5	11.40	9.0	23.35	19	45.90	40	86.45
4.0	12.36	9.5	24.55	20	48.02	45	94.25
4.5	13.30	10.0	25.80	22	52.30		
5.0	14.41	11	28.09	24	56.60		

Run 8 air pressure 75.58 cm Hg.

time	pressure	time	pressure	time	pressure	time	pressure
0.0	4.60	6.0	10.45	14	20.88	32	46.25
0.5	6.12	6.5	10.87	15	22.29	34	48.98
1.0	6.85	7.0	11.25	16	23.55	36	51.80
1.5	7.20	7.5	11.80	17	24.70	40	57.6
2.0	7.52	8.0	12.30	18	26.47	45	64.07
2.5	7.82	8.5	12.86	19	27.87	50	70.21
3.0	8.13	9.0	13.48	20	29.17	55	75.97
3.5	8.50	9.5	14.20	22	32.00	60	81.40
4.0	8.82	10.0	14.88	24	34.94	65	86.60
4.5	9.22	11	16.14	26	37.89	70	91.25
5.0	9.65	12	17.45	28	40.70	75	95.25
5.5	10.08	13	19.59	30	43.53		

Run 9 air pressure 75.58 cm Hg.

time	pressure	time	pressure	time	pressure	time	pressure
0.5	7.0	6.5	10.00	15	20.75	36	51.44
1.0	7.45	7.0	10.30	16	22.27	38	54.37
1.5	7.95	7.5	10.82	17	23.51	40	57.28
2.0	8.25	8.0	11.30	18	24.90	45	64.07
2.5	8.41	8.5	11.85	19	26.30	50	70.76
3.0	8.60	9.0	12.35	20	27.75	55	77.09
3.5	8.75	9.5	12.92	22	30.89	60	83.31
4.0	8.92	10.0	13.58	24	33.92	65	89.41
4.5	9.12	11	15.37	26	36.85	70	95
5.0	9.30	12	16.70	28	39.85		
5.5	9.42	13	18.24	30	42.70		
6.0	9.56	14	19.51	32	45.67		

Run 10 air pressure 75.77 cm Hg.

time	pressure	time	pressure	time	pressure	time	pressure
0.0	8.0	6.0	12.87	14	22.10	32	45.00
0.5	8.85	6.5	13.30	15	23.30	34	47.49
1.0	9.20	7.0	13.82	16	24.51	36	50.15
1.5	9.80	7.5	14.42	17	25.70	38	52.60
2.0	10.30	8.0	14.92	18	26.92	40	55.49
2.5	10.65	8.5	15.37	19	28.20	45	61.59
3.0	10.98	9.0	15.85	20	29.50	50	67.66
3.5	11.25	9.5	16.60	22	32.01	55	73.80
4.0	11.57	10.0	17.22	24	34.60	60	79.60
4.5	11.89	11	18.77	26	37.23	65	85.38
5.0	12.22	12	19.98	28	39.86	70	90.98
5.5	12.55	13	20.91	30	42.60	75	95.55

Run 11 air pressure 75.75 cm Hg.

time	pressure	time	pressure	time	pressure	time	pressure
0.0	7.50	7.0	12.53	19	20.18	55	45.90
0.5	8.91	7.5	12.78	20	20.70	60	49.45
1.0	10.18	8.0	13.00	22	22.20	65	52.95
1.5	10.40	8.5	13.27	24	23.56	75	59.50
2.0	10.60	9.0	13.48	26	24.80	90	69.01
2.5	10.78	9.5	13.71	28	26.30	95	72.28
3.0	10.90	10.0	13.89	30	27.77	100	75.24
3.5	11.05	11	14.66	32	29.05	110	81.02
4.0	11.21	12	15.34	34	30.49	120	87.03
4.5	11.33	13	15.91	36	31.95	130	92.77
5.0	11.60	14	16.60	38	33.40		
5.5	11.87	16	17.47	40	34.99		
6.0	12.06	17	18.86	45	38.67		
6.5	12.33	18	19.53	50	42.32		

Run 12 air pressure 75.51 cm Hg.

time	pressure	time	pressure	time	pressure	time	pressure
0	7.0	16	9.55	30	16.20	50	27.32
1	7.10	17	9.90	31	16.95	55	31.60
2	7.19	18	10.35	32	17.35	60	32.64
4	7.60	19	10.80	33	17.40	65	35.30
6	7.80	20	11.23	34	19.00	70	37.93
7	7.88	21	11.65	35	20.04	75	40.60
8	8.00	22	12.50	36	20.50	80	43.21
9	8.10	23	12.50	38	21.00	85	45.78
10	8.25	24	12.91	39	21.80	90	48.43
11	8.40	25	13.35	40	22.20	95	51.01
12	8.61	26	13.80	41	22.80	105	56.41
13	8.85	27	14.55	42	23.39	111	61.81
14	9.05	28	15.20	43	24.06	120	64.4
15	9.30	29	15.80	46	25.05		

Run 13 air pressure 73.67 cm Hg.

time	pressure	time	pressure	time	pressure	time	pressure
0.0	6.50	5.0	19.83	10.0	33.88	20	61.45
0.5	9.20	5.5	20.98	11	36.85	22	66.12
1.0	10.08	6.0	22.40	12	39.70	24	70.50
1.5	11.10	6.5	23.77	13	42.70	26	75.08
2.0	12.12	7.0	25.30	14	45.30	28	79.54
2.5	13.18	7.5	26.80	15	47.90	30	84.00
3.0	14.32	8.0	28.12	16	50.70	32	88.20
3.5	15.38	8.5	29.50	17	53.40	34	92.07
4.0	16.90	9.0	31.50	18	56.20	36	95.54
4.5	18.50	9.5	32.40	19	58.74		

Run 14      air pressure 73.63 cm Hg.

time	pressure	time	pressure	time	pressure	time	pressure
0.0	4.50	5.0	19.30	10.0	34.60	20	62.70
0.5	5.75	5.5	20.65	11	37.65	22	67.55
1.0	7.22	6.0	22.18	12	40.65	26	77.02
1.5	9.08	6.5	23.80	13	43.67	28	81.60
2.0	10.40	7.0	25.40	14	46.45	30	85.87
2.5	11.62	7.5	26.97	15	49.20	32	90.07
3.0	12.83	8.0	28.50	16	51.90	34	93.80
3.5	14.35	8.5	30.00	17	54.61		
4.0	15.84	9.0	31.55	18	57.57		
4.5	17.40	9.5	33.00	19	60.15		

The volume of the apparatus was found to be 236 ccs.

(iii) Theory

Since small bore tubing was used in the manometers (~1mm I.D.) the change in volume with increasing pressure is negligible and thus from the gas equation

$$\frac{PV}{T} = nR$$

under conditions of constant volume and temperature, the change in pressure is directly proportional to the change in the number of moles.



Appendix 7Kinetic results cont.

Calculation of  $\bar{n}$  at  $[\text{OH}^-] = 0.20\text{M}$  for a solution containing  $0.0920\text{MTi(III)}$  and  $0.334\text{M Cl}^-$ .

$$\begin{aligned}\text{For this solution } [\text{H}^+] &= [\text{Cl}^-] - 3 [\text{Ti(III)}] \\ &= 0.334 - 0.276 = 0.058\text{M}\end{aligned}$$

∴ Concentration of base after neutralisation of free acid =  $0.200 - 0.058$

$$\text{i.e. effective } [\text{OH}^-] = 0.142\text{M}$$

$$\begin{aligned}\bar{n} &= \text{ratio } [\text{OH}^-] : [\text{Ti(III)}] \\ &= \frac{0.142}{0.092} = 1.54\end{aligned}$$

i.e. From Figures 13 and 15, hydrogen evolution occurs in solutions where

$$\bar{n} > 1.5.$$

Appendix 8Calculation of  $pK_w$  in 0.41M NaCl at 22°C

The variation of  $pK_w$  with temperature for water<sup>29</sup> is given in Figure 49. Thus at 22°C the ionic product of water is

$$\frac{[H^+][OH^-]}{[H_2O]} = 10^{-14.1}$$

For 0.41M NaCl<sup>30</sup>,  $\frac{\gamma_H \gamma_{OH}}{a_{H_2O}} = 0.530$

$$\text{now } K_w = \frac{\gamma_H \gamma_{OH}}{a_{H_2O}} \cdot \frac{[H^+][OH^-]}{[H_2O]}$$

$$\therefore pK_w = -\log \left( \frac{\gamma_H \gamma_{OH}}{a_{H_2O}} \right) - \log \left( \frac{[H^+][OH^-]}{[H_2O]} \right)$$

$$= 0.275 + 14.100$$

i.e.  $pK_w = 14.375$  for 0.41M NaCl solution at 22°C.

## Appendix 9

Theory for the calculation of  $K_{12}$ ,  $K_{22}$ ,  $K_3$  and  $K_{sp}$  $K_{12}$ 

From equation (16) of Chapter 2

$$K_{12} = \frac{[\text{Ti}_2(\text{OH})_2(\text{H}_2\text{O})_8^{4+}]^{\frac{1}{2}}}{[\text{Ti}(\text{H}_2\text{O})_6^{3+}][\text{OH}^-]} \quad (1)$$

$$= \frac{[\text{H}_2\text{O}]}{[\text{H}^+][\text{OH}^-]} \cdot \frac{[\text{Ti}_2(\text{OH})_2(\text{H}_2\text{O})_8^{4+}]^{\frac{1}{2}}[\text{H}^+]}{[\text{Ti}(\text{H}_2\text{O})_6^{3+}][\text{H}_2\text{O}]} \quad (2)$$

From equation (13) of Chapter 2

$$\beta_{12} = \frac{[\text{Ti}_2(\text{OH})_2(\text{H}_2\text{O})_8^{4+}]^{\frac{1}{2}}[\text{H}^+]}{[\text{Ti}(\text{H}_2\text{O})_6^{3+}][\text{H}_2\text{O}]} \quad (3)$$

$$\therefore \log K_{12} = \text{p}K_w + \log \beta_{12} \quad (4)$$

 $K_{22}$ 

From equation (17) of Chapter 2

$$K_{22} = \frac{[\text{Ti}_2(\text{OH})_2(\text{H}_2\text{O})_8^{4+}]}{[\text{Ti}(\text{OH})(\text{H}_2\text{O})_5^{2+}]^2} \quad (5)$$

From equation (6) of Chapter 2

$$\beta_1 = \frac{[\text{Ti}(\text{OH})(\text{H}_2\text{O})_5^{2+}][\text{H}^+]}{[\text{Ti}(\text{H}_2\text{O})_6^{3+}][\text{H}_2\text{O}]} \quad (6)$$

$$\text{Thus from equations (3) and (6)} \quad K_{22} = \frac{\beta_{12}^2}{\beta_1^2} \quad (7)$$

$$\therefore \log K_{22} = 2(\log \beta_{12} - \log \beta_1) \quad (8)$$

 $K_3$ 

From equation (23) of Chapter 2

$$K_3 = \frac{1}{[\text{Ti}(\text{OH})(\text{H}_2\text{O})_5^{2+}][\text{OH}^-]^2} \quad (9)$$

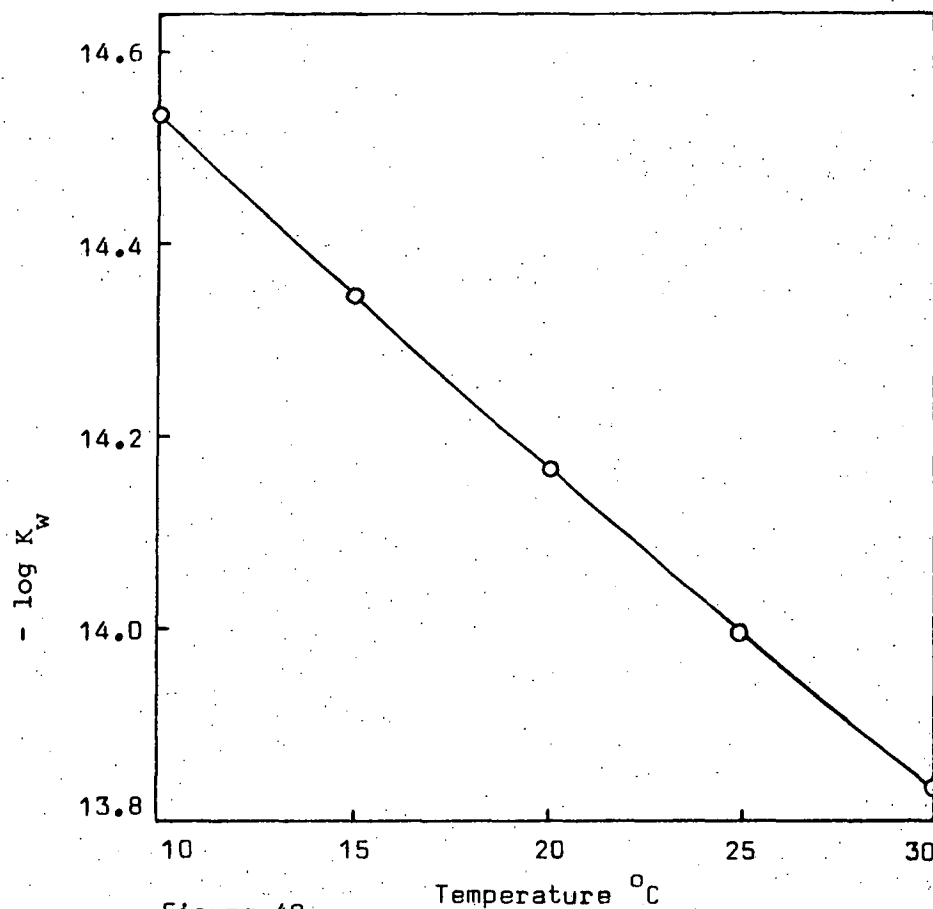


Figure 49.

$$K_3 = \frac{1}{[H^+]^2 [OH^-]^2} \cdot \frac{[H^+]^2}{[Ti(OH)(H_2O)_5^{2+}]} \quad (10)$$

From equation (19) of Chapter 2

$$\beta_3 = \frac{[H^+]^2}{[Ti(OH)(H_2O)_5^{2+}]} \quad (11)$$

$$\therefore \log K_3 = 2pK_w + \log \beta_3 \quad (12)$$

K<sub>sp</sub>

For  $Ti(OH)_3$  (solid)

$$K_{sp} = [Ti(H_2O)_6^{3+}][OH^-]^3 \quad (13)$$

$$= \frac{[Ti(H_2O)_6^{3+}][OH]}{[Ti(OH)(H_2O)_5^{2+}]} \cdot \frac{[Ti(OH)(H_2O)_5^{2+}][OH^-]^2}{1} \quad (14)$$

From equation (10) of Chapter 2

$$K_1 = \frac{[\text{Ti}(\text{OH})(\text{H}_2\text{O})_5^{2+}]}{[\text{Ti}(\text{H}_2\text{O})_6^{3+}][\text{OH}^-]} \quad (15)$$

Thus from equations (9) and (15)

$$K_{sp} = \frac{1}{K_1} \cdot \frac{1}{K_3} \quad (16)$$

$$\text{i.e. } \log K_{sp} = -\log K_1 - \log K_3 \quad (17)$$

### Appendix 10

#### Calculation of extinction coefficient of dark blue species

Absorbance data at 740 nm for equilibrated individual solutions in the region  $1 < \bar{n} < 3$  (i.e.  $0 < \bar{m} < 1$ ) containing the dark blue species are shown in Table 9. Each solution contained

Table 9

Absorbance(A) per cm	$\bar{m}$	$(1-\bar{m})A_{\text{Ti}_2(\text{OH})_2(\text{H}_2\text{O})_8}^*$	$A_{\text{complex}}$
0.777	0.000	0.777	0.000
5.07	0.074	0.720	4.35
7.60	0.158	0.654	6.95
10.67	0.242	0.589	10.08
14.78	0.326	0.524	14.26
15.23	0.411	0.458	14.77
17.15	0.495	0.392	16.76
19.85	0.579	0.327	19.52
22.85	0.663	0.262	22.59
28.7	0.747	0.197	28.5
24.3	0.832	0.131	24.2
0.62	0.916	0.065	0.55
0.04	1.000	0.000	0.04

\*  $A_{\text{Ti}_2(\text{OH})_2(\text{H}_2\text{O})_8}^*$  at 740 nm calculated from absorbance data Fig. 6.

initially 0.0950M Ti(III) and 0.364M  $\text{Cl}^-$  and varying amounts of 2.000M NaOH. The absorbance was measured using 0.1 cm cells. The absorption values for the dark blue complex ( $A_{\text{complex}}$ ) were calculated using the theory outlined in Appendix 5. A plot of  $A_{\text{complex}}$  versus  $\bar{m}$  should be a straight line of slope  $a_{\text{complex}}$  (Figure 50). The scatter of points at the higher  $\bar{m}$  values is largely due to small amounts of the complex settling as a colloidal gel. In the last two solutions most of the species is precipitated. The slope in Figure 50 is 43.6. Thus from equation(5) of Appendix 5,  $\epsilon_{\text{complex}} = \frac{43.6}{0.0950}$

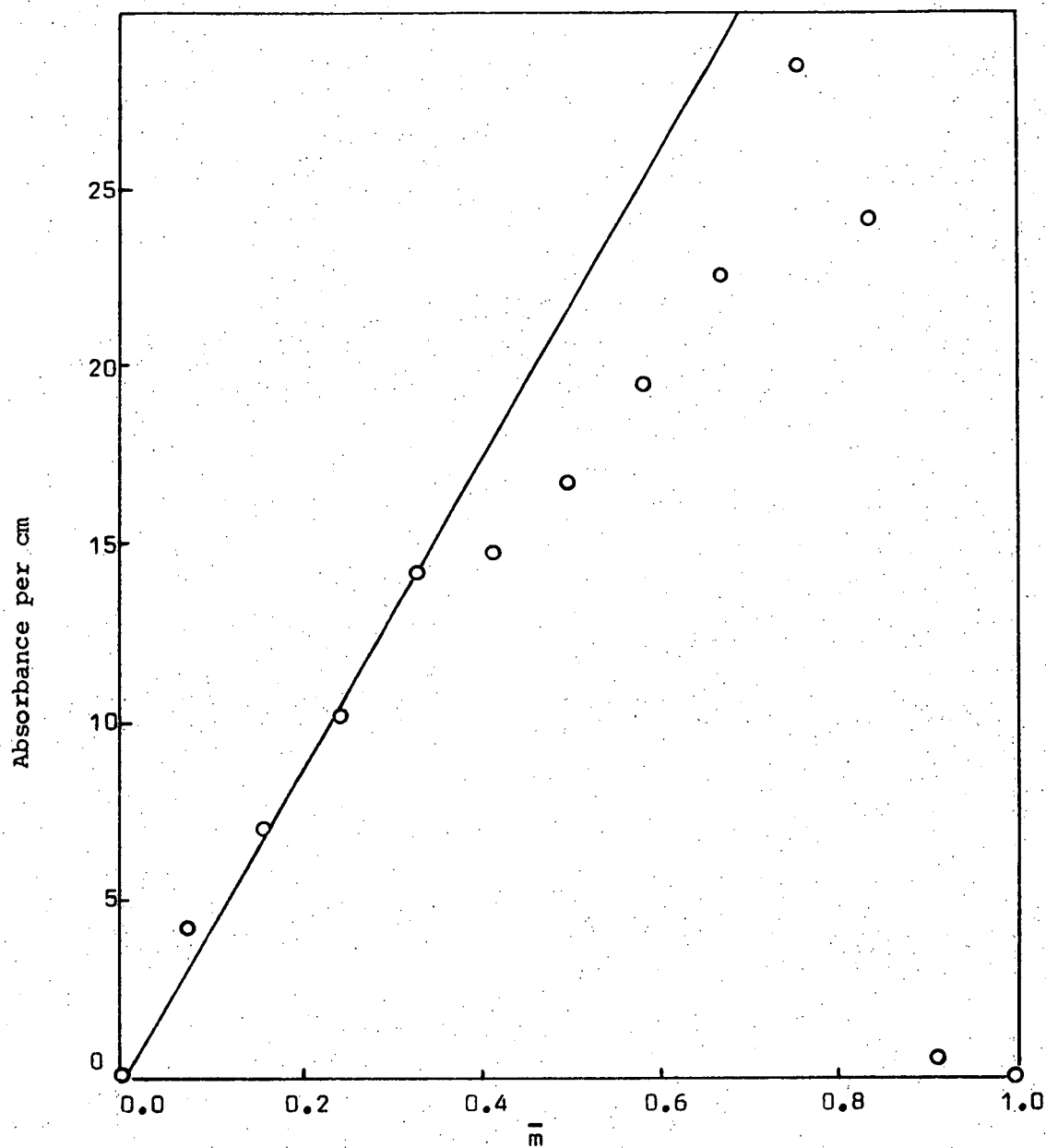
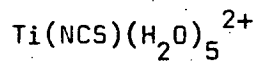


Figure 50

i.e.  $\epsilon_{\text{complex}} = 460 \pm 20^* \text{ moles}^{-1} \text{ litres cm}^{-1}$ , at 740 nm.

\*Estimated error.

## Appendix 11

Calculation of stability constant for the 1:1 complex.

For the reaction  $\text{Ti(H}_2\text{O)}_6^{3+} + \text{NCS}^- \rightleftharpoons \text{Ti(NCS)(H}_2\text{O)}_5^{2+} + \text{H}_2\text{O}$

$$K_1 = \frac{[\text{Ti(NCS)(H}_2\text{O)}_5^{2+}]}{[\text{Ti(H}_2\text{O)}_6^{3+}][\text{NCS}^-]} \quad (1)$$

Assuming that the formation of a 1:4 complex can be neglected in dilute thiocyanate solutions, the absorbance of the solution will be given by:

$$A = \epsilon_{\text{Ti}^{3+}} [\text{Ti}^{3+}] + \epsilon_{\text{TiNCS}^{2+}} [\text{TiNCS}^{2+}] \text{ for 1 cm cells} \quad (2)$$

(note: ammonium thiocyanate solutions have zero absorbance in the wavelength region studied). The total titanium concentration is given by:

$$[\text{Ti(III)}] = [\text{Ti}^{3+}] + [\text{TiNCS}^{2+}] = \text{constant} \quad (3)$$

Substituting 3 in 2 and rearranging gives

$$A = [\text{TiNCS}^{2+}] \left\{ \epsilon_{\text{TiNCS}^{2+}} - \epsilon_{\text{Ti}^{3+}} \right\} + [\text{Ti(III)}] \epsilon_{\text{Ti}^{3+}} \quad (4)$$

But  $[\text{Ti(III)}] \epsilon_{\text{Ti}^{3+}} = A_o = \text{Initial absorbance reading. Thus}$

$$[\text{TiNCS}^{2+}] = \frac{A - A_o}{\epsilon_{\text{TiNCS}^{2+}} - \epsilon_{\text{Ti}^{3+}}} \quad (5)$$

$$[\text{Ti}^{3+}] = [\text{Ti(III)}] - \frac{A - A_o}{\epsilon_{\text{TiNCS}^{2+}} - \epsilon_{\text{Ti}^{3+}}} \quad (6)$$

$$[\text{NCS}^-] = [\text{NCS}^-]_T - \frac{A - A_o}{\epsilon_{\text{TiNCS}^{2+}} - \epsilon_{\text{Ti}^{3+}}} \quad (7)$$

where  $[\text{NCS}^-]_T = \text{total thiocyanate ion concentration. The values of the concentration terms in equation 1 are given by equations 5, 6 and 7.}$



The value of  $\epsilon_{\text{TiNCS}^{2+}}$  was obtained by substituting varying numerical values in the above equations until the best fit of the data was obtained, since, from equation 1 a plot of  $\frac{[\text{TiNCS}^{2+}]}{[\text{Ti}^{3+}]}$  versus  $[\text{NCS}^-]$  should be a straight line of slope  $K_1$ . The absorbance data at 500 nm and 600 nm for a series of individual solutions are shown in Tables 10 and 11. Each solution contained 0.0920M Ti(III), 0.334M  $\text{Cl}^-$  and varying amounts of  $\text{NH}_4\text{NCS}$  up to 0.84M. Total volume of each solution was 50 mls. Absorbance values were measured using 0.5 cm cells.

Table 10

Data at 500 nm

A (Absorbance per cm)	$\frac{A - A_0}{\Delta \epsilon}$	$\frac{A - A_0}{\Delta \epsilon}$ [Ti(III)]	[NCS] <sub>T</sub>	[NCS <sup>-</sup> ]	$\frac{[TiNCS^{2+}]}{[Ti^{3+}]}$
0.342	0.0000	0.0920	0.000	0.0000	0.0000
0.444	0.0051	0.0869	0.030	0.0249	0.0587
0.540	0.0099	0.0821	0.060	0.0501	0.1206
0.638	0.0148	0.0772	0.090	0.0752	0.1917
0.720	0.0189	0.0731	0.120	0.1011	0.2585
0.794	0.0226	0.0694	0.150	0.1274	0.3256
0.864	0.0261	0.0659	0.180	0.1539	0.3961
0.926	0.0295	0.0628	0.210	0.1808	0.4650
0.982	0.0320	0.0600	0.240	0.2080	0.5333
1.044	0.0351	0.0569	0.270	0.2349	0.6169
1.096	0.0377	0.0543	0.300	0.2623	0.6943
1.176	0.0417	0.0503	0.360	0.3183	0.8290
1.248	0.0453	0.0467	0.420	0.3747	0.9700
1.306	0.0482	0.0438	0.480	0.4318	1.1005
1.364	0.0511	0.0409	0.540	0.4889	1.2494
1.420	0.0539	0.0381	0.600	0.5461	1.4147
1.506	0.0582	0.0338	0.720	0.6618	1.7219
1.584	0.0621	0.0299	0.840	0.7779	2.0769

$$\epsilon_{TiNCS^{2+}} = 23.7^* \text{ moles}^{-1} \text{ l cm}^{-1}, \therefore \text{calculated } \epsilon_{TiNCS^{2+}}^{(540 \text{ nm})}$$

$$= 27.3 \text{ moles}^{-1} \text{ l cm}^{-1}, \epsilon_{Ti^{3+}} = 3.72 \text{ moles}^{-1} \text{ l cm}^{-1},$$

$$\therefore \epsilon_{TiNCS^{2+}} - \epsilon_{Ti^{3+}} = \Delta \epsilon = 20.0 \text{ moles}^{-1} \text{ l cm}^{-1}$$

\* value giving best fit of experimental data.

Table 11

Data at 600 nm

A (Absorbance per cm)	$\frac{A-A_0}{\Delta \xi}$	$[\text{Ti(III)}] \frac{A-A_0}{\Delta \xi}$	$[\text{NCS}^-]_T$	$[\text{NCS}^-]$	$\frac{[\text{TiNCS}^{2+}]}{[\text{Ti}^{3+}]}$
0.192	0.0000	0.0920	0.000	0.0000	0.0000
0.282	0.0050	0.0870	0.030	0.0250	0.0575
0.370	0.0099	0.0821	0.060	0.0501	0.1206
0.452	0.0144	0.0776	0.090	0.0756	0.1856
0.524	0.0184	0.0736	0.120	0.1016	0.2500
0.594	0.0223	0.0697	0.150	0.1277	0.3199
0.656	0.0258	0.0662	0.180	0.1542	0.3897
0.716	0.0291	0.0629	0.210	0.1809	0.4626
0.764	0.0318	0.0602	0.240	0.2082	0.5282
0.820	0.0349	0.0571	0.270	0.2351	0.6112
0.856	0.0369	0.0551	0.300	0.2631	0.6697
0.936	0.0413	0.0507	0.360	0.3187	0.8146
1.008	0.0453	0.0467	0.420	0.3747	0.9700
1.066	0.0486	0.0434	0.480	0.4314	1.120
1.124	0.0518	0.0402	0.540	0.4882	1.289
1.178	0.0548	0.0372	0.600	0.5452	1.473

$$\xi_{\text{TiNCS}^{2+}} = 20.1^* \text{ moles}^{-1} \text{ l cm}^{-1}, \therefore \text{calculated } \xi_{\text{TiNCS}^{2+}}(540 \text{ nm})$$

$$= 26.7 \text{ moles}^{-1} \text{ l cm}^{-1}, \xi_{\text{Ti}^{3+}} = 2.09 \text{ moles}^{-1} \text{ l cm}^{-1}, \Delta \xi = 18.0 \text{ moles}^{-1} \text{ l cm}^{-1}.$$

Plots of the data at 500 nm and 600 nm are shown in Figures 51 and 52. A good straight line fit was obtained up to thiocyanate ion concentrations of 0.4M. At higher concentrations the curve deviated from the straight line, indicating that the formation of the 1:4 species was beginning to be

\* value giving best fit of experimental data

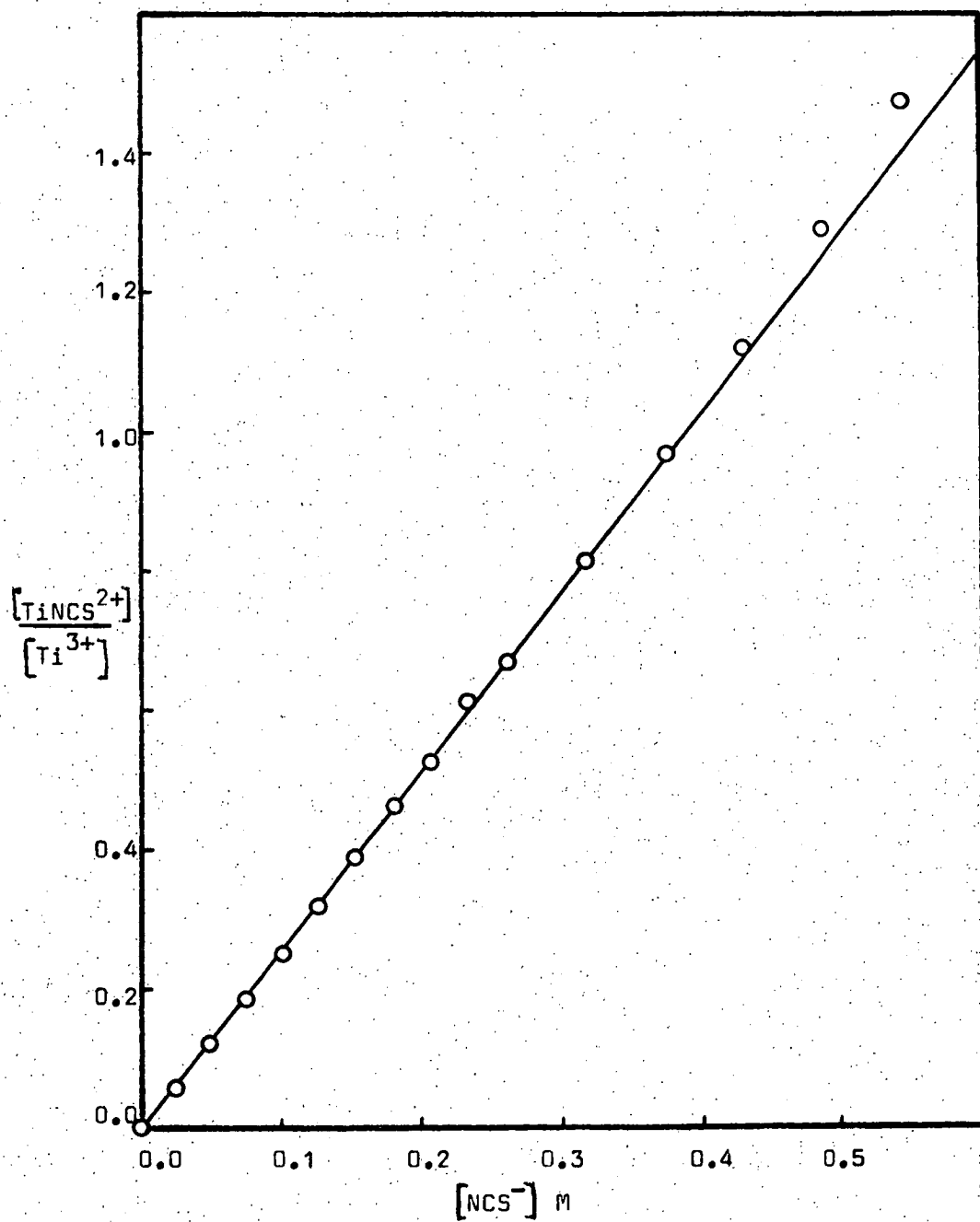


Figure 51.

significant in these solutions. From the slopes of the curves,  $K_1$  was found to be 2.57 and 2.55 respectively.

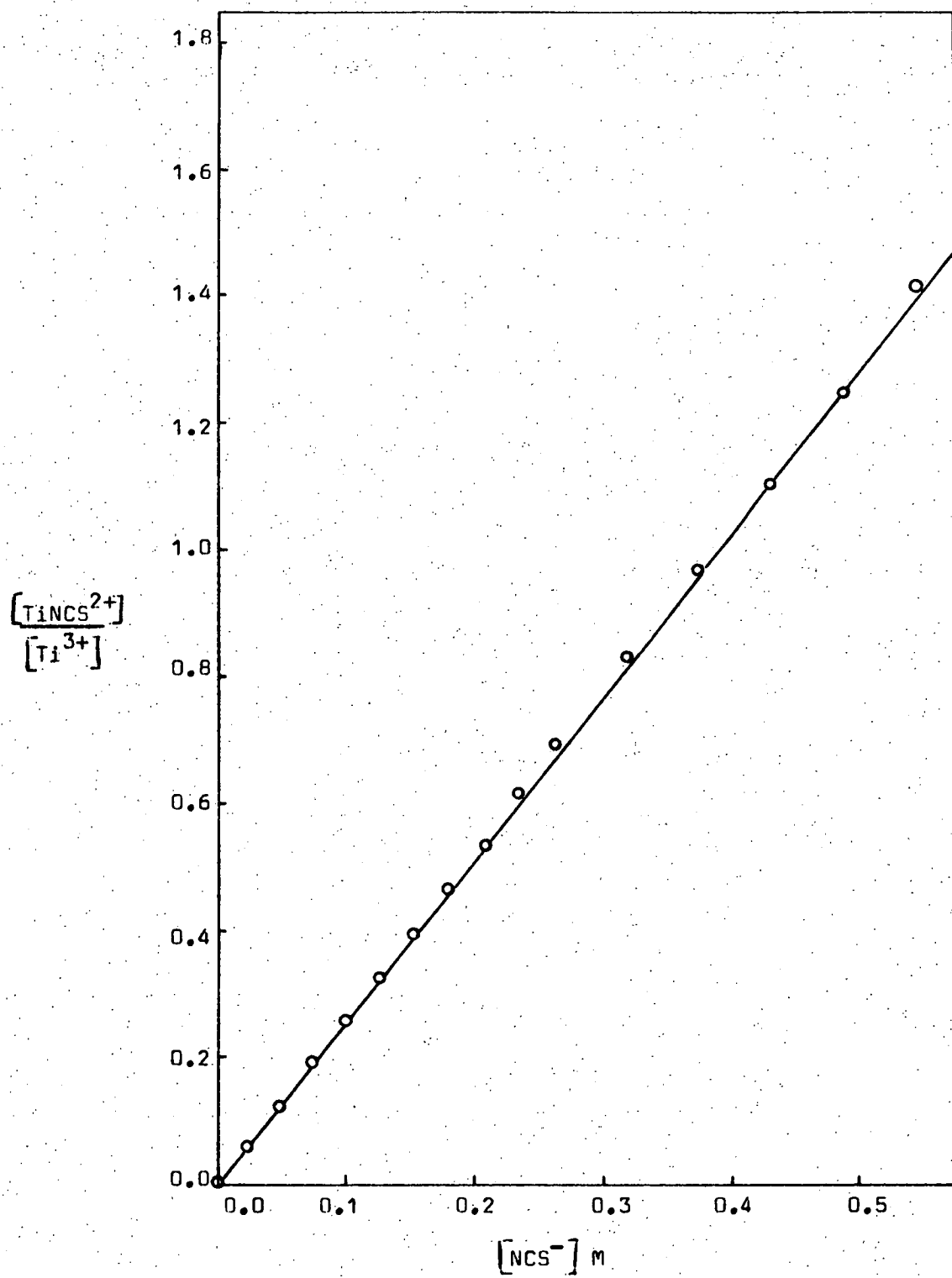


Figure 52.

## Appendix 12

Calculation of stability constant for the 1:4 complex  $\text{Ti}(\text{NCS})_4(\text{H}_2\text{O})_2^-$ .

For the reaction  $\text{Ti}(\text{NCS})(\text{H}_2\text{O})_5^{2+} + 3\text{NCS}^- \rightleftharpoons \text{Ti}(\text{NCS})_4(\text{H}_2\text{O})_2^-$

$$K_{14} = \frac{[\text{Ti}(\text{NCS})_4(\text{H}_2\text{O})_2^-]}{[\text{Ti}(\text{NCS})(\text{H}_2\text{O})_5^{2+}][\text{NCS}^-]^3} \quad (1)$$

In concentrated solutions, the absorbance of the solution is given by:

$$A = \epsilon_{\text{Ti}^{3+}}[\text{Ti}^{3+}] + \epsilon_{\text{TiNCS}^{2+}}[\text{TiNCS}^{2+}] + \epsilon_{\text{Ti}(\text{NCS})_4^-}[\text{Ti}(\text{NCS})_4^-] \quad (2)$$

for 1 cm cells. From equation 1 of Appendix 11,

$$[\text{TiNCS}^{2+}] = K_1 [\text{Ti}^{3+}][\text{NCS}^-] \quad (3)$$

$$\text{and from equation 1, } [\text{Ti}(\text{NCS})_4^-] = K_{14} K_1 [\text{Ti}^{3+}] [\text{NCS}^-]^4 \quad (4)$$

The total titanium(III) content of the solution is given by:

$$[\text{Ti(III)}] = [\text{Ti}^{3+}] + [\text{TiNCS}^{2+}] + [\text{Ti}(\text{NCS})_4^-] = \text{constant} \quad (5)$$

After substituting equations 3 and 4, equation 5 becomes:

$$[\text{Ti(III)}] = [\text{Ti}^{3+}] \{1 + K_1 [\text{NCS}^-] + K_{14} K_1 [\text{NCS}^-]^4\} \quad (6)$$

Substituting equations 3, 4 and 6 into equation 2 and rearranging to separate  $K_{14}$  gives:

$$K_{14} \{A - \epsilon_{\text{Ti}(\text{NCS})_4^-} [\text{Ti(III)}]\} K_1 [\text{NCS}^-]^4 = \epsilon_{\text{Ti}^{3+}} [\text{Ti(III)}] - A + \epsilon_{\text{TiNCS}^{2+}} [\text{Ti(III)}] K_1 [\text{NCS}^-] - A K_1 [\text{NCS}^-] \quad (7)$$

Writing  $A_0$  for  $\epsilon_{\text{Ti}^{3+}} [\text{Ti(III)}]$ ,  $A_1$  for  $\epsilon_{\text{TiNCS}^{2+}} [\text{Ti(III)}]$  and  $A_4$  for  $\epsilon_{\text{Ti}(\text{NCS})_4^-} [\text{Ti(III)}]$ , equation 7 simplifies to

$$K_{14} \{A - A_4\} K_1 [\text{NCS}^-]^4 = A - A_0 + (A - A_1) K_1 [\text{NCS}^-] \quad (8)$$

$A_0$  is known for  $\text{Ti}^{3+}$ , and  $K_1$  and  $A_1$  are known for  $\text{TiNCS}^{2+}$ . The equilibrium thiocyanate concentration is given by:

$$[\text{NCS}^-] = [\text{NCS}^-]_{\text{total}} - [\text{TiNCS}^{2+}] - 4[\text{Ti}(\text{NCS})_4^-] \quad (9)$$

However, for a weak 1:4 complex in solutions containing high thiocyanate ion concentrations, equation 10 becomes a good approximation and equilibrium thiocyanate concentrations were calculated this way.

$$[\text{NCS}^-] = [\text{NCS}^-]_{\text{total}} - [\text{Ti(III)}] \quad (10)$$

Since a graph of  $(A - A_0) + (A - A_1)K_1 [\text{NCS}^-]$  versus  $(A_4 - A)K_1 [\text{NCS}^-]^4$  should be a straight line of slope  $K_{14}$ , the value of  $A_4$  was obtained by substituting varying numerical values in equation 8 until the best fit of the data was obtained.

The absorbance data at 520 nm and 560 nm for a series of individual solutions are shown in Tables 12 and 13. Each solution contained 0.0344M Ti(III), 0.263M  $\text{Cl}^-$  and varying amounts of  $\text{NH}_4\text{NCS}$  up to 7.20M. Total volume of each solution was 50 mls. Absorbance values were measured using 0.5 cm cells.

Table 12

Data at 520 nm for 1 cm cells.

$[\text{NCS}^-]_T$	$[\text{NCS}^-]$	A (Absorbance per cm)	$(A_4 - A)K_1 [\text{NCS}^-]^4$	$\frac{(A + A_0) + (A - A_1)K_1 [\text{NCS}^-]}{(A_4 - A)K_1 [\text{NCS}^-]^4}$
0.00	0.000	0.126	0.00	0.000
1.60	1.573	0.812	10.94	0.360
2.40	2.371	0.958	44.67	1.227
3.20	3.170	1.098	106.53	2.636
4.00	3.969	1.178	210.83	3.948
4.80	4.769	1.268	320.36	5.720
5.60	5.568	1.354	383.78	7.798
6.40	6.368	1.402	454.62	9.574
7.20	7.168	1.436	500.10	11.273

$$K_1 = 2.56, \quad A_1 = 0.893, \quad A_4 = 1.510^*$$

$$\text{i.e. } \epsilon_4 = \frac{A_4}{[\text{Ti(III)}]} = 44.4 \text{ moles}^{-1} \text{ l cm}^{-1}, \quad \therefore \text{calculated } \epsilon_{\text{Ti}(\text{NCS})_4^-} (550 \text{ nm}) = 49.9 \text{ moles}^{-1} \text{ l cm}^{-1}.$$

Table 13

Data at 560 nm for 1 cm cells.

$[\text{NCS}^-]_T$	$[\text{NCS}^-]$	A (Absorbance per cm)	$(A_4 - A)K_1[\text{NCS}^-]^4$	$\frac{(A + A_0) + (A - A_1)K_1[\text{NCS}^-]}{K_1[\text{NCS}^-]}$
0.00	0.000	0.106	0.0	0.000
1.60	1.573	0.824	14.5	0.372
2.40	2.371	0.988	61.7	1.355
3.20	3.170	1.130	160.3	2.809
4.00	3.969	1.256	313.7	4.666
4.80	4.769	1.368	505.7	6.853
5.60	5.568	1.460	713.4	9.194
6.40	6.368	1.544	867.1	11.772
7.20	7.168	1.604	986.7	14.233

$$K_1 = 2.56, \quad A_1 = 0.910, \quad A_4 = 1.750^*$$

i.e.  $\xi_4 = 51.5 \text{ moles}^{-1} \text{ l cm}^{-1}$ ,  $\therefore$  calculated  $\xi_{\text{Ti}(\text{NCS})_4^-}$  (550 nm)

=  $51.8 \text{ moles}^{-1} \text{ l cm}^{-1}$ . \*value giving best fit of experimental data.

Plots of the data at 520 nm and 560 nm are shown in Figures 53 and 54.

Some scatter in the data was observed due to magnification of experimental errors by the 4th power term in the calculation. From the slopes of the curves,  $K_{14}$  was found to be  $2.1 \times 10^{-2}$  and  $1.4 \times 10^{-2}$  respectively.



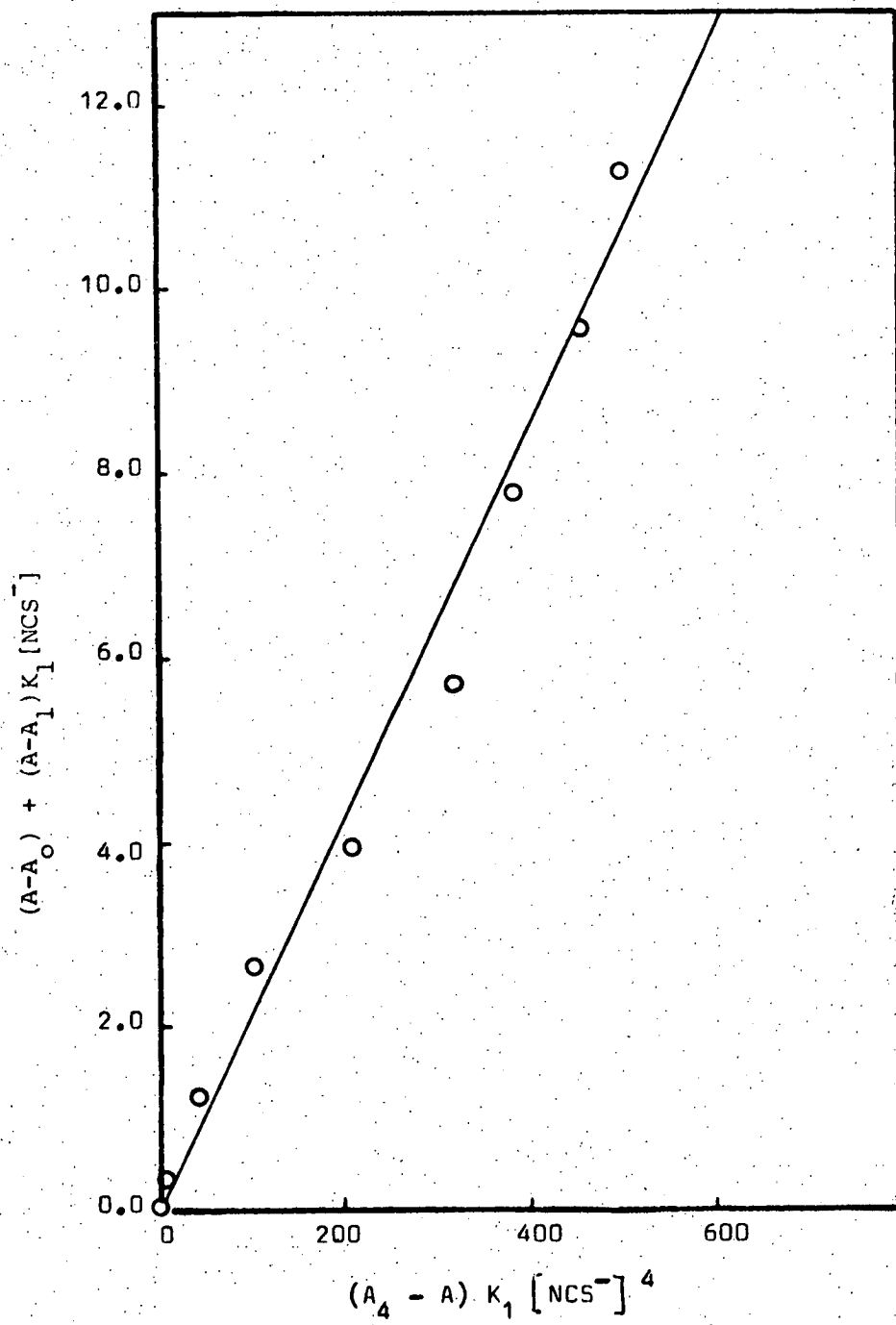


Figure 53.

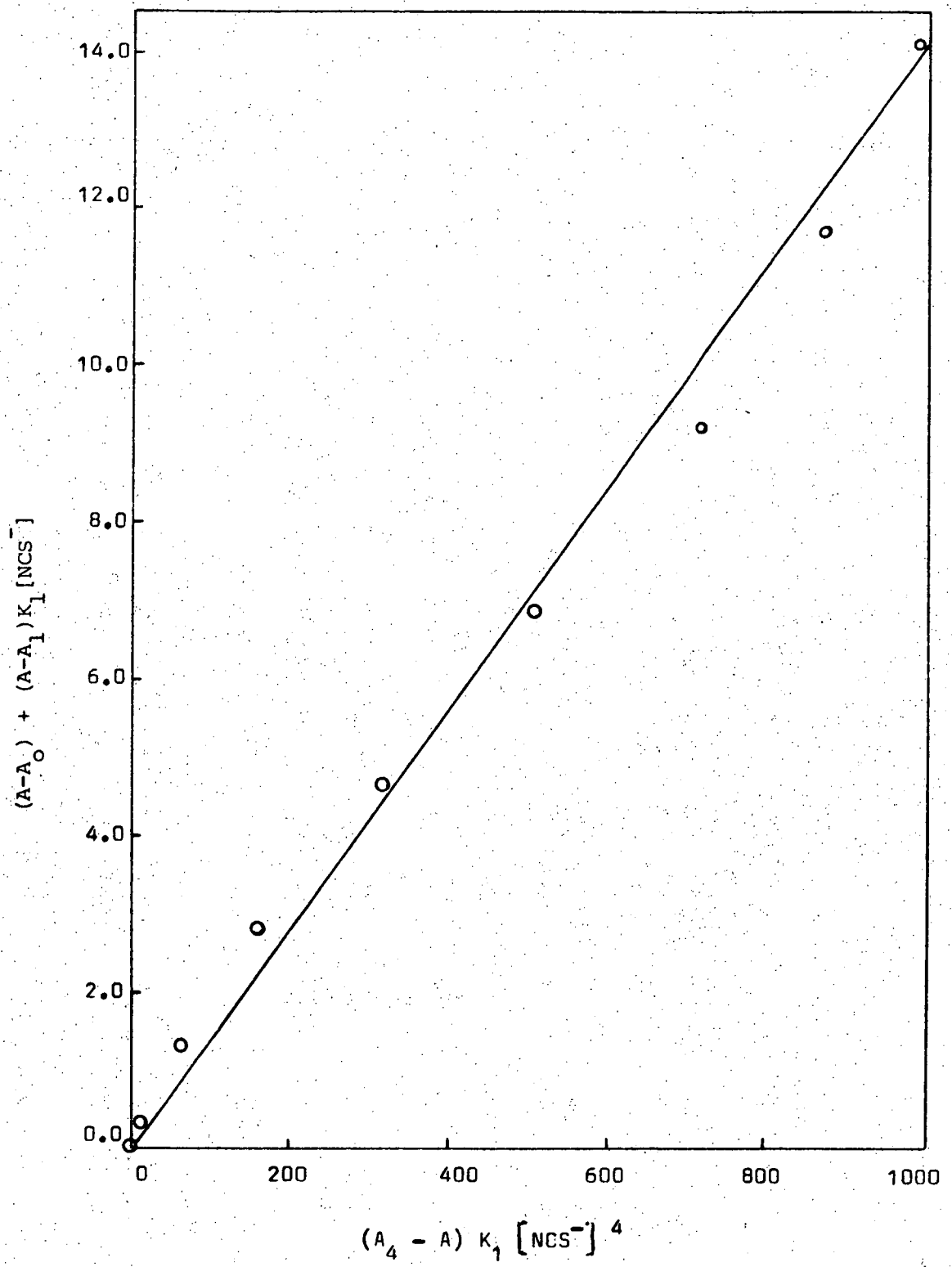


Figure 54.

Appendix 13Calculation of formation constant for 1:1 mixed oxidation state species.(i) Theory

For the reaction  $\text{Ti(III)} + \text{Ti(IV)} \rightleftharpoons \text{Ti(III)Ti(IV)}$

$$K_{11} = \frac{[\text{Ti(III)Ti(IV)}]}{[\text{Ti(III)}][\text{Ti(IV)}]} \quad (1)$$

For continuous variation solutions, total absorbance is given by:

$$A = a_4(v - c) + a_3(1 - v - c) + a_c c \quad (2)$$

where  $v$  = total mole fraction of Ti(IV) present,  $1 - v$  = total mole fraction of Ti(III) present, and  $c$  = mole fraction of dimer formed.  $a_3$ ,  $a_4$  and  $a_c$  = the relative absorptivity coefficients of Ti(III), Ti(IV) and dimer respectively. Rearranging equation 2 gives

$$A - a_4 v - a_3(1-v) = c(a_c - a_4 - a_3) \quad (3)$$

$$\text{i.e. } \Delta D = c \Delta a \quad (4)$$

where  $\Delta D = A - a_4 v - a_3(1 - v)$  being the Job difference parameter. In the limit as  $v \rightarrow 0$ ,  $c = v$ , and similarly, in the limit as  $(1 - v) \rightarrow 0$ ,  $c = (1 - v)$ . Therefore, from equation 4

$$\frac{(d\Delta D)}{(dv)_{v=0}} = - \frac{(d\Delta D)}{(dv)_{(1-v)=0}} = \Delta a \quad (5)$$

That is, the slope of the tangents to the curve at  $v = 0$  and  $1$ , give the relative absorptivity coefficient difference ( $\Delta a$ ) of the complex. Using these values of  $\Delta a$ , and equations 4 and 6, and  $\Delta D_{\max}$  data, the equilibrium constant  $K_{11}$  was calculated.

$$K_{11} = \frac{c}{(v-c)(1-v-c)} \quad (6)$$

(ii) Thiocyanate system data

100 ml solution containing 0.0340M titanium, 0.261M  $\text{Cl}^-$ , and 6.40M  $\text{NH}_4\text{SCN}$ . The titanium(III) content of the solution at various stages

was determined by titrating 2 ml aliquots with 0.02110M  $\text{Fe}(\text{NH}_4)(\text{SO}_4)_2$  solution, using a 5 ml micro-burette. The absorbance data for the solution at 450 nm and 470 nm are given in Tables 14 and 15. [0.5 cm cells used].

Table 14

Data at 450 nm

$$a_3 = 0.248 \text{ moles}^{-1} \text{ l cm}^{-1}, a_4 = 1.302 \text{ moles}^{-1} \text{ l cm}^{-1}$$

A (Absorbance per cm)	1-v	$a_3(1-v)$	$a_4v$	$\Delta D$
0.248	1.000	0.2480	0.0000	0.0000
0.578	0.891	0.2210	0.1420	0.2150
0.856	0.755	0.1872	0.3190	0.3498
1.216	0.525	0.1302	0.6184	0.4674
1.296	0.304	0.0754	0.9062	0.3144
1.324	0.109	0.0270	1.1600	0.1370
1.302	0.000	0.0000	1.3020	0.0000

Table 15

Data at 470 nm

$$a_3 = 0.486 \text{ moles}^{-1} \text{ l cm}^{-1}, a_4 = 0.422 \text{ moles}^{-1} \text{ l cm}^{-1}$$

(Absorbance per cm)	1-v	$a_3(1-v)$	$a_4v$	$\Delta D$
0.486	1.000	0.4860	0.0000	0.0000
0.584	0.891	0.4330	0.0460	0.1070
0.646	0.755	0.3670	0.1034	0.1756
0.688	0.525	0.2552	0.2004	0.2324
0.622	0.304	0.1478	0.2938	0.1604
0.500	0.109	0.0530	0.3760	0.0710
0.422	0.000	0.0000	0.4220	0.0000

Plots of  $\Delta D$  versus  $v$  are shown in Figure 26. The slope of the tangent to the curve at  $v=0$  and 1, gives the relative absorptivity coefficient of the complex,  $a_c$ . Unless a stable complex is formed, these tangents cannot be estimated with any accuracy. However tangents to the curves were estimated and the values obtained together with the calculated corresponding  $K_{11}$  values are given in Table 16.

Table 16

Wavelength(nm)	$\left(\frac{d\Delta D}{dv}\right)_{v=0}$	$K_{11}$	$-\left(\frac{d\Delta D}{dv}\right)_{v=1}$	$K_{11}$
450	2.37	2.2	1.33	16.3
470	1.60	1.2	0.67	14.7

The large variations in  $K_{11}$  are a result of the experimental errors in estimating the tangents to the curves, because of the low stability of the complex.

(iii) Sulphate system data.

Using the data reported by Goroshchenko and Godneva<sup>63</sup> replotted in Figure 39, the tangents to the curve were estimated and the values obtained together with the calculated corresponding  $K_{11}$  values are given in Table 17.

Table 17

limit	value	$K_{11}$
$\left(\frac{d\Delta D}{dv}\right)_{v=0}$	0.3218	10.13
$-\left(\frac{d\Delta D}{dv}\right)_{v=0}$	0.3127	8.91

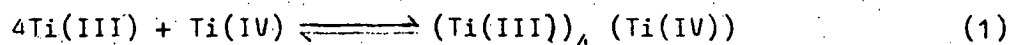
Appendix 14Calculation of formation constant for 4:1 mixed oxidation state species.

Let the total mole fraction of titanium(IV) present =  $v$

Let the total mole fraction of titanium(III) present =  $1 - v$

Let the total mole fraction of dimer present =  $c$

Let  $a_3$  and  $a_c$  = the absorptivity per cm, per mole fraction of titanium(III) and dimer respectively. Titanium(IV) does not absorb under these conditions in the wavelength region studied. For the reaction



the total absorbance of the solution is given by

$$A = a_3 (1 - v - 4c) + a_c c \quad (2)$$

rearranging equation (45) gives

$$A - a_3 (1 - v) = c (a_c - 4a_3) \quad (3)$$

$$\text{i.e. } \Delta D = c \Delta a \quad (4)$$

Where  $\Delta D = A - a_3(1-v)$  is the Job difference parameter.

Absorbance data at 476 nm and 530 nm are shown in Tables 18 and 19.

Total titanium concentration = 0.0826M, total chloride ion concentration = 0.478M, total sulphate ion concentration (as ammonium sulphate) = 0.894M.

Table 18Data at 476 nm

A (Absorbance per cm)	(1-v)	$a_3(1-v)$	$\Delta D$
0.258	1.000	0.258	0.000
0.292	0.993	0.256	0.036
0.352	0.985	0.254	0.098
0.436	0.973	0.251	0.185
0.550	0.955	0.246	0.304
0.630	0.937	0.242	0.388
0.723	0.904	0.233	0.490
0.775	0.881	0.227	0.548
0.804	0.797	0.205	0.599
0.763	0.701	0.181	0.582
0.678	0.540	0.139	0.539
0.572	0.433	0.112	0.460
0.496	0.344	0.089	0.407
0.378	0.252	0.065	0.313
0.232	0.144	0.037	0.195

Table 19

Data at 530 nm

A (Absorbance per cm)	(1-v)	$a_3(1-v)$	$\Delta D$
0.388	1.000	0.388	0.000
0.415	0.993	0.385	0.030
0.459	0.985	0.382	0.077
0.524	0.973	0.378	0.146
0.610	0.955	0.370	0.240
0.667	0.937	0.364	0.303
0.733	0.904	0.351	0.382
0.783	0.881	0.342	0.441
0.790	0.797	0.309	0.481
0.742	0.701	0.272	0.470
0.648	0.540	0.210	0.438
0.550	0.433	0.168	0.382
0.473	0.344	0.133	0.340
0.359	0.252	0.098	0.261
0.217	0.144	0.056	0.161

In the limit as  $v \rightarrow 0$ ,  $c = v$  and  $\left(\frac{d\Delta D}{dv}\right)_{v=0} = \Delta a$ . i.e. For a plot of  $\Delta D$  versus  $v$ , the slope of the tangent to the curve at  $v=0$  gives the absorptivity coefficient of the complex  $a_c$ . Thus for equation (1)

$$K_{41} = \frac{[Ti(III)_4(Ti(IV))]}{[Ti(III)]^4 [Ti(IV)]} \quad (5)$$

$$\text{i.e. } K_{41} = \frac{c}{(1-v-4c)^4 (v-c)} \quad (6)$$

Using a values obtained from the tangents to the curve Figure 40 and



$\Delta D$  values at  $v=0.203$ ,  $C$  at  $v=0.203$  was calculated using equation (4), and  $K_{41}$  was calculated from this data using equation (6). Also, from equation (3)

$$\Delta a = a_c - 4a_3$$

The absorptivity per titanium(III) atom for the complex is

$$\frac{a_c}{4} = \frac{\Delta a}{4} + a_3 \quad (7)$$

and the extinction coefficient of the complex per titanium(III) atom is

given by  $\xi = \frac{a_c}{4 [Ti]}$  (8)

The results obtained are summarised below

Wavelength (nm)	$\left(\frac{d\Delta D}{dv}\right)_{v=0}$	$C_{(v=0.203)}$	$K_{41}$	$\xi$ (moles <sup>-1</sup> l cm <sup>-1</sup> )
476	6.60	0.0908	22.8	23.1
530	5.85	0.0822	14.2	22.4

References

1. Latimer W.M., Oxidation Potentials, Prentice Hall, New York 1952.
2. Polyakova V.M. and Chernyavskaya E.I., Tr. Inst. Khim., Akad. Nauk SSSR, Ural. Filial, 1970, 17, 148.
3. Mackenzie H.A.E. and Tompkins F.C., Trans. Faraday Soc., 1942, 38, 465.
4. Polyakova V.M. and Chernyavskaya E.I., Tr. Inst. Khim., Akad. Nauk SSSR, Ural. Filial, 1970, 20, 94.
5. Hartmann H. and Schlafer H.L., Z. Physik. Chem., 1951, 197, 116.
6. Ilse F.E. and Hartmann H., Z. Physik. Chem., 1951, 197, 239.
7. Gardner H.J., Aust. J. Chem., 1967, 20, 2357.
8. Clark R.J.H., The Chemistry of Titanium and Vanadium, Elsevier, London 1968.
9. Karpinskaya N.M. and Andreev S.N., Zh. Neorg. Khim., 1968, 13, 50.
10. Klygin A.E. et al., Zh. Neorg. Khim., 1971, 16, 1590.
11. Morozov I.S., Toptygina G.M. and Lipatova N.P., Zh. Neorg. Khim., 1961, 6, 2528.
12. Schlafer H.L. and Fritz H.P., Spectrochimica Acta, 1967, 23A, 1409.
13. Straumanis M.E. and Chen P.C., J. Electrochem. Soc., 1951, 98, 234.
14. Straumanis M.E. et al., J. Electrochem. Soc., 1956, 103, 439.
15. Woods P.H. and Cockerell L.D., J. Am. Chem. Soc., 1958, 80, 1534.
16. Anselmi D. and Farnia G., Electrochim. Metal, 1968, 3, 51.
17. Titova I.E. and Dement'eva M.I., Zh. Prikl. Khim., 1968, 41, 280.
18. Reznichenko V.A., Izv. Akad. Nauk SSSR, Metal, 1970, 4, 62.
19. Morgan L.O., Proc. 6th ICCC, 1961, 471.
20. Pecsok R.L. and Fletcher A.N., Inorg. Chem., 1962, 1, 155.
21. Paris M.R. and Gregoire Cl., Anal. Chim. Acta, 1968, 42, 439.
22. Krentzien H. and Brito F., Ion (Madrid), 1970, 30, 14.
23. Pajdowski L., Inorg. Nuc. Chem., 1966, 28, 433.
24. Sillen L.G., Quart. Rev., 1959, 13, 146.

25. Sillen L.G. and Martell A.E., Stability Constants of Metal-ion Complexes, Special Publication Nos. 17 and 25, The Chemical Society London, 1964 and 1971.
26. Schaffer C.E. and Jorgensen C.K., Inorg. Nucl. Chem., 1958, 8, 149.
27. Pajdowski L. and Jezowska-Trzebiatowska B., Inorg. Nucl. Chem., 1966, 28, 443.
28. Akitt J.W. et al., J. Chem., Soc., 1972, D, 604.
29. Weast R.C., Handbook of Chemistry and Physics, The Chemical Rubber Co. Cleveland Ohio, 52nd Ed. 1972, p D-122.
30. Harned H.S. and Owen B.B., The Physical Chemistry of Electrolyte Solutions, Reinhold, New York 1943, p578.
31. Sylva R.N., Rev. Pure and Appl. Chem., 1972, 22, 115.
32. Atkinson R.J., Posner A.M. and Quirk J.P., Inorg. Nucl. Chem., 1968, 30, 2371.
33. Spiro T.G. et al., J. Am. Chem. Soc., 1966, 88, 2721.
34. Sheka I.A., Chaus I.S. and Mityreva T.T., The Chemistry of Gallium, Elsevier, London 1966, p41.
35. Kroon D.J. and Stolpe C., Nature, 1959, 183, 945.
36. Critchfield F.E. and Johnson J.B., Anal. Chem., 1958, 30, 1247.
37. Critchfield F.E. and Johnson J.B., Anal. Chem., 1959, 31, 570.
38. Roberts N.K. and van der Woude H., J. Chem. Soc., 1968, A, 940.
39. Mellor J.W., A Comprehensive Treatise on Inorganic and Theoretical Chemistry, Longmans, Green and Co. Ltd., 1927, 7, p29,77.
40. Jorgensen C.K., Acta. Chem. Scand., 1957, 11, 73.
41. Cordfunke E.H.P., The Chemistry of Uranium, Elsevier, Amsterdam 1969, p100.
42. Barnard R. et al, J. Chem. Soc.(Dalton) 1973, p604.
43. Mellor J.W., A Comprehensive Treatise on Inorganic and Theoretical Chemistry, Longmans, Green and Co. Ltd., 1927, 9, p740.
44. Cotton F.A. and Wilkinson G., Advanced Inorganic Chemistry, Interscience, New York 1966, p820.

45. Mellor J.W., A Comprehensive Treatise on Inorganic and Theoretical Chemistry, Longmans, Green and Co. Ltd., 1927, 11, 174.
46. Rechnitz G.A. and Catherino H.A., Inorg. Chem., 1965, 4, 112.
47. Glebov V.A., J. Structural Chemistry, 1970, 11, 750.
48. Schenk M., Helv. Chim. Acta, 1936, 19, 625.
49. Tribalat S. and Delafosse D., Anal. Chim. Acta, 1958, 19, 74.
50. Diebler H., Z. Phys. Chem., 1969, 68, 64.
51. Samuni A., Meisel D. and Czapski G., J. Chem. Soc., 1972, p1273.
52. Sutton G.J., Aust. J. Chem., 1959, 12, 122.
53. Van der Pfordten O.F., Liebigs Ann., 1886, 234, 257.
54. Bohland H. and Malitzke P., Z. Anorg. Allgem. Chem., 1967, 350, 70.
55. Jones G. and Bollinger D.M., J. Am. Chem. Soc., 1931, 53, 411.
56. Leong T.H., Hons. Thesis, University of Tasmania, 1971, p31.
57. Rossotti F.J.C. and Rossotti H., The Determination of Stability Constants, McGraw-Hill, New York 1961, p52.
58. Cotton F.A. and Wilkinson G., Advanced Inorganic Chemistry, Interscience, New York 1966, p438.
59. Arris J. and Duffy J.A., J. Chem. Soc. Suppl. No.1, 1964, p5850.
60. Guggenheim E.A. and Stokes R.H., Equilibrium Properties of Aqueous Solutions of Single Strong Electrolytes, Pergamon Press, Oxford 1969, p143.
61. Hamer W.J., The Structure of Electrolytic Solutions, John Wiley and Sons, New York 1959, p48.
62. Beck M.T., Chemistry of Complex Equilibria, Van Nostrand Reinhold Co. London 1970, p89.
63. Goroshchenko Ya.G. and Godneva M.M., Russ. J. Inorg. Chem., 1961, 6, 744.
64. Demenev N.V. et al., Zh. Neorg. Khim., 1957, 2, 465.
65. Mellor J.W., A Comprehensive Treatise on Inorganic and Theoretical Chemistry, Longmans, Green and Co. Ltd., 1927, 7, p92.
66. Yamanaka M., Higihira Y. and Akazawa Y., Yakugaku Zasshi, 1960, 80, 236.

67. Rems P., Orel B. and Sifter J., *Inorg. Chimica Acta*, 1971, 5, 33.
68. Eve D.J. and Fowles G.W.A., *J. Chem. Soc.*, 1966, A, 1183.
69. Nakamoto K., *Infrared Spectra of Inorganic and Co-ordination Compounds*, John Wiley, New York 1970, p173.
70. Miller F.A. and Wilkins C.H., *Anal. Chem.*, 1952, 24, 1253.
71. Meyer J. and Markowez E., *Z. Anorg. Allgem. Chem.*, 1926, 157, 211.
72. Weinland R.F. and Ensgraber Fr., *Z. Anorg. Chem.*, 1913, 84, 340.
73. Patscheke G. and Schaller W., *Z. Anorg. Allgem. Chem.*, 1938, 235, 257.
74. Vogel A.I., *Quantitative Inorganic Analysis*, Longmans, London 1961.
75. Gandeboeuf J. and Souchay P., *J. Chim. Phys.*, 1959, 56, 358.
76. Erdmann H., *Angew. Chem.*, 1952, 64, 500.
77. Kuntzel A., Erdmann H. and Spahrkas H., *Das Leder*, 1952, 3, 73.
78. Schlafer H.L. and Gotz R., *Z. Anorg. Allgem. Chem.*, 1961, 309, 104.
79. Podmore L.P., Smith P.W. and Stoessiger R., *J. Chem. Soc.(Dalton)* 1973, p125.
80. Robin M.B., and Day P., *Adv. Inorg. Chem. and Radiochem.*, 1967, 10, 247.
81. Heintz E.A., *Nature*, 1963, 197, 690.
82. Lo G.Y.S. and Brubaker C.H., *Inorg. Nucl. Chem.*, 1972, 34, 2375.
83. Kutner E.A., Matseevskii B.P. and Lepin L.K., *Russ. J. Phys. Chem.*, 1971, 45, 813.
84. Bishop E. and Evans N., *Talanta*, 1970, 17, 1125.
85. Milligan L.H. and Gillette G.R., *J. Phys. Chem.*, 1924, 28, 744.
86. Johnson C.E. and Winstein S., *J. Am. Chem. Soc.*, 1951, 73, 2601.
87. Duke F.R. and Quinney P.R., *J. Am. Chem. Soc.*, 1954, 76, 3800.
88. Polyakova V.M. and Chernyavskaya E.I., *Tr. Inst. Khim., Akad. Nauk SSSR, Ural. Filial*, 1970, 17, 155.
89. Anderson I.R. and Sheldon J.C., *Aust. J. Chem.*, 1965, 18, 271.
90. Meites L., *Handbook of Analytical Chemistry*, McGraw-Hill, New York 1963.

91. Vogel A.I., Quantitative Inorganic Analysis, Longmans. Green and Co., London, 1951, p403
92. Feldmane Dz., Berdnikov V.M., Matseevskii, Zh. Fiz. Khim. 1975, 49, 3148.
93. Marov I. N., Yakovleva E.G., Pechurova N.I. Evtikova G.A., Russ J. Inorg. Chem., 1975, 20, 48.